from space to core earthsciences UCL

Equilibrium Isotope Fractionation Factors: Insights from First-principles calculations

Wenzhong Wang (王文忠)

wenzhong.wang@ucl.ac.uk

Department of Earth Sciences
University College London

Summer School, 08/11

All models are **wrong**, but some are **useful**.

\- George Box

Content

1. Background

thermodynamics, Urey equation, First-principles calculations

2. EIFFs among minerals: controlling factors

Temperature, pressure, concentration, occupancy site, ...

3. EIFFs for aqueous solutions

Mg, Ba, ...

4. Future prospects

Part 1. Background

thermodynamics, Urey equation, First-principles calculations

Keywords -- Equilibrium

Thermal Equilibrium: The temperature of the system does not change with time and has same value at all points of the system.

Mechanical Equilibrium: There are no unbalanced forces within the system or between the surroundings. The pressure in the system is same at all points and does not change with respect to time.

Chemical Equilibrium: No chemical reaction takes place in the system and the chemical composition which is same throughout the system does not vary with time.

Keywords -- Equilibrium

Thermal Equilibrium: The temperature of the system does not change with time and has same value at all points of the system.

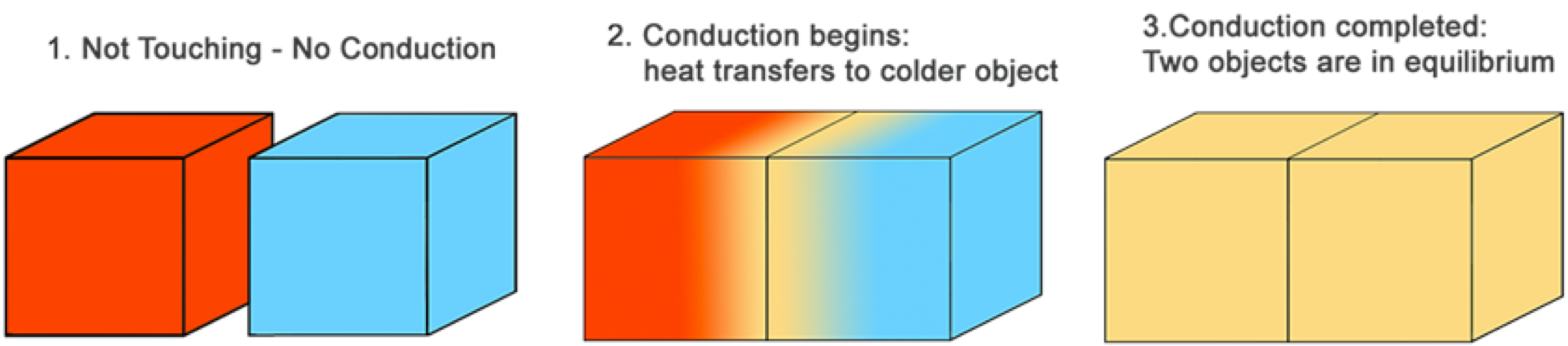

Keywords -- Equilibrium

Mechanical Equilibrium: There are no unbalanced forces within the system or between the surroundings. The pressure in the system is same at all points and does not change with respect to time.

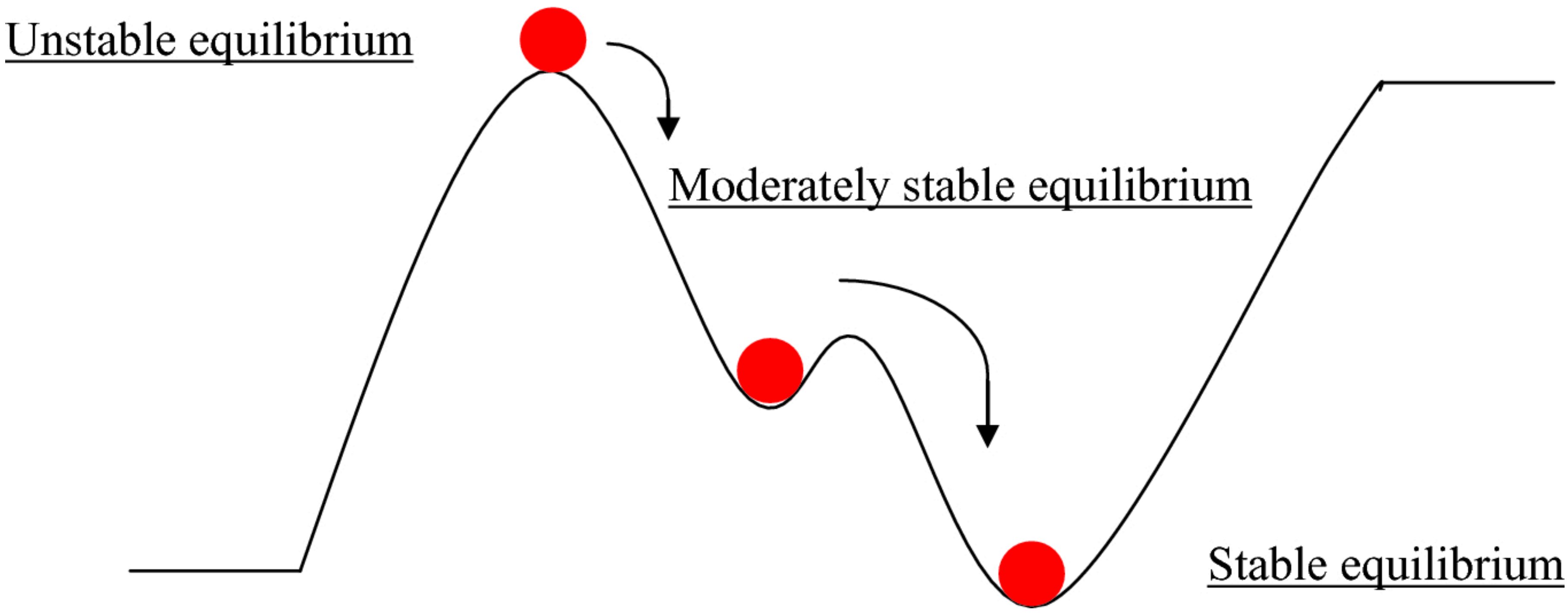

Keywords -- Equilibrium

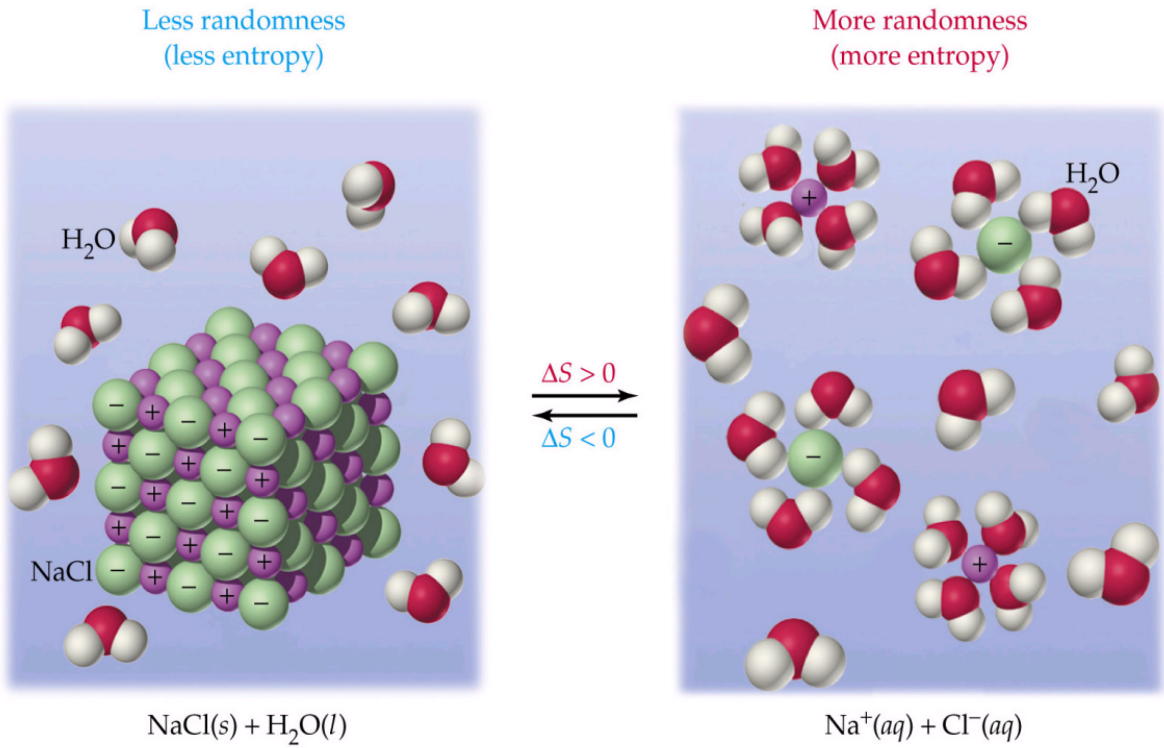

Chemical Equilibrium: No chemical reaction takes place in the system and the chemical composition which is same throughout the system does not vary with time.

Laws of thermodynamics

1. Zeroth law: A=B & B=C, A=C; Temperature (T)
2. First law: energy is conservative; Internal energy (U)
3. Second law: heat cannot be fully converted to work
4. Third law: The entropy of perfect crystal at 0 K is zero.

- ✓ Enthalpy $H = U + PV$
- ✓ Helmholtz free energy $F = U - TS$
- ✓ Gibbs free energy $G = H - TS = F + PV$

Maxwell relations

$$dU = TdS - PdV$$
$$dH = TdS + VdP$$
$$dG = -SdT + VdP$$

If we know G (T, P), we can derive all the other thermodynamic functions:

Equilibrium Constants and ΔG

Equilibrium constant for a reaction: $aA + bB \leftrightarrow mM + nN$

$$K=[M]^m[N]^n/[A]^a[B]^b$$

$$\mu = \mu^* + RT\ln f_i$$

$\Delta G = m(\mu^*_M + RT\ln f_M) + n(\mu^*_N + RT\ln f_N) - a(\mu^*_A + RT\ln f_A) - b(\mu^*_B + RT\ln f_B)$

$= \Delta G^* + RT\ln([f_M]^m * [f_N]^n / [f_A]^a / [f_B]^b)$

$[f_M]^m * [f_N]^n / [f_A]^a / [f_B]^b = [M]^m[N]^n/[A]^a[B]^b = K$

At equilibrium, $\Delta G = 0$:

$$K=\exp(-\Delta G^*/RT)$$

Urey equation (Bigeleisen-Mayer)

Equilibrium constant for a isotope exchange reaction:

$$AX + X^* \rightleftharpoons AX^* + X$$

K=[AX*][X]/[AX][X*]=exp(-ΔG*/RT)= exp(-ΔF*/kT)

F=-kTlnZ, Z is partition function: Z=$\boldsymbol{z_{tran}\, z_{rot}\, z_{vib}\, z_{elec}}$

$$z_{tran} = \left(\frac{\sqrt{2\pi M k_b T}}{h_p}\right)^3 V \quad z_{rot} = \frac{1}{\sigma}\sqrt{\pi (k_b T)^3 I_X I_Y I_Z} \quad z_{vib} = \prod_{i=1}^{3N-6} \frac{e^{-\frac{h_p \omega_i}{4\pi k_b T}}}{1-e^{-\frac{h_p \omega_i}{2\pi k_b T}}} \quad z_{elec} = e^{-\frac{\varepsilon_0}{k_b T}}$$

$$\boldsymbol{\beta_{AX-X} = \frac{z(AX^*)/z(AX)}{z(X^*)/z(X)} = \sqrt{\frac{{M^*}^3 I_X^* I_Y^* I_Z^*}{M^3 I_X I_Y I_Z}} \prod_{i=1}^{3N-6} \frac{e^{-\frac{h_p {\omega_i}^*}{4\pi k_b T}}}{1-e^{-\frac{h_p {\omega_i}^*}{2\pi k_b T}}} \frac{1-e^{-\frac{h_p \omega_i}{2\pi k_b T}}}{e^{-\frac{h_p \omega_i}{4\pi k_b T}}} \Bigg/ \sqrt{\frac{{m^*}^3}{m^3}}}$$

$$\sqrt{\frac{{M^*}^3 I_X^* I_Y^* I_Z^*}{M^3 I_X I_Y I_Z}} \sqrt{\frac{m^3}{{m^*}^3}} = \prod_{i=1}^{3N-6} \frac{{\omega_i}^*}{\omega_i}$$

Reduced Partition Function Ratio

$$\beta_A = \frac{Q_h}{Q_l} = \prod_i^{3N} \frac{u_i^*}{u_i} \frac{e^{-\frac{1}{2}u_i^*}}{1 - e^{-u_i^*}} \frac{1 - e^{-u_i}}{e^{-\frac{1}{2}u_i}} \qquad u_i^*\ (u_i) = \hbar\omega_i^*(\omega_i)/k_B T$$

$$\Delta_{A-B} \approx 10^3 ln\alpha_{A-B} = 10^3 ln\beta_A - 10^3 ln\beta_B$$

We only need vibrational frequencies ω_i

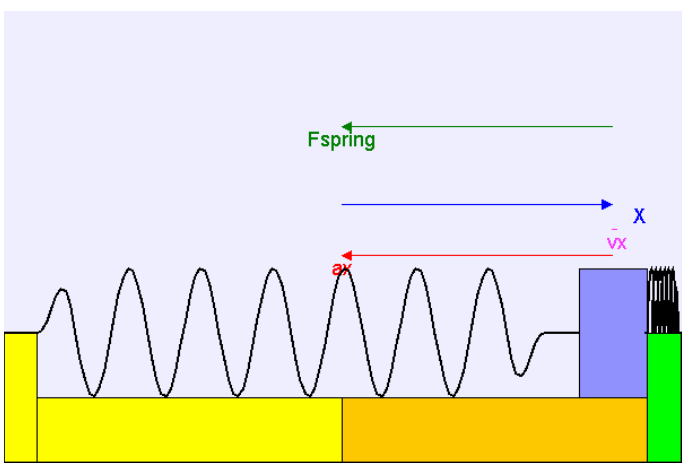

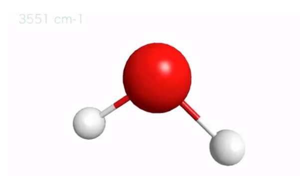

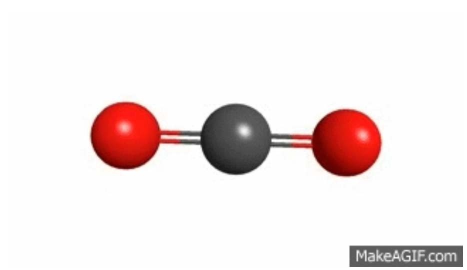

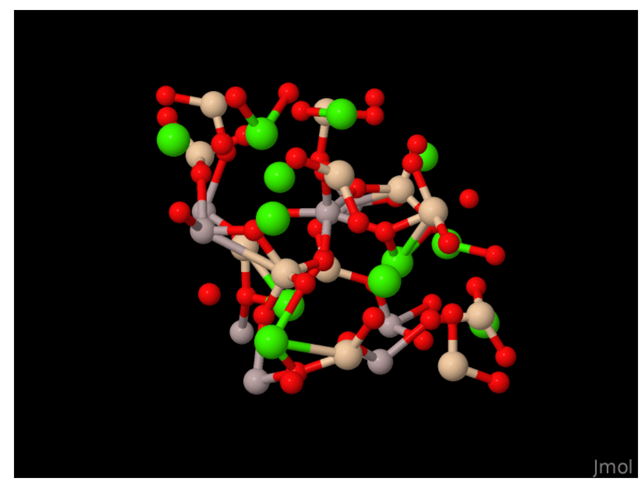

The Thermodynamic Properties of Isotopic Substances.

LIVERSIDGE LECTURE, DELIVERED BEFORE THE CHEMICAL SOCIETY IN THE ROYAL INSTITUTION ON DECEMBER 18TH, 1946.

By HAROLD C. UREY.
(Institute of Nuclear Studies, University of Chicago.)

THE discovery of the isotopes of the elements resulted from the careful study of the properties of radioactive substances during the first years of this century. The conclusion that certain species of atoms had identical chemical properties but different radioactive properties came from chemical studies which accompanied the study of radioactivity. Boltwood [1] noted that thorium and ionium were very similar in chemical properties, so similar, in fact, that he was unable to separate them if they were mixed. Marckwald and Keetman [2] investigated this problem with greater care, as did Auer v. Welsbach [3], and all these authors came to the conclusion that ionium and thorium are identical in chemical properties. Further, Marckwald [4] and Soddy [5] showed that radium and mesothorium constitute another such pair of substances. At present many such radio-elements which are chemically the same elements or are identical with non-radioactive elements are known. Soddy was able to conclude that this occurrence of two or more varieties of elements of identical chemical properties was probably of general occurrence, and that such identical elements differed in atomic weight as well as radioactive properties, and

THE JOURNAL OF CHEMICAL PHYSICS VOLUME 15, NUMBER 5 MAY, 1947

Calculation of Equilibrium Constants for Isotopic Exchange Reactions

JACOB BIGELEISEN AND MARIA GOEPPERT MAYER
Argonne National Laboratory, Chicago, Illinois and Institute for Nuclear Studies, University of Chicago*

(Received February 5, 1947)

It is pointed out that the possibility of chemical separation of isotopes is a quantum effect. This permits a direct calculation of the difference in the free energies of two isotopic molecules. Tables and approximation methods are given which permit a rapid calculation of equilibrium constants if the frequency shifts on isotopic substitution are known. Several applications are discussed.

Scope of Urey equation

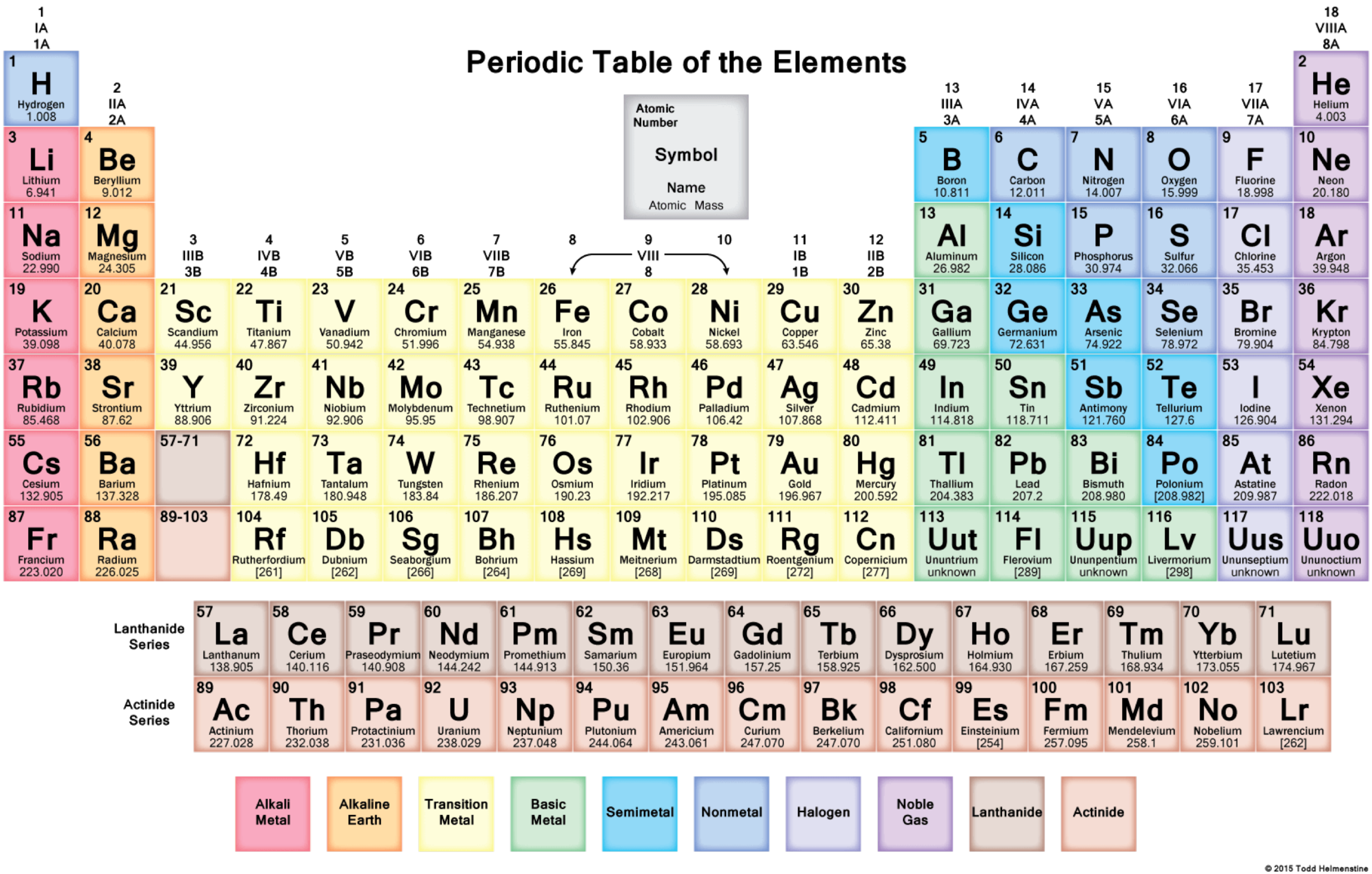

Quantum mechanics

A. Piccard, E. Henriot, P. Ehrenfest, E. Herzen, Th. de Donder, E. Schrödinger, J.E. Verschaffelt, W. Pauli, W. Heisenberg, R.H. Fowler, L. Brillouin;
P. Debye, M. Knudsen, W.L. Bragg, H.A. Kramers, P.A.M. Dirac, A.H. Compton, L. de Broglie, M. Born, N. Bohr;
I. Langmuir, M. Planck, M. Curie, H.A. Lorentz, A. Einstein, P. Langevin, Ch.-E. Guye, C.T.R. Wilson, O.W. Richardson

Schrödinger equation

Single particle

$$\left[-\frac{\hbar^2}{2m}\nabla^2 + V(\vec{r})\right]\psi(\vec{r}) = E\psi(\vec{r})$$

Multiple particles

$$\hat{H}\psi(\boldsymbol{r},\boldsymbol{R}) = E\psi(\boldsymbol{r},\boldsymbol{R})$$

$$-\sum_I \frac{\hbar^2}{2M_I}\nabla_I^2 - \sum_i \frac{\hbar^2}{2m_i}\nabla_i^2 - \sum_I\sum_i \frac{e^2 Z_I}{\boldsymbol{r}_{iI}} + \sum_{i<j}\frac{e^2}{\boldsymbol{r}_{ij}} + \sum_{I<J}\frac{e^2 Z_I Z_J}{\boldsymbol{R}_{IJ}}$$

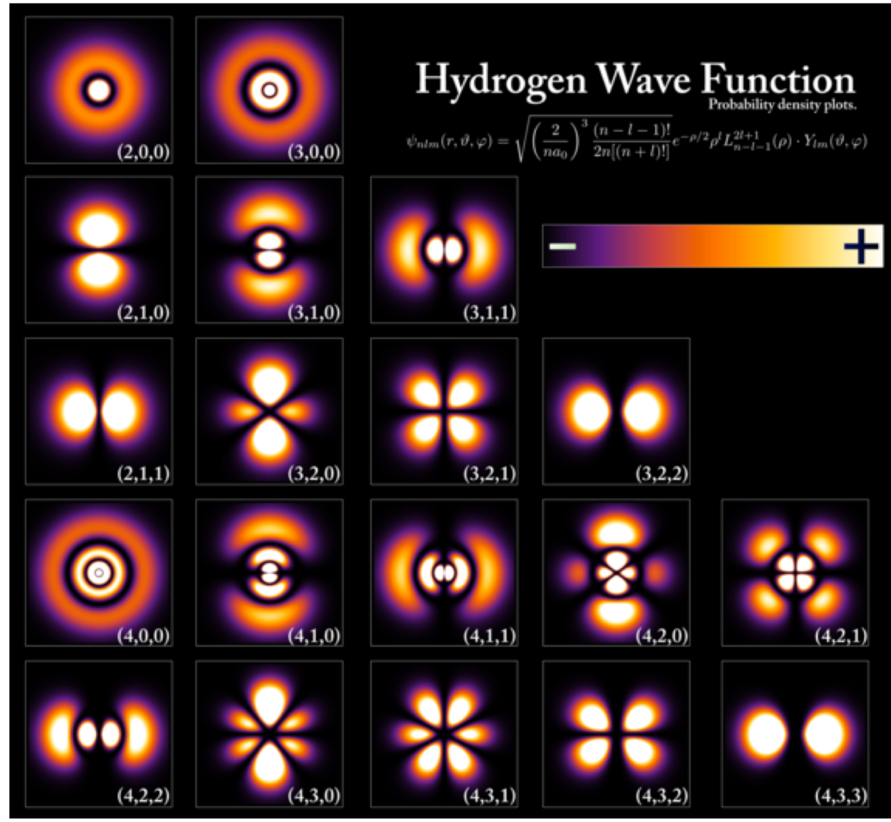

Born-Oppenheimer approximation

$$\hat{H}_e\psi_e(\boldsymbol{r},\boldsymbol{R}) = E(\boldsymbol{R})\psi_e(\boldsymbol{r},\boldsymbol{R})$$

$$\hat{H}_e = -\sum_i \frac{\hbar^2}{2m_i}\nabla_i^2 - \sum_I\sum_i \frac{e^2 Z_I}{\boldsymbol{r}_{iI}} + \sum_{i<j}\frac{e^2}{\boldsymbol{r}_{ij}}$$

Simple to write,
yet hard to solve equation

Solving Schrödinger equation

Single particle

$$\left[-\frac{\hbar^2}{2m}\nabla^2 + V(\vec{r})\right]\psi(\vec{r}) = E\psi(\vec{r})$$

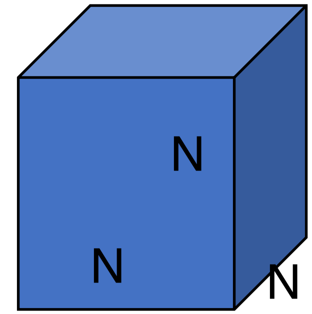

Multiple particles

$$\hat{H}\psi(\boldsymbol{r},\boldsymbol{R}) = E\psi(\boldsymbol{r},\boldsymbol{R})$$

$$-\sum_I \frac{\hbar^2}{2M_I}\nabla_I^2 - \sum_i \frac{\hbar^2}{2m_i}\nabla_i^2 - \sum_I \sum_i \frac{e^2 Z_I}{\boldsymbol{r}_{iI}} + \sum_{i<j} \frac{e^2}{\boldsymbol{r}_{ij}} + \sum_{I<J} \frac{e^2 Z_I Z_J}{\boldsymbol{R}_{IJ}}$$

n = # electrons	Ψ (N^{3n})	ρ (N^3)
1	8	8
10	10^9	8
100	10^{90}	8
1000	10^{900}	8

Born-Oppenheimer approximation

$$\hat{H}_e\psi_e(\boldsymbol{r},\boldsymbol{R}) = E(\boldsymbol{R})\psi_e(\boldsymbol{r},\boldsymbol{R})$$

$$\hat{H}_e = -\sum_i \frac{\hbar^2}{2m_i}\nabla_i^2 - \sum_I \sum_i \frac{e^2 Z_I}{\boldsymbol{r}_{iI}} + \sum_{i<j} \frac{e^2}{\boldsymbol{r}_{ij}}$$

Simple to write,
yet hard to solve equation

Density functional theory

First theorem

Energy of the system is a unique functional of the charge density

Second theorem

The correct ground state charge density minimizes the energy functional and the resulting energy is the ground state energy

$$E_{\text{tot}}[n(\mathbf{r})] = T[n(\mathbf{r})] + E_{\text{int}}[n(\mathbf{r})] + \int d\mathbf{r}\, V_{\text{ext}}(\mathbf{r})\, n(\mathbf{r}) + E_{\text{ion-ion}}$$

Pierre Hohenberg
(1934/10 ~ 2017/12)

Walter Kohn
(1923/03 ~ 2016/04)

1998 Nobel Prize in Chemistry

Kohn-Sham equation

$$\left(-\frac{\hbar^2}{2m}\nabla^2 + \int \frac{n(r)dr'}{|r-r'|} + V_{ext}(r) + V_{xc}(r)\right)\psi_i(r) = \varepsilon_i \psi_i(r)$$

The exchange-correlation functional

Local density approximation (LDA) VS. Generalized Gradient Approximation (GGA)

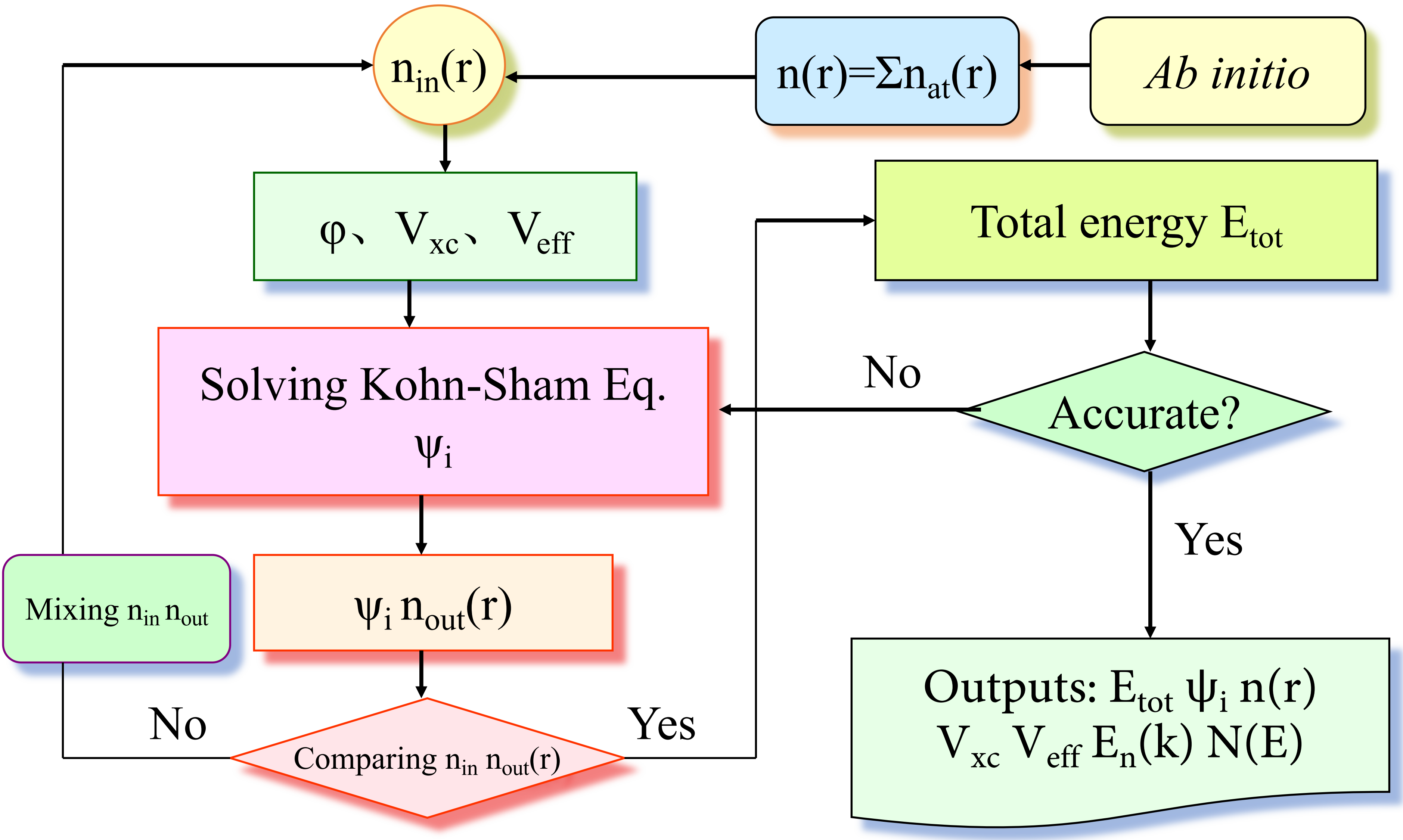

n_in(r)
n(r)=Σn_at(r)
Ab initio
φ、 V_xc、 V_eff
Total energy E_tot
Solving Kohn-Sham Eq.
ψ_i
No
Accurate?
Yes
Mixing n_in n_out
ψ_i n_out(r)
No
Comparing n_in n_out(r)
Yes
Outputs: E_tot ψ_i n(r)
V_xc V_eff E_n(k) N(E)

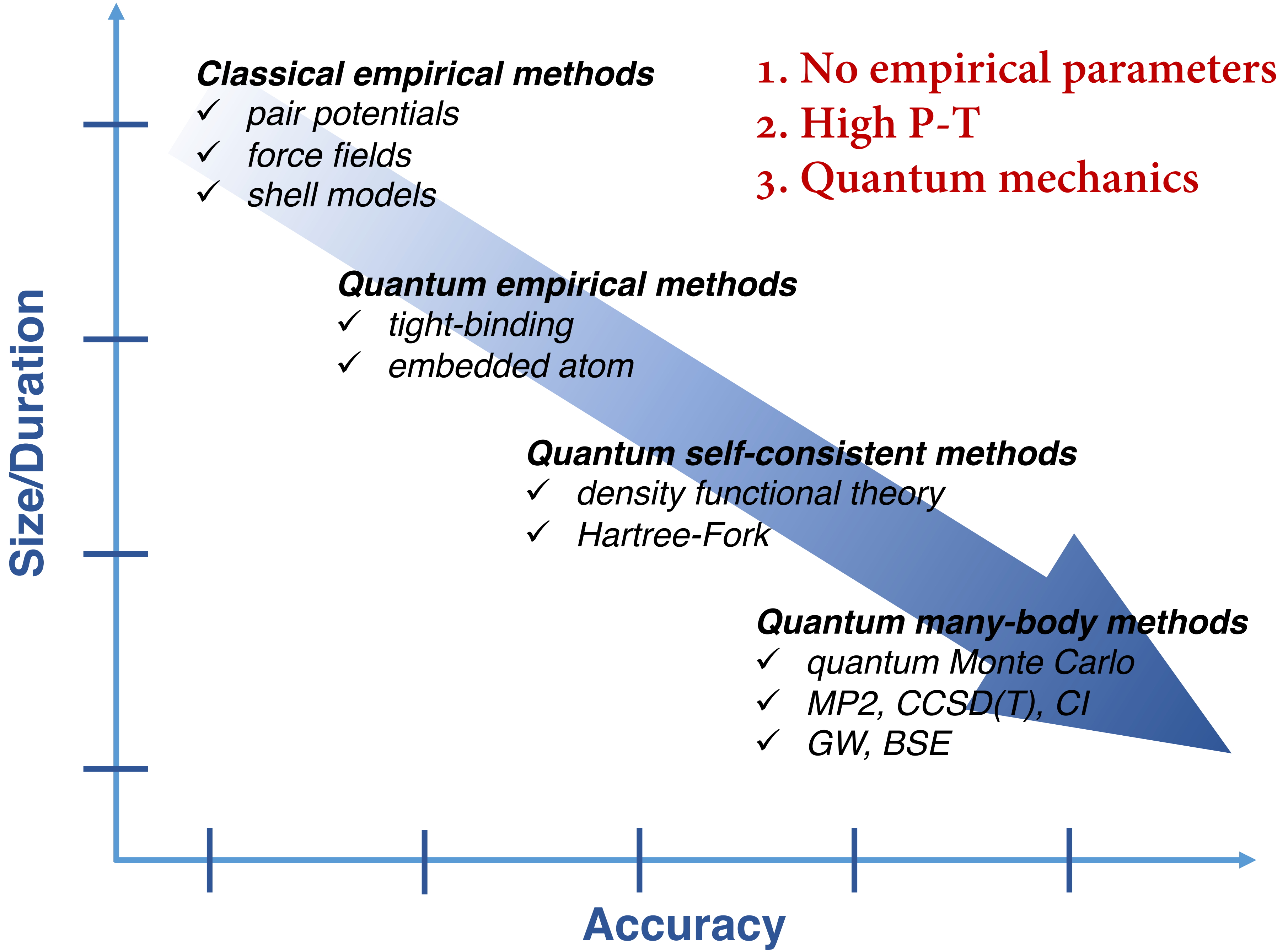

Classical empirical methods
✓ pair potentials
✓ force fields
✓ shell models
1. No empirical parameters
2. High P-T
3. Quantum mechanics
Quantum empirical methods
✓ tight-binding
✓ embedded atom
Quantum self-consistent methods
✓ density functional theory
✓ Hartree-Fork
Quantum many-body methods
✓ quantum Monte Carlo
✓ MP2, CCSD(T), CI
✓ GW, BSE
Size/Duration
Accuracy

Package	License†	Language	Basis	Periodic‡	Mol. mech.	Semi-emp.	HF	Post-HF	MRCI	CC	DFT	GPU
Yambo Code	Free, GPL	Fortran	PW	3d	No	No	Yes	Yes	No	No	No	No
xtb	Academic	Fortran	Minimal GTO	3d	No	Yes	No	No	No	No	No	No
WIEN2k	Commercial	Fortran, C	FP-(L)APW+lo	3d	Yes	No	Yes	No	No	No	Yes	No
VASP	Academic (AT), commercial	Fortran	PW	3d	Yes	No	Yes	Yes	No	No	Yes	Yes
TURBOMOLE	Commercial	Fortran	GTO	Yes	Yes	Yes	Yes	Yes	No	up to (T)	Yes	No
TeraChem [8]	Commercial	C, CUDA	GTO	No	Yes	No	Yes	Yes	No	No	Yes	Yes
TB-LMTO	Academic	Fortran	LMTO	3d	No	No	No	No	No	No	Yes	No
SPHInX	Free, Apache License	C++	PW	3d	No	No	No	No	No	No	Yes	No
Spartan	Commercial	Fortran, C, C++	GTO	No	Yes	Yes	Yes	Yes	No	up to (T)	Yes	No
SIESTA	Free, GPL	Fortran	NAO	3d[12]	Yes	No	No	No	No	No	Yes	No
Siam Quantum	Free, GPL	C	GTO	No	Yes	No	Yes	Yes	No	No	Yes	No
Scigress	Commercial	C++, C, Java, Fortran	GTO	Yes	Yes	Yes	No	No	No	No	Yes	No
SAMSON	Free	C++, Python	Multiple	No	Yes	Yes	No	No	No	No	Yes	No
RSPt	Academic	Fortran, C	FP-LMTO	3d	No	No	No	No	No	No	Yes	Yes
RMG	Free, GPL	C, C++	Grid	Any	Yes	No	No	No	No	No	Yes	Yes, CUDA
Quantum ESPRESSO[6]	Free, GPL	Fortran	PW	3d	Yes	No	Yes	No	No	No	Yes	Yes, CUDA
Quantemol-N	Academic, commercial	Fortran, Java	GTO	No	Yes	Yes	Yes	Yes	No	No	No	No
Quantemol-EC	Academic, commercial	Fortran, Python	GTO	No	Yes	Yes	Yes	Yes	No	No	No	No
QSite	Unknown	Unknown	GTO	No	Yes	No[11]	Yes	Yes	No	No	Yes	No
QMCPACK (QMC)	Free, U. Illinois Open Source	C++	GTO, PW, Spline, Grid, STO	Any	No	No	Yes	Yes	Yes[18]	No	No	Yes, CUDA


ICTP
The Abdus Salam
International Centre
for Theoretical Physics
United Nations
Educational, Scientific and
Cultural Organization
IAEA
International Atomic Energy Agency
Advanced Workshop on High-Performance & High-Throughput Materials Simulations
using Quantum ESPRESSO
16 - 27 January 2017
Miramare, Trieste - Italy

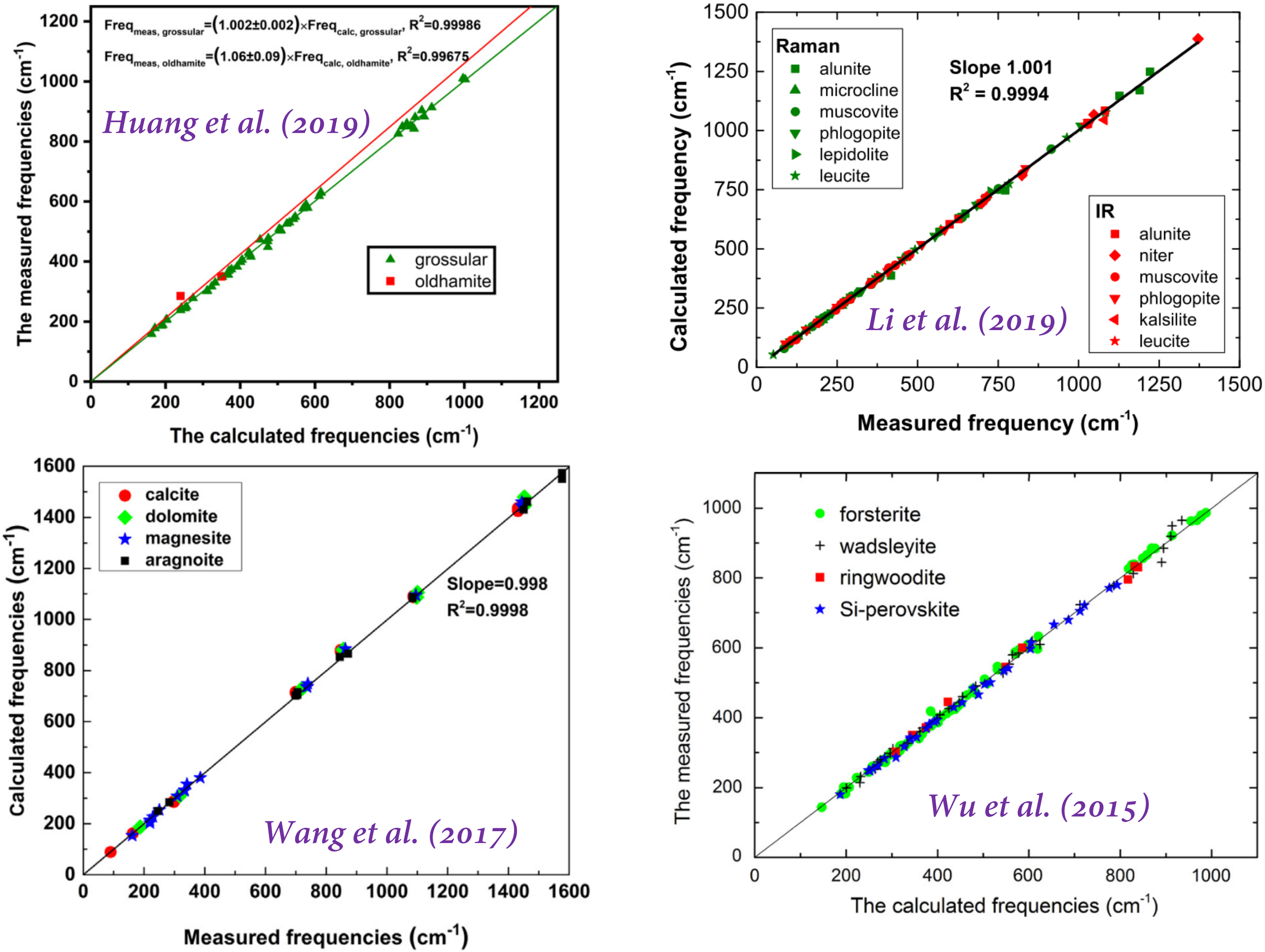
Freq_meas, grossular=(1.002±0.002)×Freq_calc, grossular, R²=0.99986
Freq_meas, oldhamite=(1.06±0.09)×Freq_calc, oldhamite, R²=0.99675
Huang et al. (2019)
grossular
oldhamite
The measured frequencies (cm⁻¹)
The calculated frequencies (cm⁻¹)
0
200
400
600
800
1000
1200
Raman
alunite
microcline
muscovite
phlogopite
lepidolite
leucite
Slope 1.001
R² = 0.9994
IR
alunite
niter
muscovite
phlogopite
kalsilite
leucite
Li et al. (2019)
Calculated frequency (cm⁻¹)
Measured frequency (cm⁻¹)
0
250
500
750
1000
1250
1500
calcite
dolomite
magnesite
aragnoite
Slope=0.998
R²=0.9998
Wang et al. (2017)
Calculated frequencies (cm⁻¹)
Measured frequencies (cm⁻¹)
0
200
400
600
800
1000
1200
1400
1600
forsterite
wadsleyite
ringwoodite
Si-perovskite
Wu et al. (2015)
The measured frequencies (cm⁻¹)
The calculated frequencies (cm⁻¹)
0
200
400
600
800
1000

Part 2. EIFFs among minerals: controlling factors

Temperature, pressure, concentration, occupancy site, …

Cluster model VS. Periodic boundary conditions

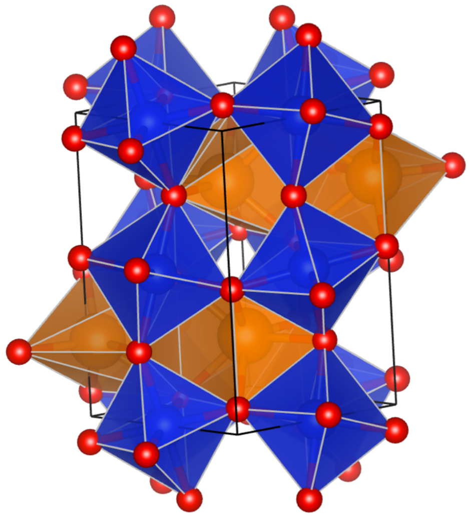

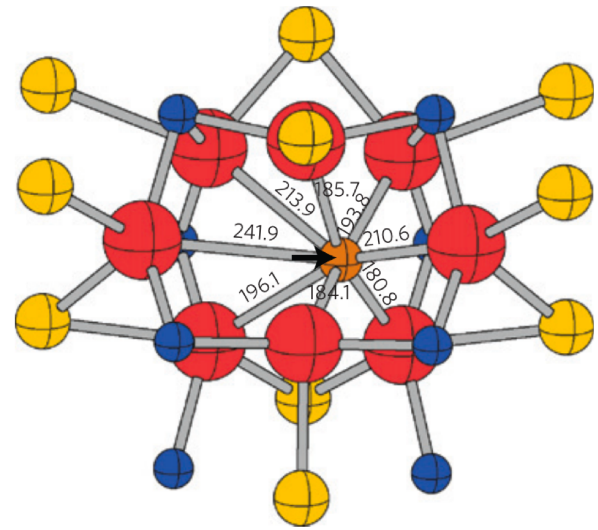

Rustad and Yin (2007)

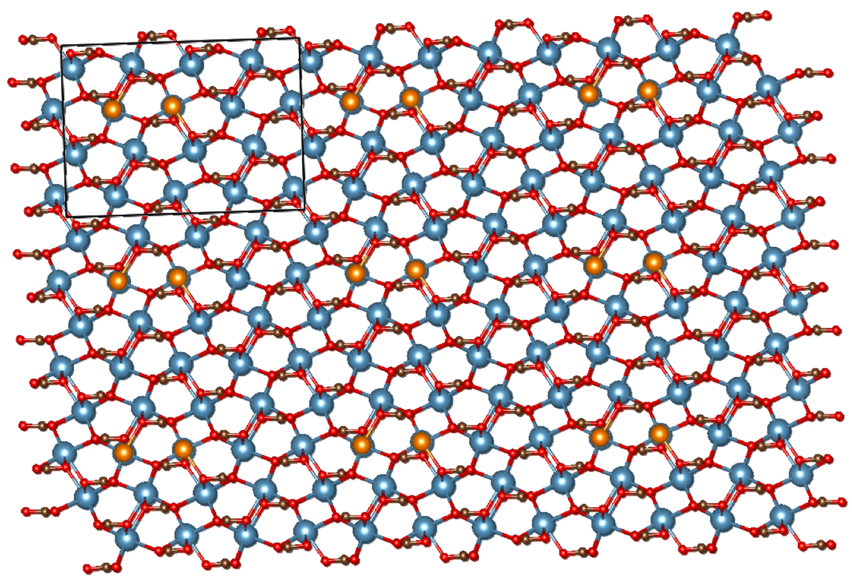

Temperature

$$\beta = \prod_{i=1}^{N_{dof}} \frac{u_i^*}{u_i} \exp\left[\frac{(u_i - u_i^*)}{2}\right] \frac{1-\exp(-u_i)}{1-\exp(-u_i^*)}$$

$$\beta = 1 + \sum_{i=1}^{N_{dof}} \left(\frac{1}{2} - \frac{1}{u_i} + \frac{1}{\exp(u_i)-1}\right)\Delta u_i$$

$$G(u) = \frac{1}{2} - \frac{1}{u} + \frac{1}{\exp(u_i)-1}$$

$$= \frac{u}{12} - \frac{u^3}{720} + \frac{u^5}{30240} - \frac{u^7}{1209600} + \ldots.$$

$$\beta = \beta_{exact} = 1 + \sum_{i=1}^{N_{dof}} \left(\frac{u_i}{12} - \frac{u_i^3}{720} + \ldots\right)\Delta u_i$$

$$u = h\nu_i / k_B T$$

$$\beta = 1 + \sum_i^{N_{dof}} \frac{u_i}{12}\Delta u_i$$

$$= 1 + \sum_{i=1}^{N_{dof}} \frac{\Delta u_i^2}{24} = 1 + \sum_{i=1}^{N_{dof}} \frac{u_i^2 - u_i^{*2}}{24}$$

$$\beta \simeq 1 + \sum_{i=1}^{N_{dof}} \frac{u_i^2 - u_i^{*2}}{24} = 1 + \frac{\Delta m}{mm^*} \frac{\hbar^2}{24 k_B^2 T^2} \sum_{i=1}^{3} A_i$$

Average Force Constant

“High-temperature” Approximation

ν [cm⁻¹] < 1.39 T [K]

Bigeleisen and Mayer (1947)

Pressure effect – Fe

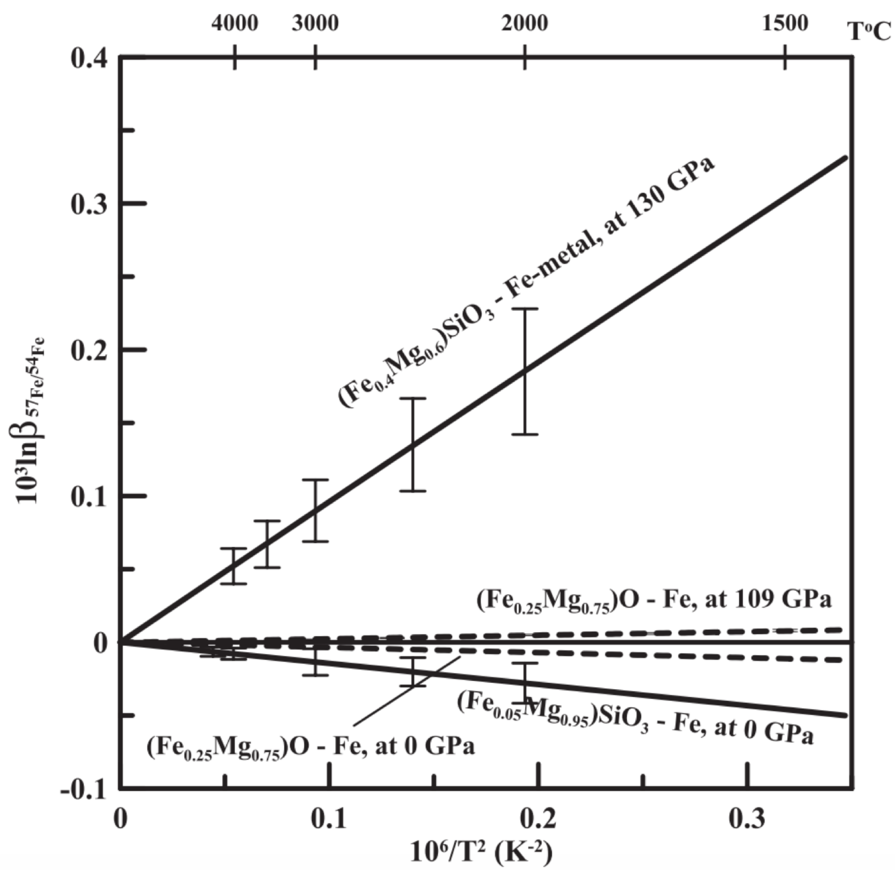

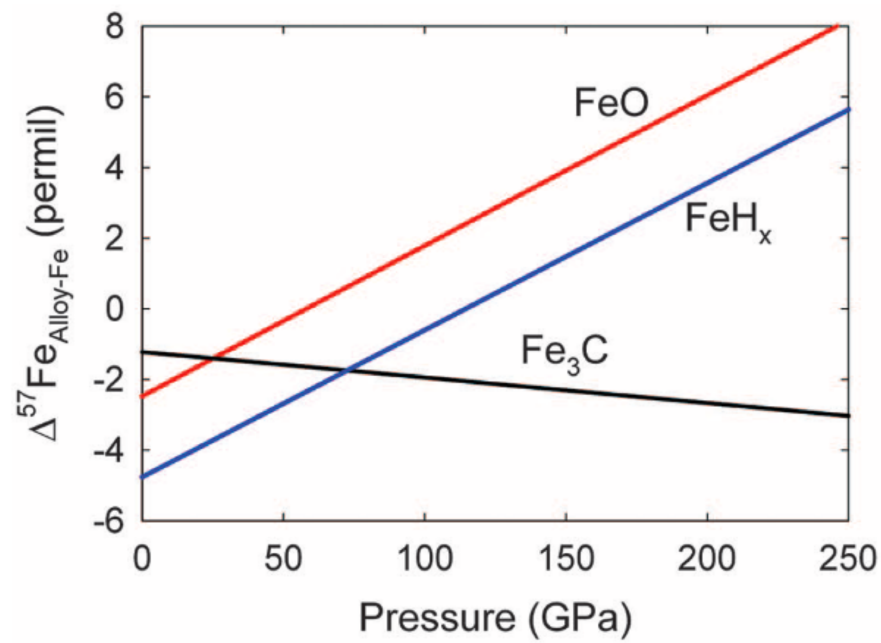

Polyakov (2009)

Shahar et al. (2016)

Inelastic nuclear resonance x-ray scattering (INRXS) spectroscopy

Pressure effect

$$\beta = \prod_{i=1}^{N_{dof}} \frac{u_i^*}{u_i} \exp\left[\frac{(u_i - u_i^*)}{2}\right] \frac{1 - \exp(-u_i)}{1 - \exp(-u_i^*)}$$

$$\boldsymbol{\beta = \beta(V, T)}$$

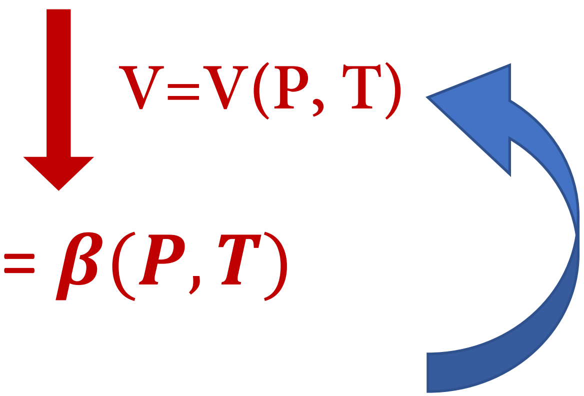

$V=V(P, T)$

$$\boldsymbol{\beta = \beta(P, T)}$$

Helmholtz free energy

$$F(V,T) = U_{st}(V) + \frac{1}{2}\sum_{q,m} \hbar\omega_{q,m}(V) + k_B T \sum_{q,m} \ln\{1 - exp[-\frac{\hbar\omega_{q,m}(V)}{k_B T}]\}$$

Equation of state

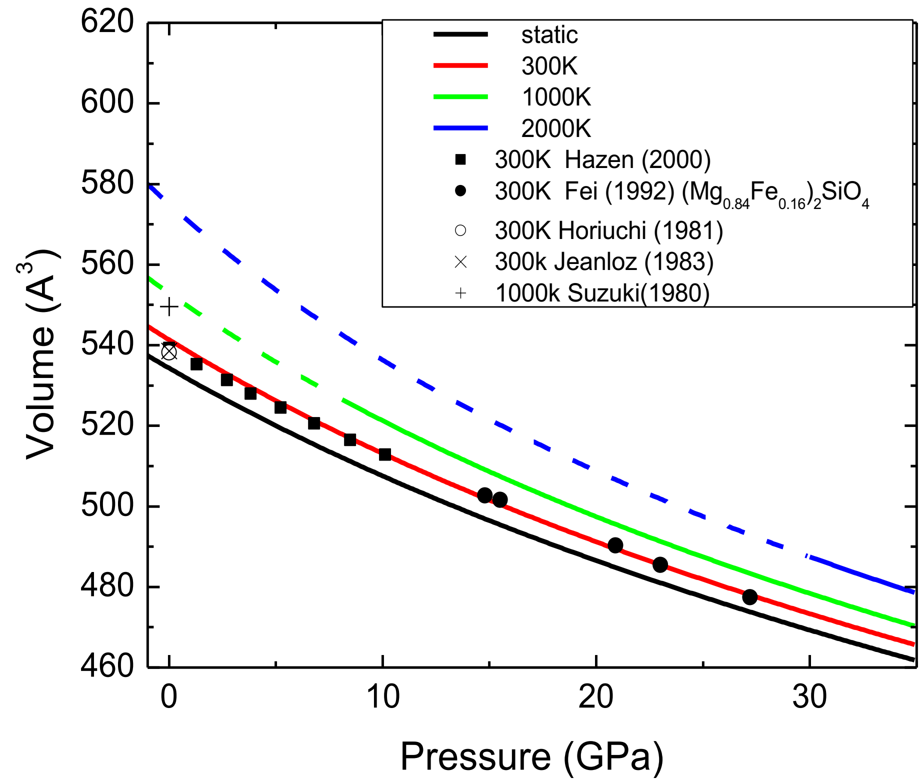

Wu & Wentzcovitch (2007)

Pressure effect– Mg, Si

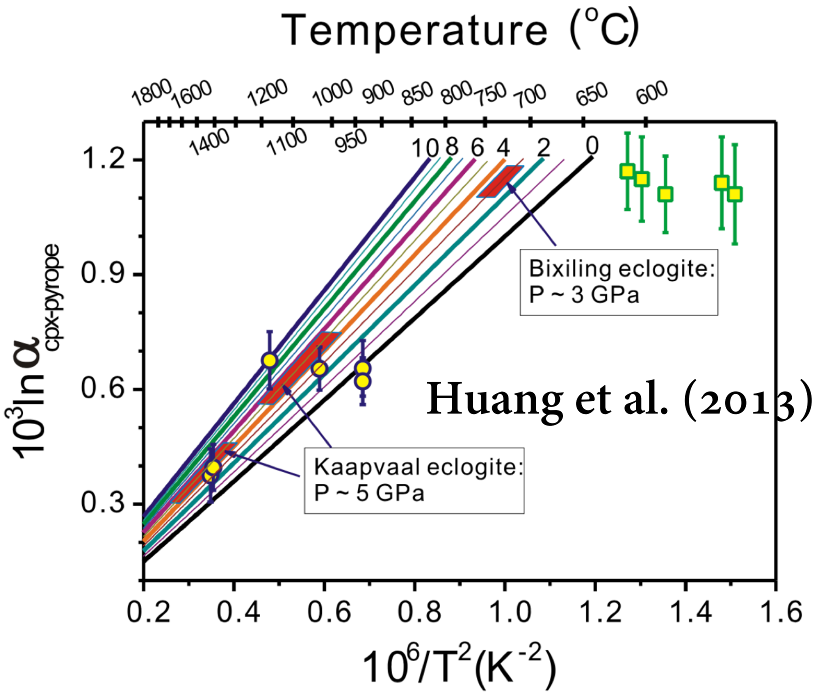

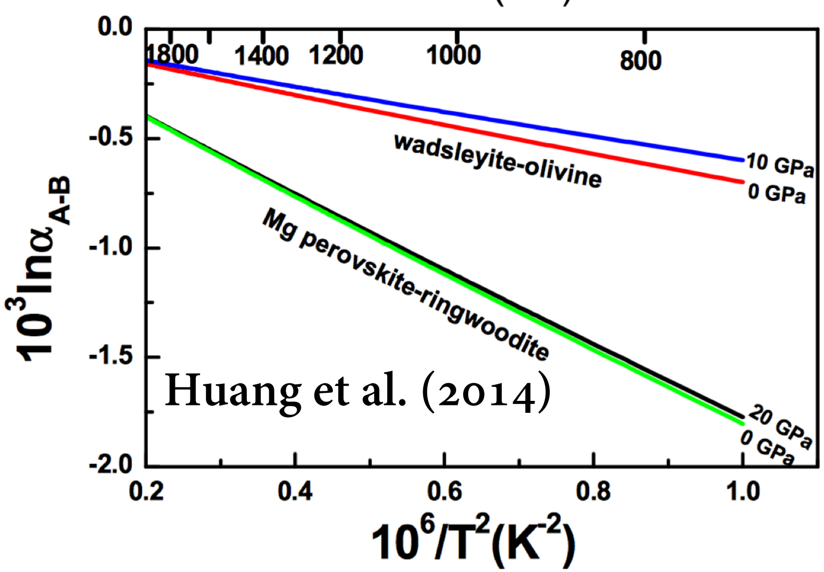

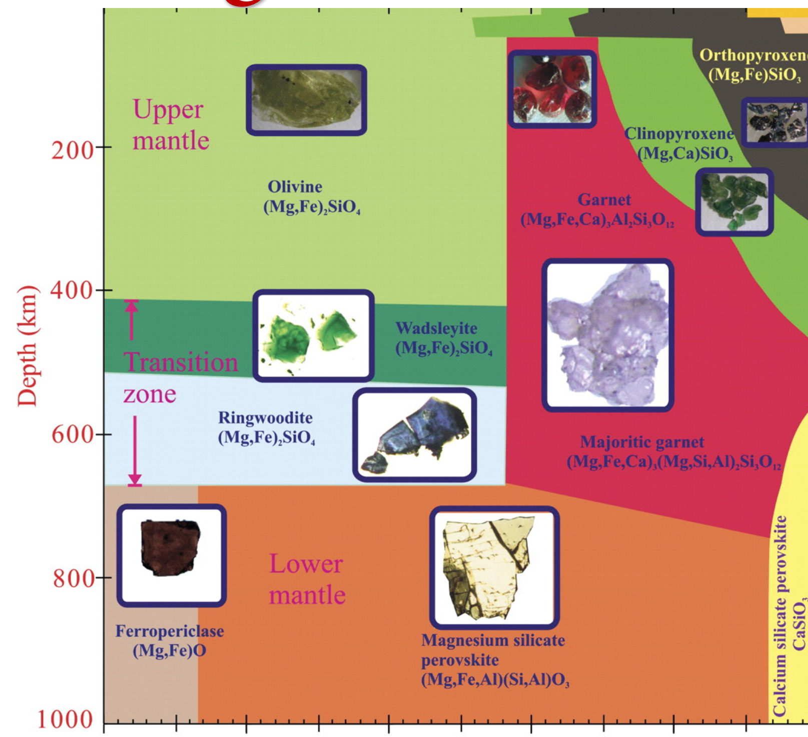

$$\left(\frac{\Delta \ln \beta(P)}{\ln \beta_0}\right)_T = 2\gamma \frac{P}{B}$$

γ: Grüneisen constant

B: Bulk modulus

Phase transition

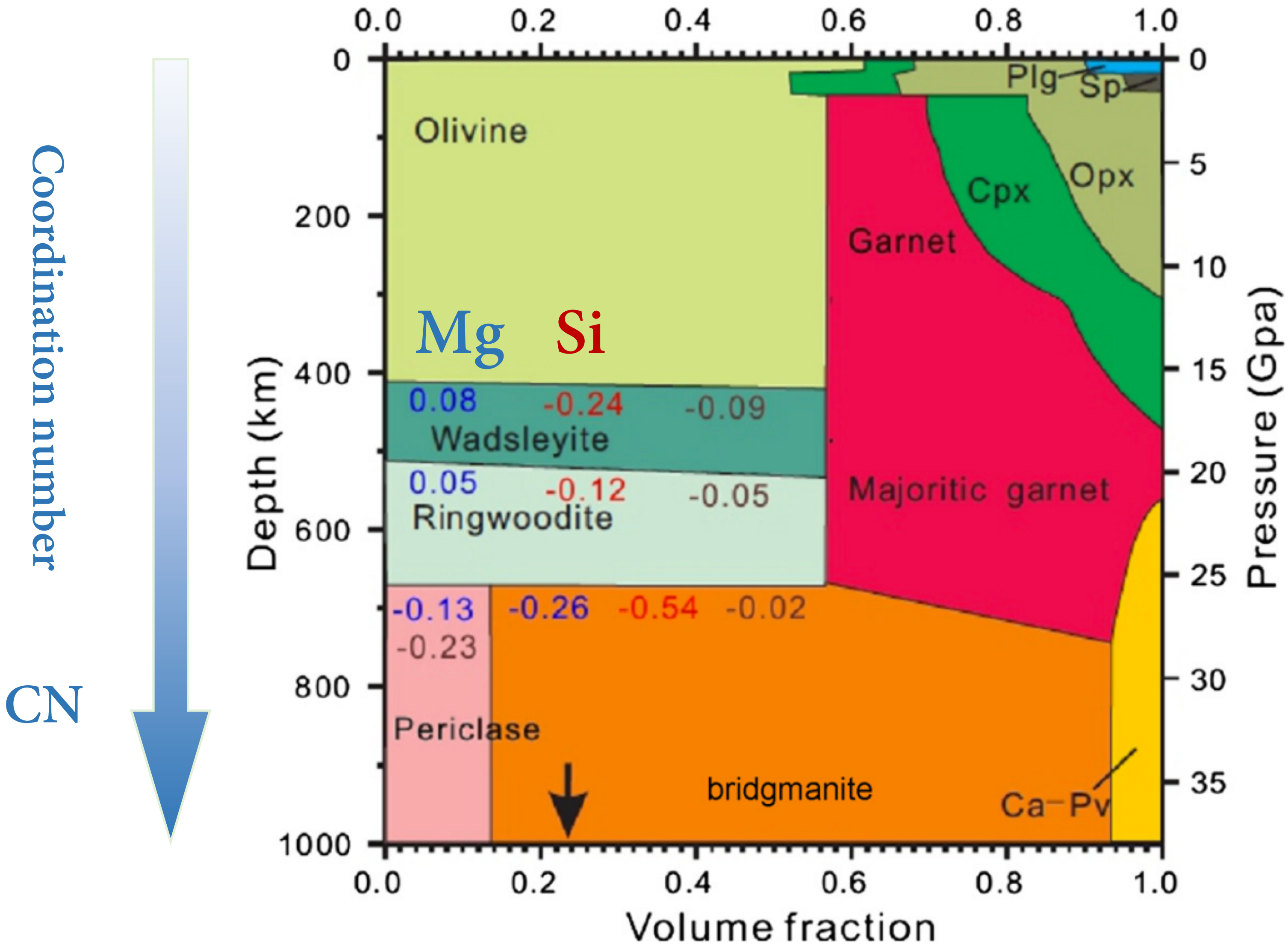

Wu et al. (2015)

Si isotope composition of the deep mantle

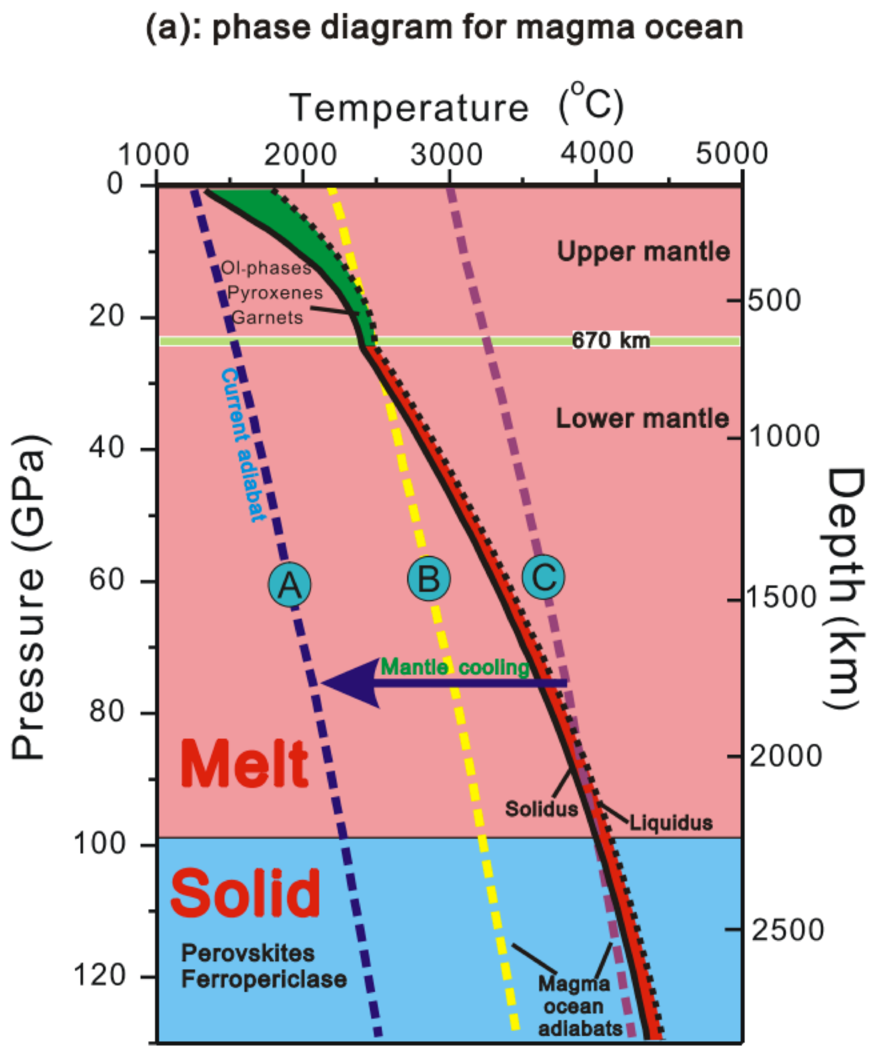

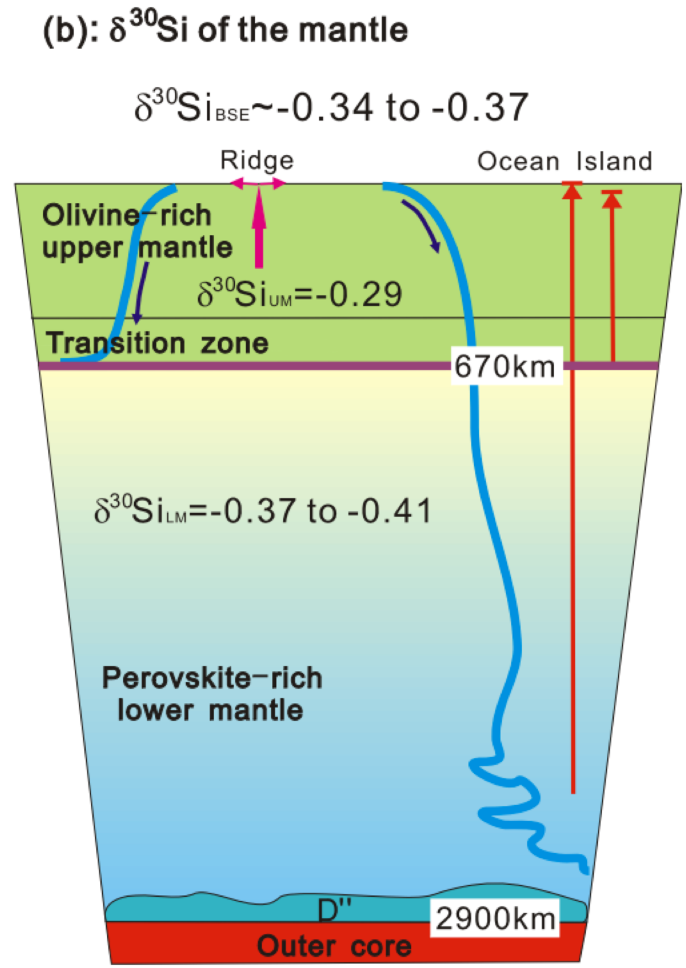

Huang et al. (2014)

Concentration effect

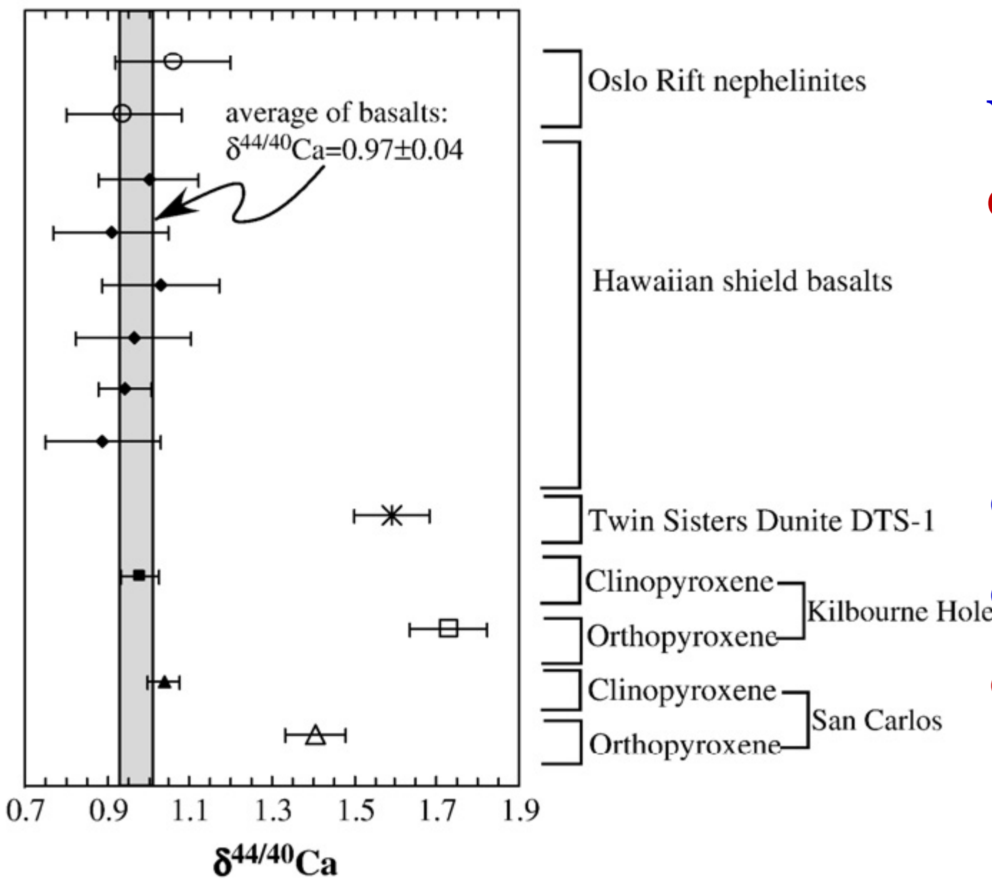

$\Delta^{44}Ca_{opx\text{-}cpx}$ in peridotites

Why $\Delta^{44}Ca_{opx\text{-}cpx}$ varies from 0.36‰ to 0.72‰?

- Disequilibrium?
- Equilibrium temperature?
- Effect of opx Ca content?

Huang et al., (2010)

Concentration effect - opx

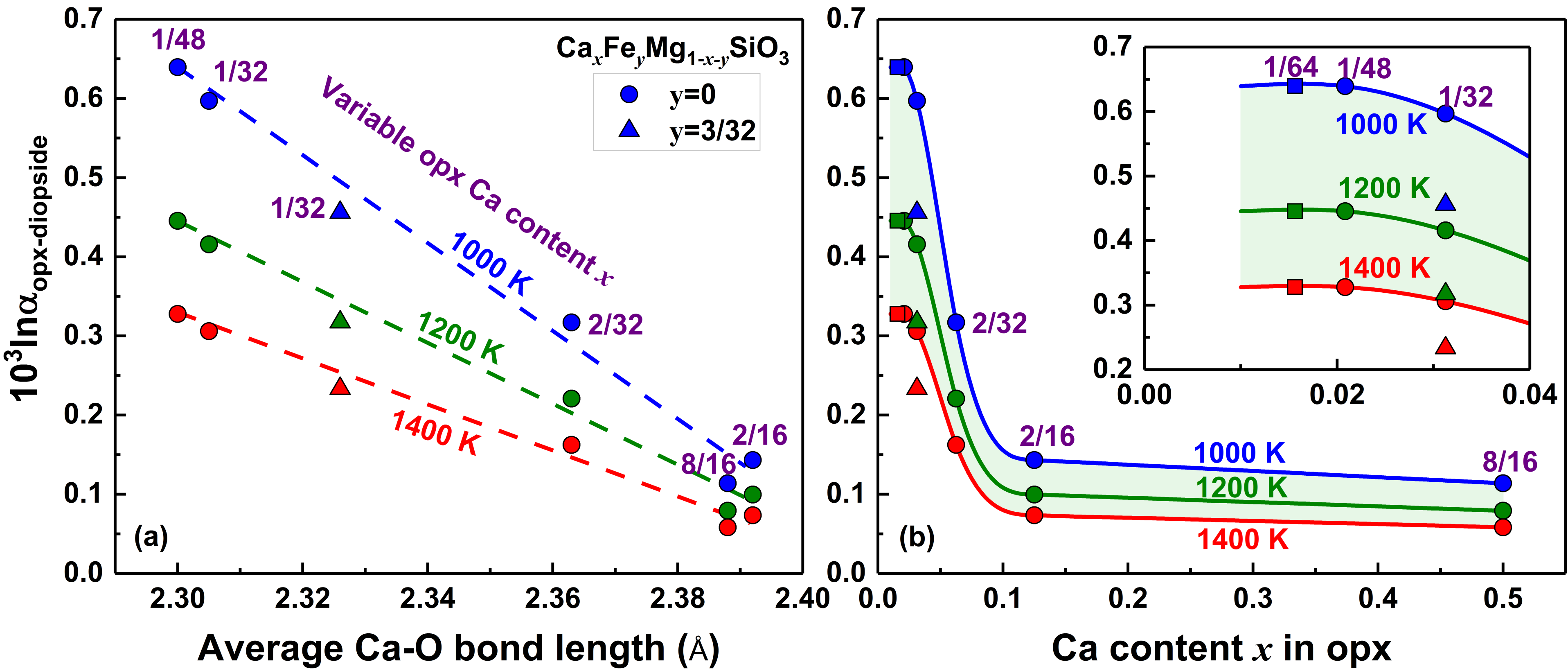

Opx Ca-O bond length determines equilibrium Ca isotope fractionation between opx and cpx

Wang et al. (2017)

Concentration effect - cpx

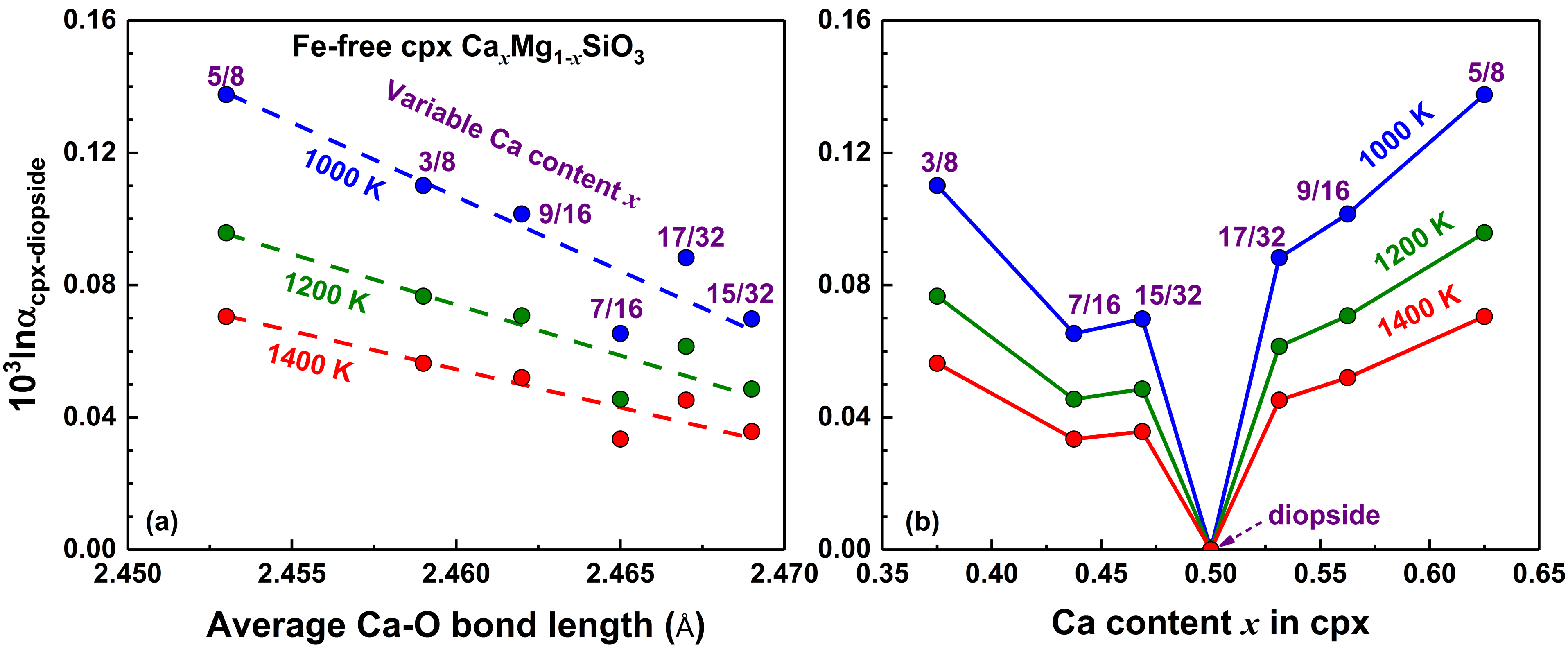

The effect of cpx Ca content is negligible

Wang et al. (2017)

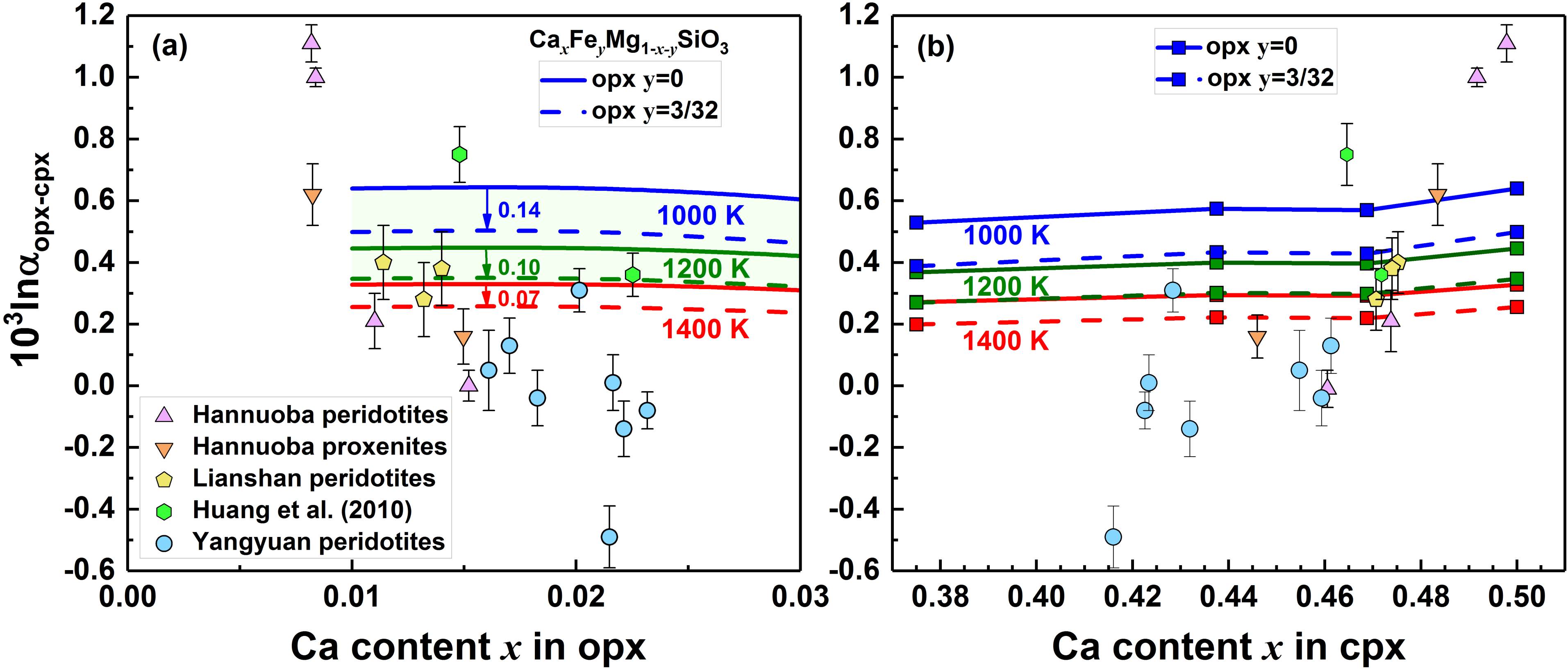

Wang et al. (2017)

Concentration effect - carbonates

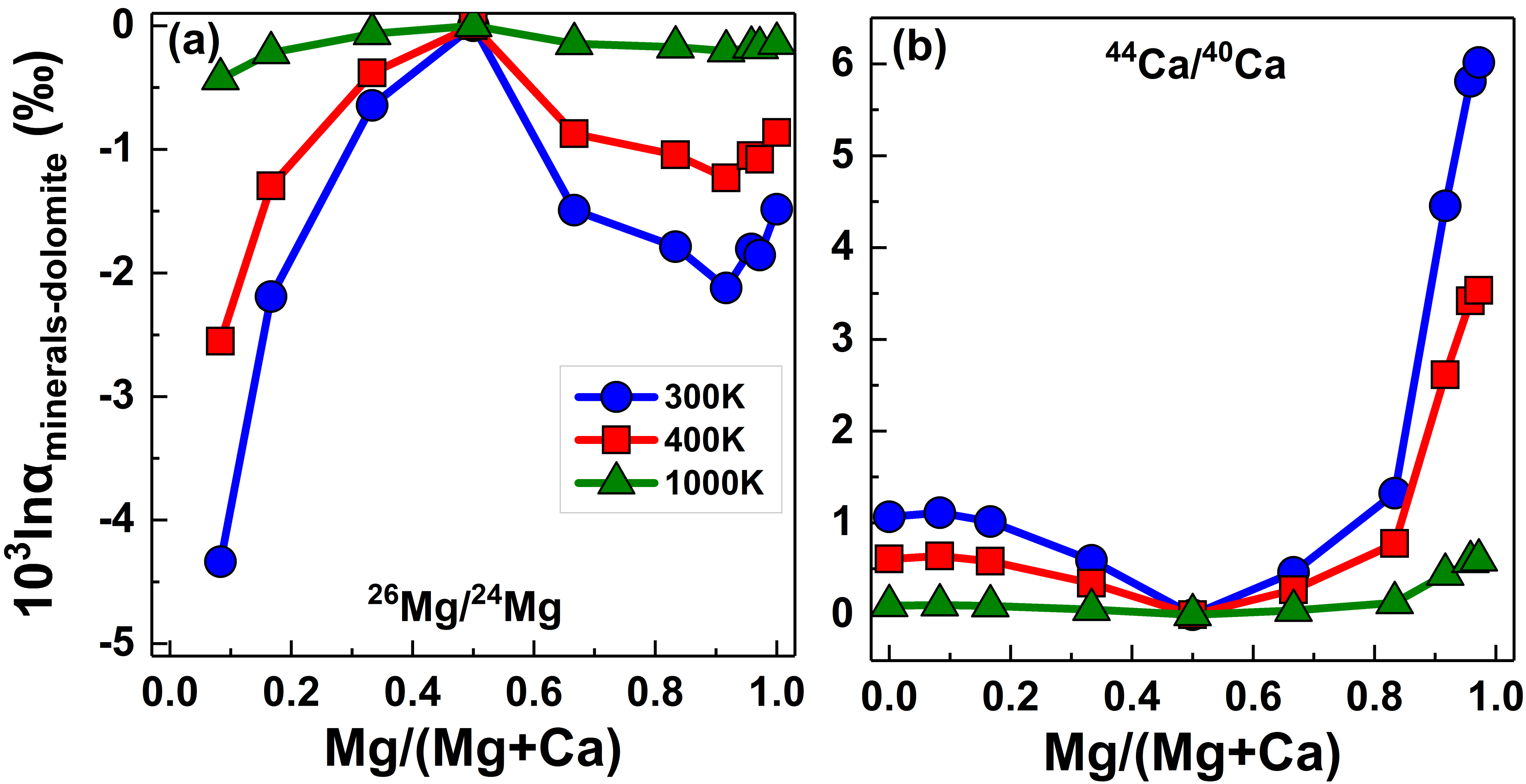

Wang et al. (2017)

Concentration effect - carbonates

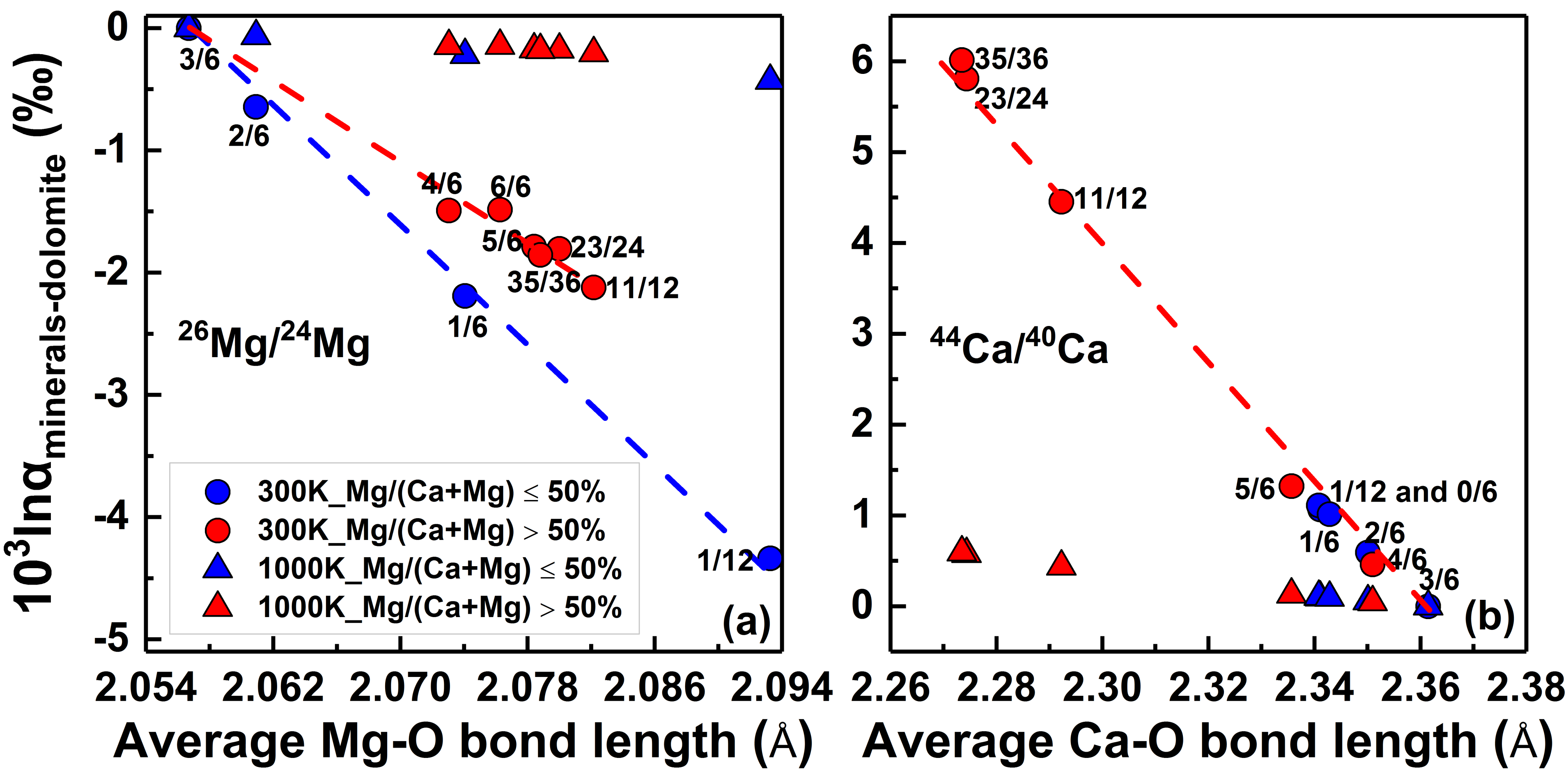

Wang et al. (2017)

Concentration effect - feldspars

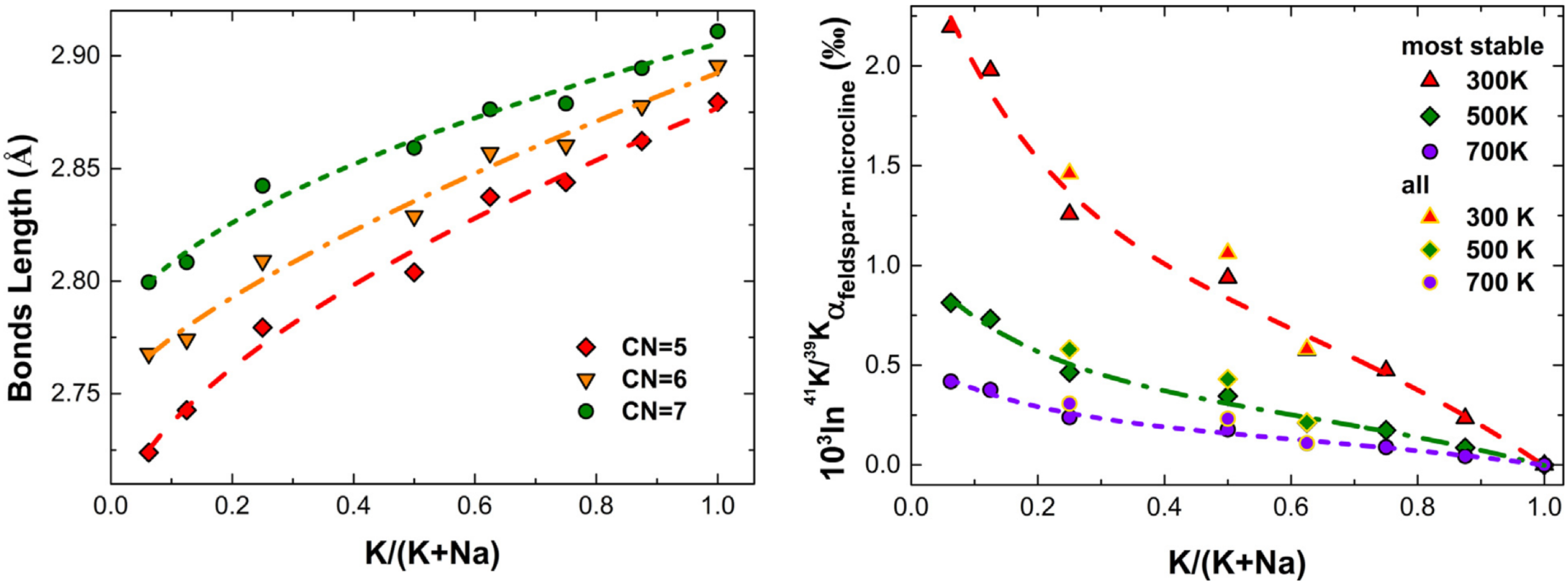

Equilibrium isotope fractionation factors are dominantly controlled by the relative bond lengths

Shorter bonds are stronger with higher vibrational frequencies and enriched in heavy isotopes

Li et al. (2019)

Isotope systems of minor elements

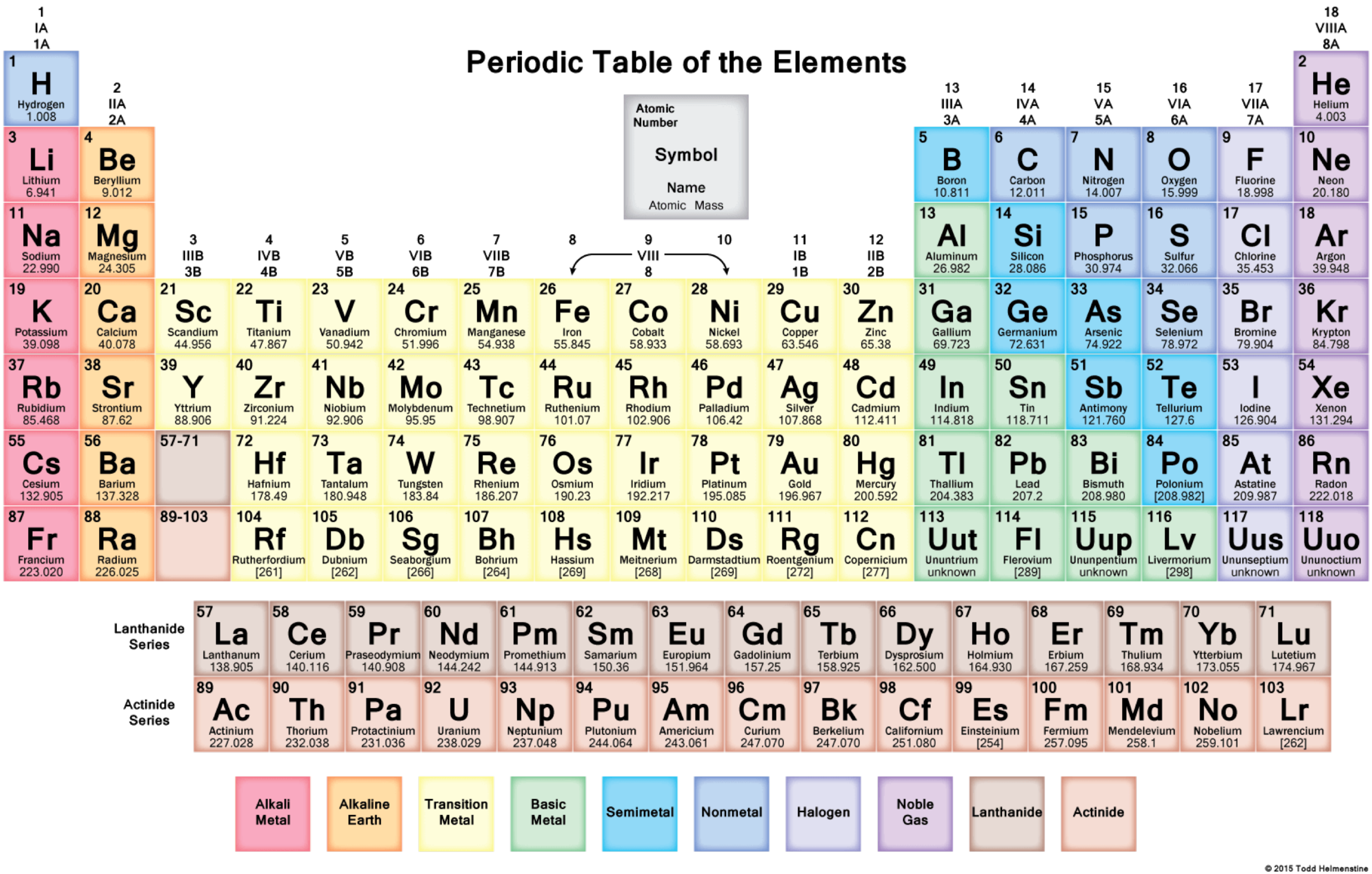

Ti isotope compositions of Basalts

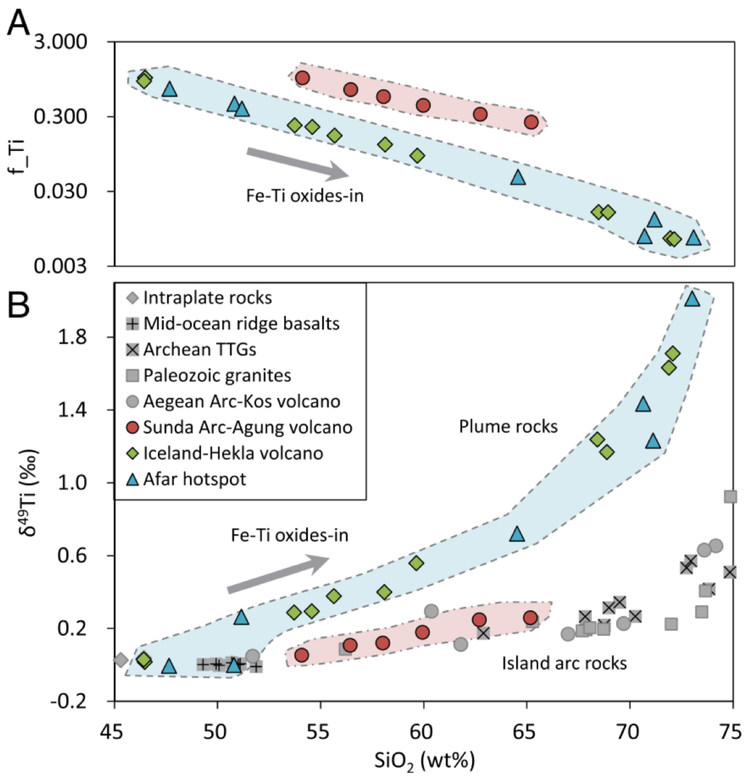

Deng et al. (2019)

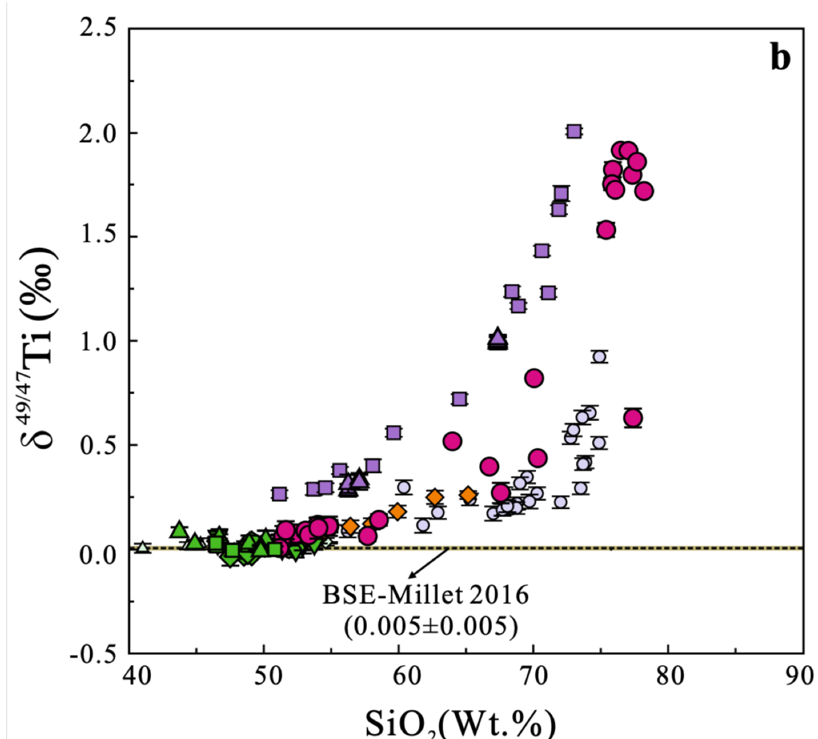

Zhao et al. (2020)

Large Ti isotopic variations have been observed in basaltic rocks

Role of Fe-Ti oxides

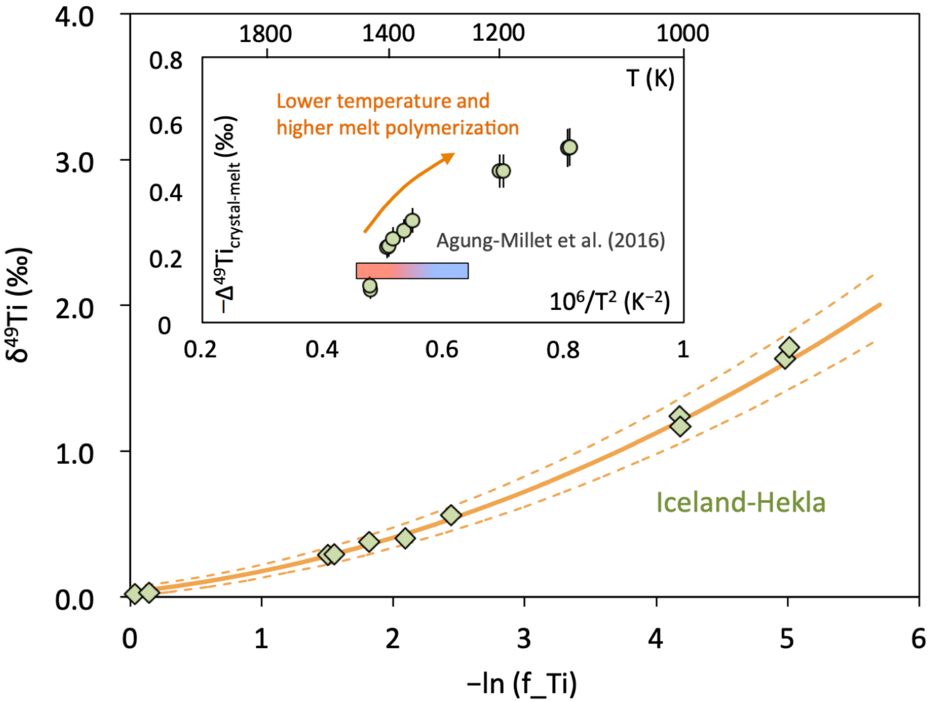

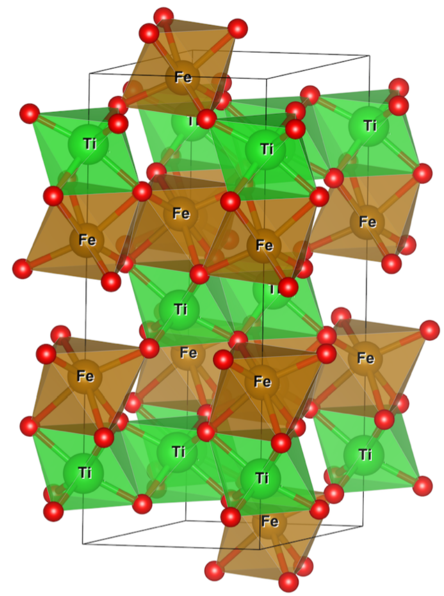

ilmenite

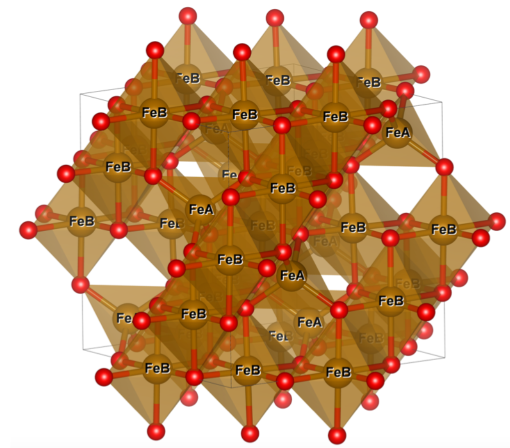

magnetite

Fe-Ti oxides were suggested to be enriched in light Ti isotopes relative to the melt during the magma differentiation

Deng et al. (2019)

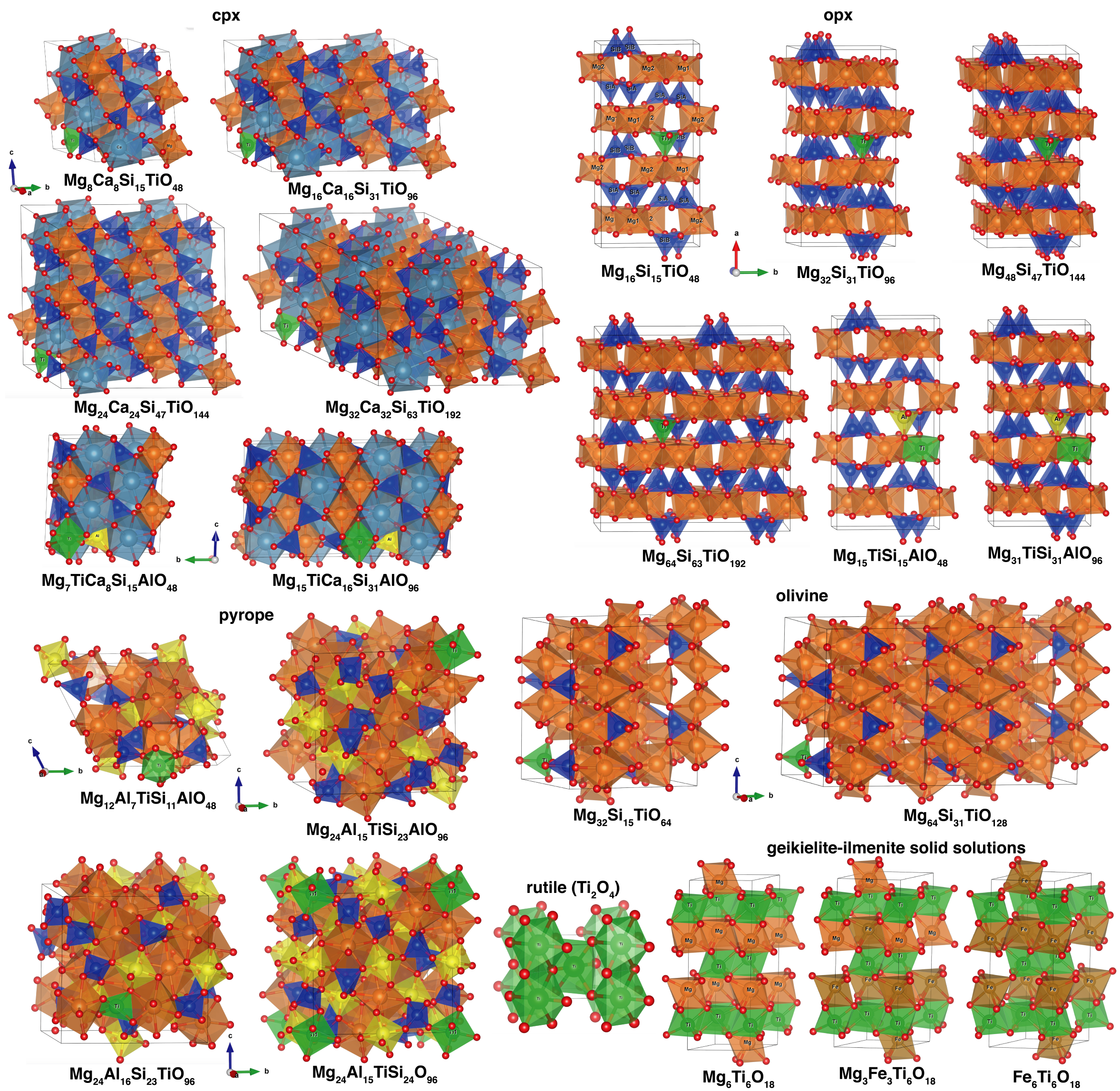

clinopyroxene

$Si^{4+} \leftrightarrow Ti^{4+}$

$Mg^{2+} + Si^{4+} \leftrightarrow Ti^{3+} + Al^{3+}$

orthopyroxene

$Si^{4+} \leftrightarrow Ti^{4+}$

$Mg^{2+} + Si^{4+} \leftrightarrow Ti^{3+} + Al^{3+}$

olivine

$Si^{4+} \leftrightarrow Ti^{4+}$

pyrope

$Al^{3+} + Si^{4+} \leftrightarrow Ti^{4+} + Al^{3+}$

$Si^{4+} \leftrightarrow Ti^{4+}$

$Al^{3+} \leftrightarrow Ti^{3+}$

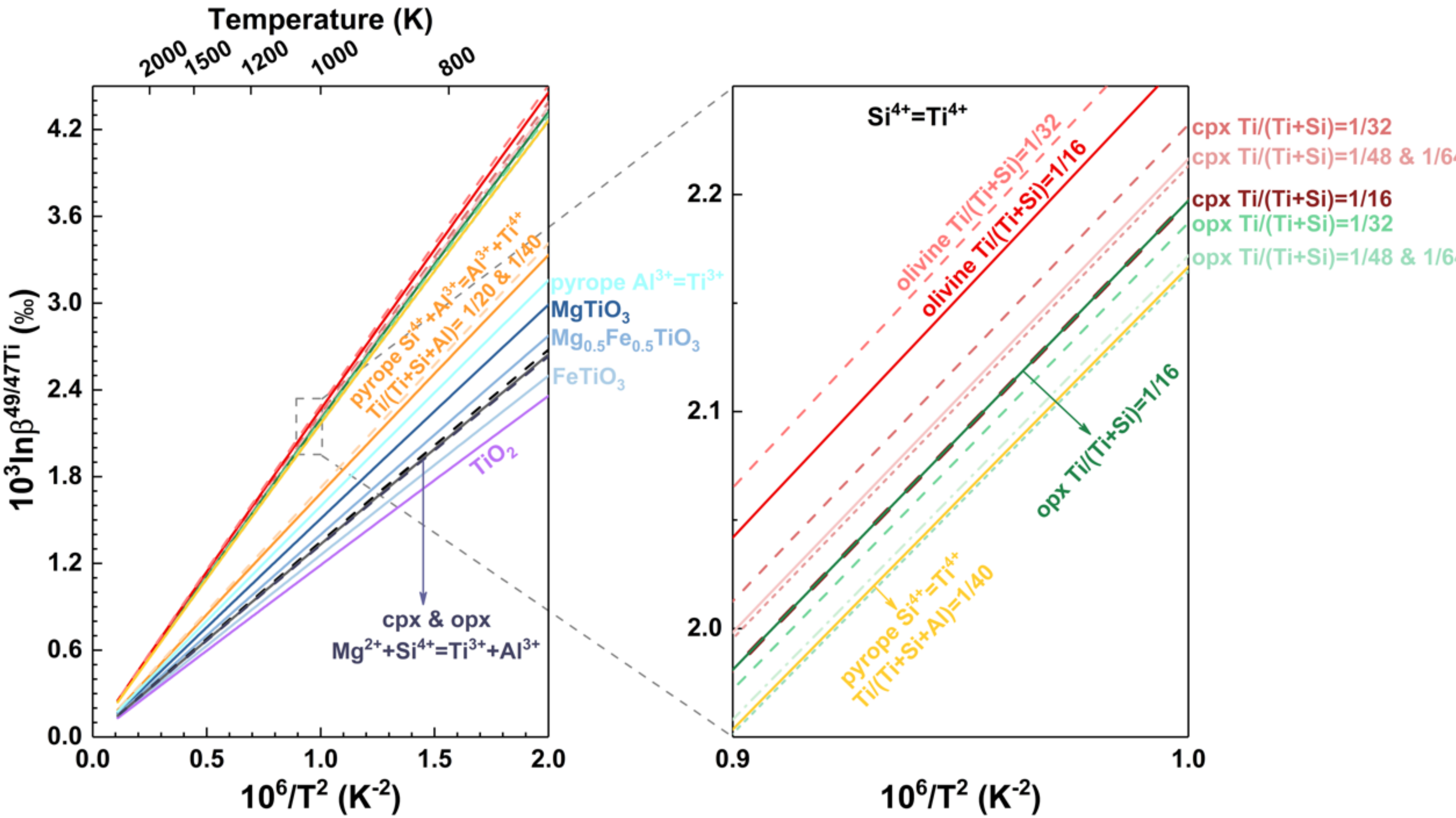

$Ti^{4+}{}_{Si}$-doped olivine, cpx, opx, and pyrope > $Ti^{4+}{}_{Al}$-doped pyrope > $Ti^{3+}{}_{Al}$-doped pyrope > geikielite ($MgTiO_3$) > $Mg_{0.5}Fe_{0.5}TiO_3$ > $Ti^{3+}{}_{Mg}$-doped cpx and opx > ilmenite ($FeTiO_3$) > rutile

Equilibrium Ti isotope fractionation

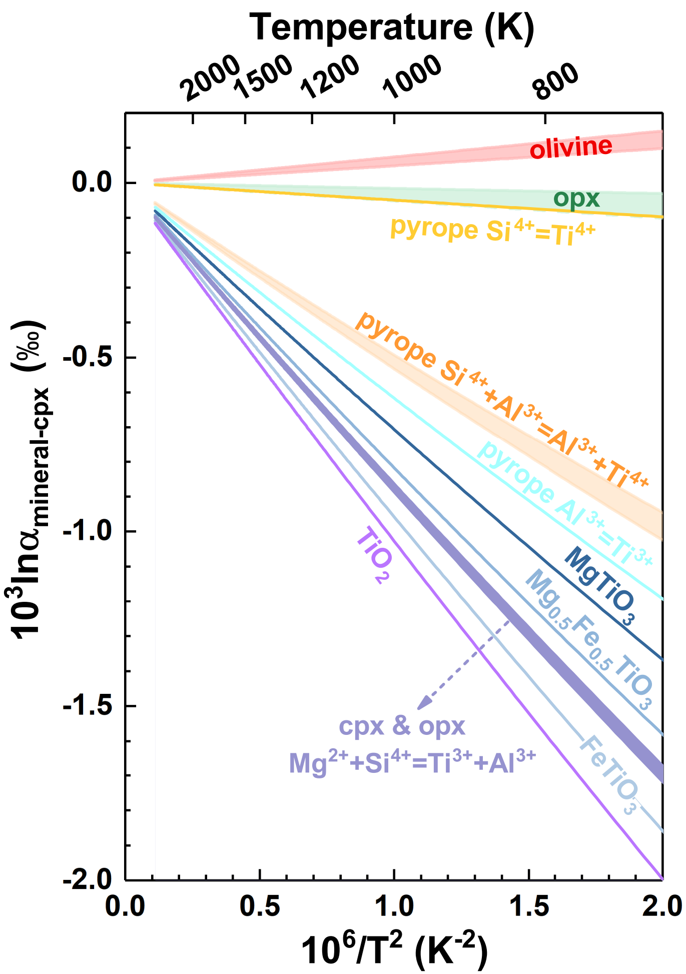

- There is **no significant Ti isotope fractionation** among $Ti^{4+}{}_{Si}$-doped cpx, opx, olivine, and pyrope
- **$Ti^{3+}{}_{Mg}$-doped** cpx and opx are extremely enriched in **light Ti isotopes** relative to those $Ti^{4+}{}_{Si}$-doped species
- The enrichment of light Ti isotopes in ilmenite relative to $Ti^{4+}{}_{Si}$-doped silicate minerals with **$10^3\ln\alpha_{FeTiO3\text{-}clinopyroxene}$** of $^{49}Ti/^{47}Ti$ is up **to -0.67‰ at 1200 K**
- The **$10^3\ln\alpha$** between ilmenite and silicates strongly **depends on the Fe/(Mg+Fe) of ilmenite**

Wang et al. (2020)

$10^3 ln\beta$ VS. bond length & CN

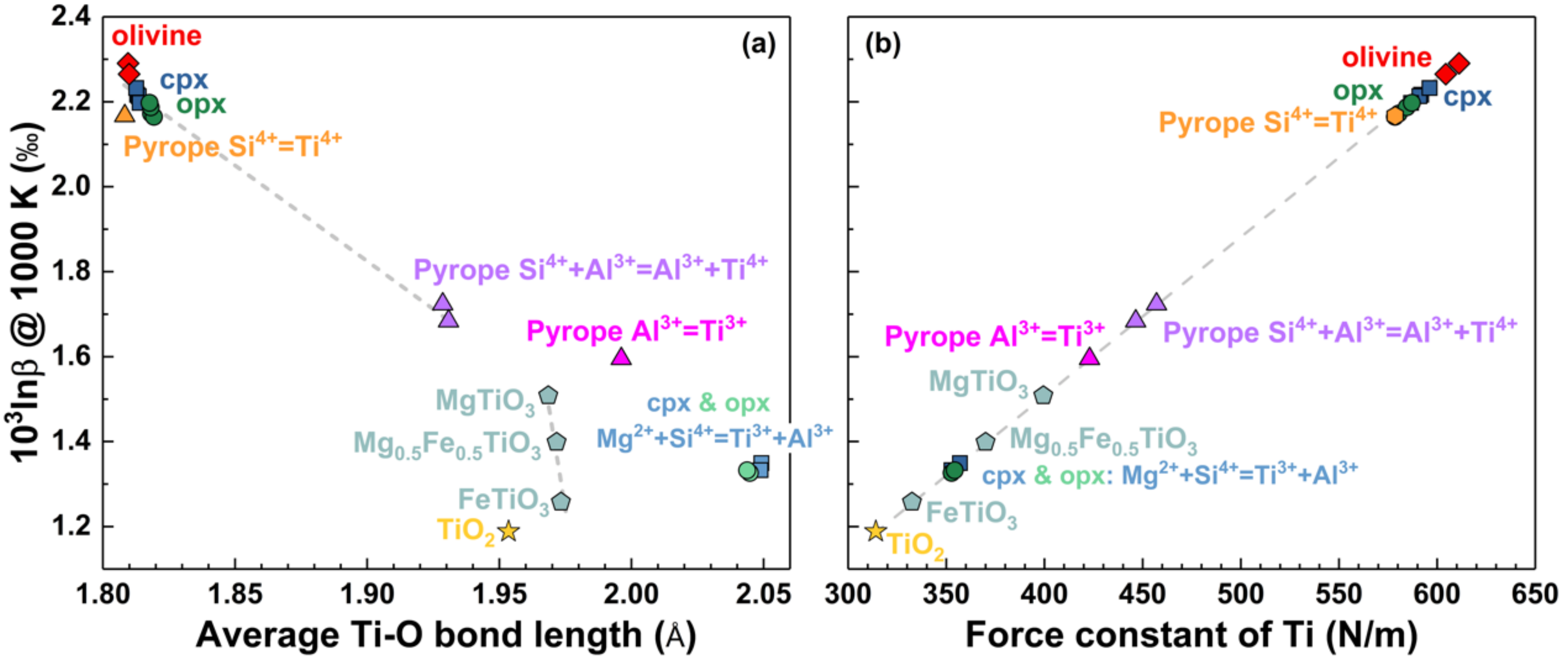

Wang et al. (2020)

$10^3 ln\beta$ VS. bond length & CN

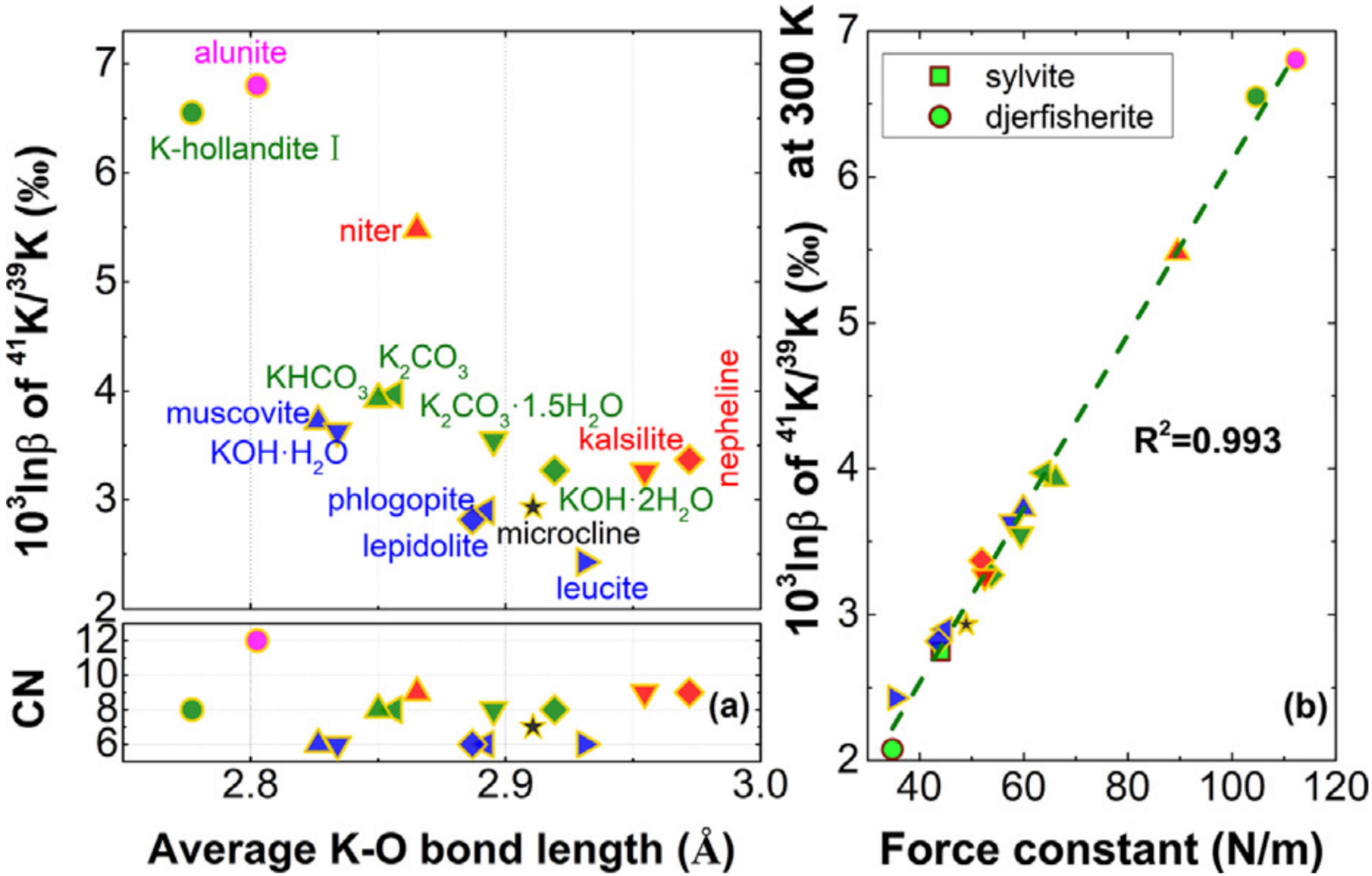

Li et al. (2019)

$10^3ln\beta$ VS. bond length & CN

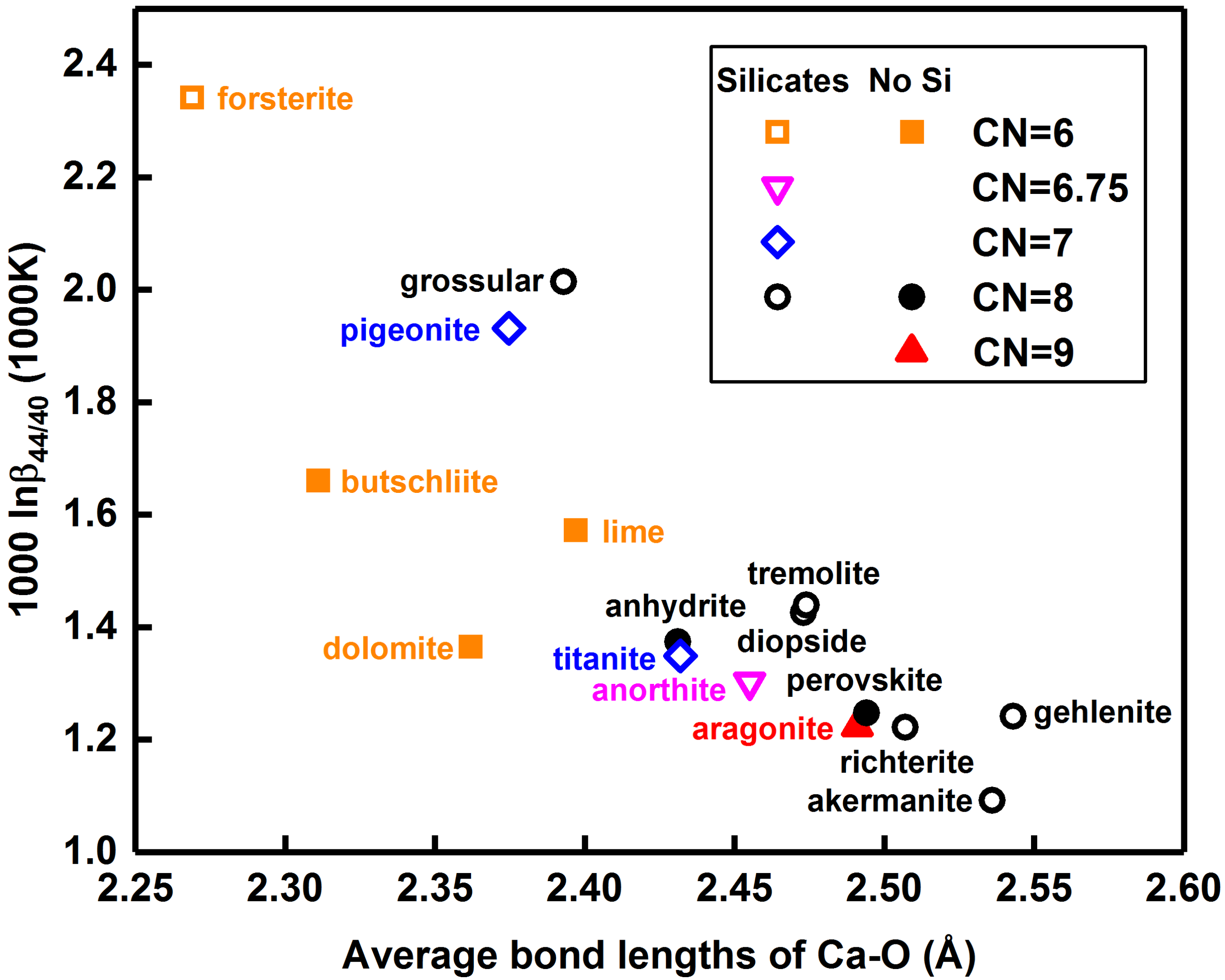

Summary

Pressure

Bond length, CN, oxidation state, and electronic configuration...

Temperature

Bond strength ≃ Force constant

$$\beta \simeq 1 + \sum_{i=1}^{N_{dof}} \frac{u_i^2 - u_i^{*2}}{24} = 1 + \frac{\Delta m}{mm^*} \frac{\hbar^2}{24k_B^2T^2} \sum_{i=1}^{3} A_i$$

lnbeta or lnalpha

Empirical formula

$$K = \frac{Z_A Z_B e^2 (1-n)}{4\pi\varepsilon_0 r_{A-B}^3}$$

Fe in Bridgmanite

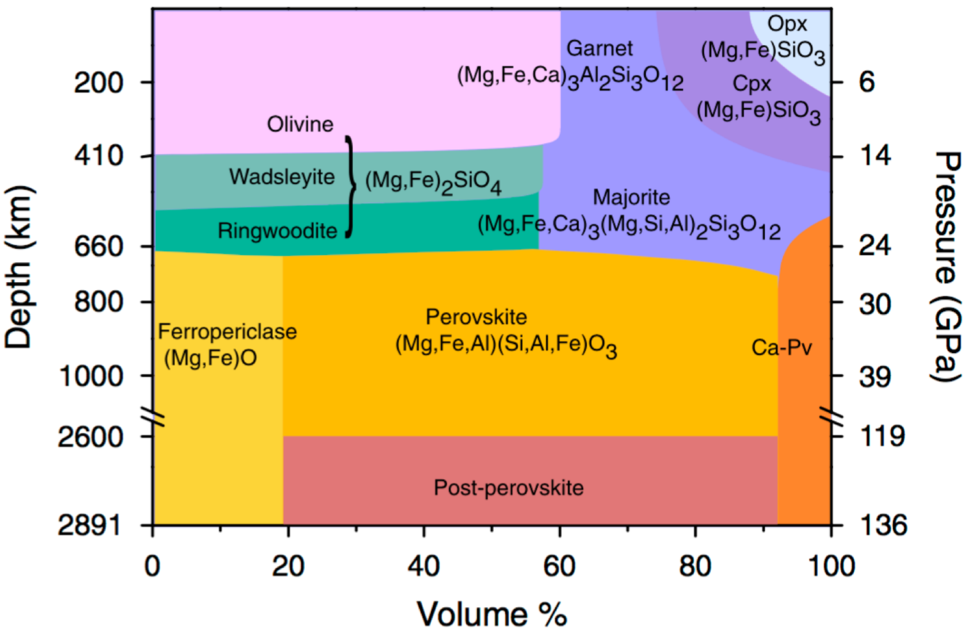

$$Mg^{2+} \leftrightarrow Fe^{2+}$$
$$Mg^{2+} + Si^{4+} \leftrightarrow Fe^{3+} + Fe^{3+}$$
$$Mg^{2+} + Si^{4+} \leftrightarrow Fe^{3+} + Al^{3+}$$

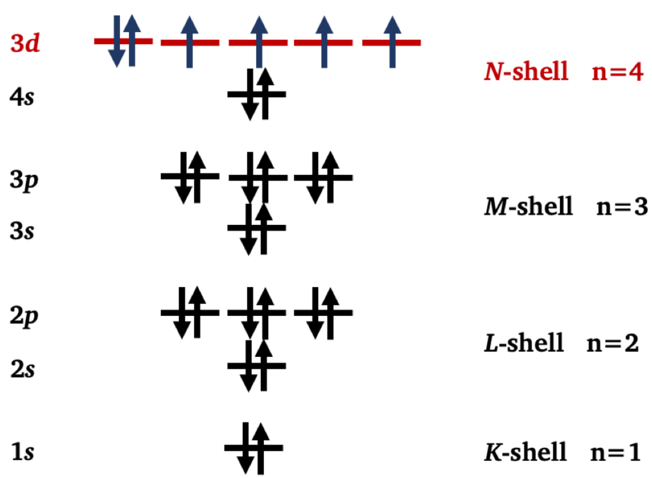

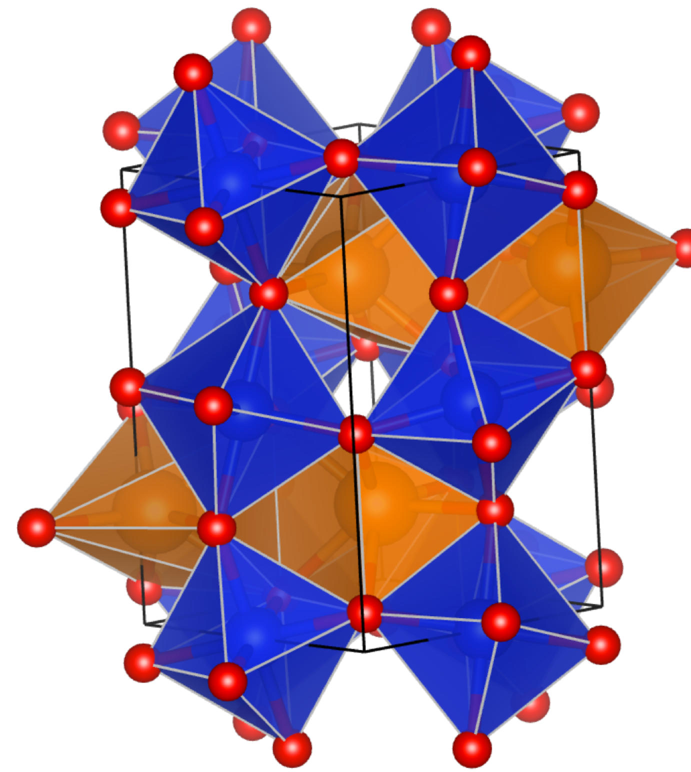

Spin transition

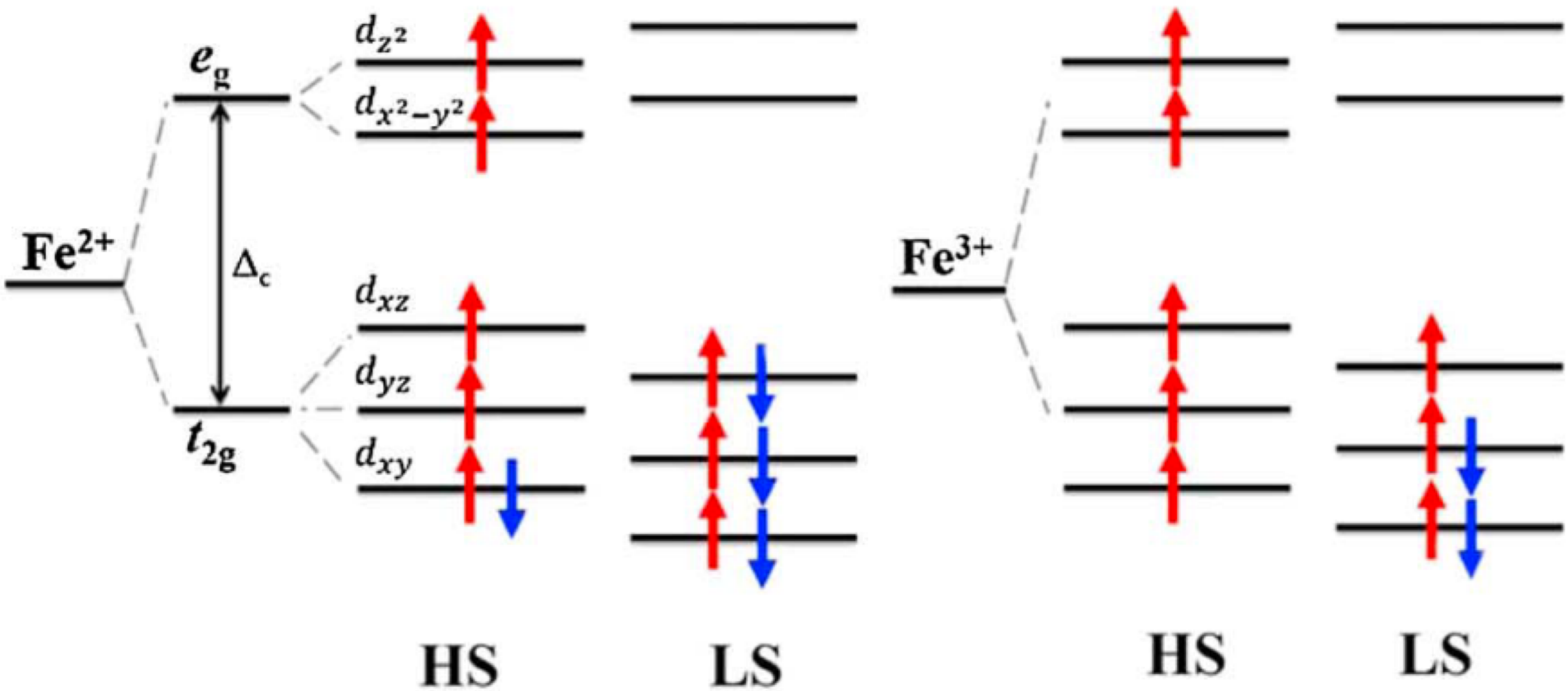

DFT+U: describe coulomb interactions among Fe 3*d* electron

Spin transition

Fe^{2+} in $FeCO_3$

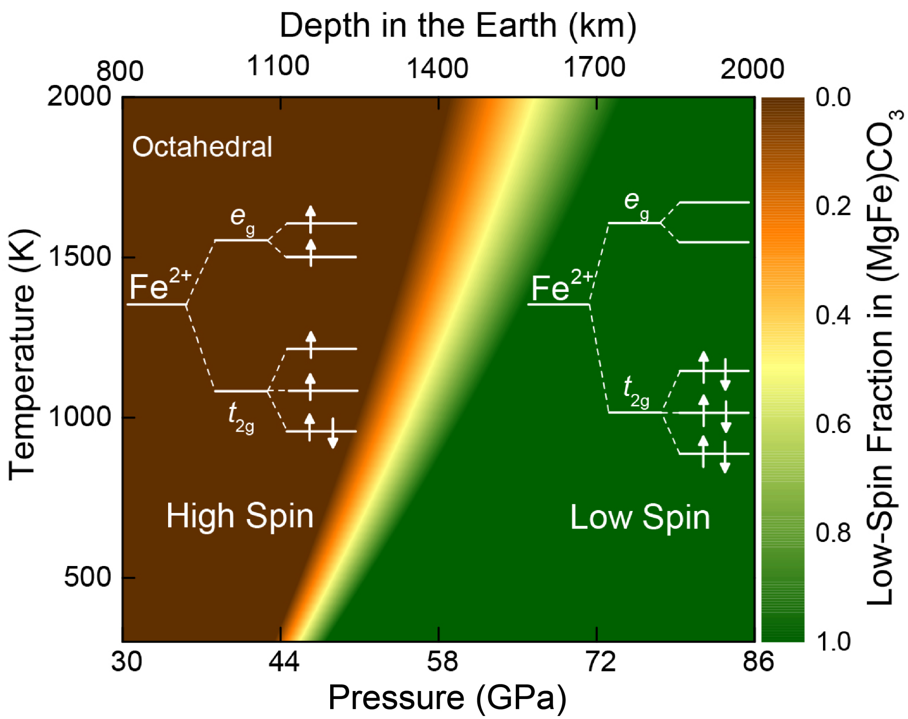

Liu et al. (2014)

Fe^{3+} in B site bridgmanite

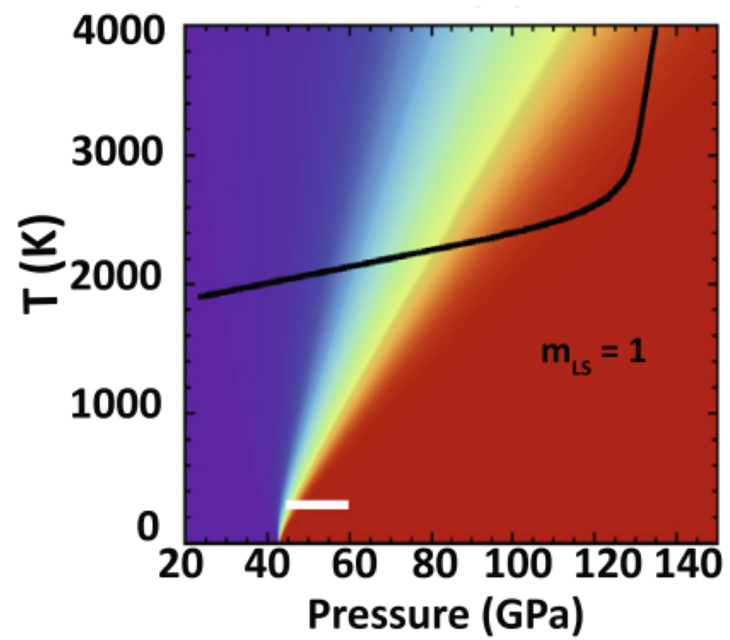

Shukla and Wentzcovitch (2016)

Experimental and Theoretical Methods

Nuclear resonant inelastic X-ray scattering spectroscopy (NRIXS)

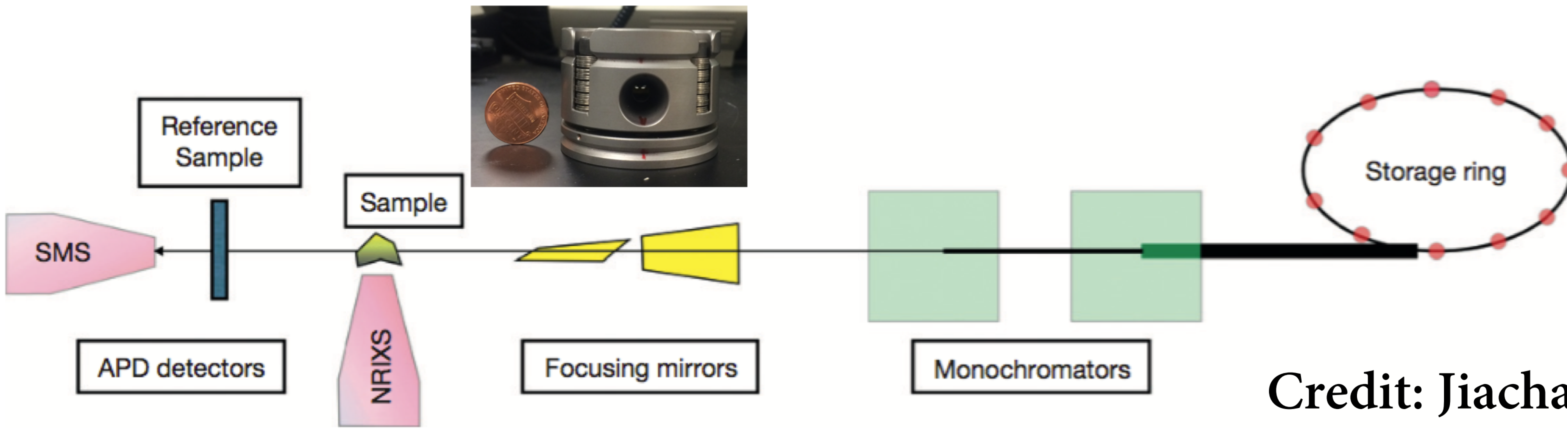

Credit: Jiachao Liu et al.

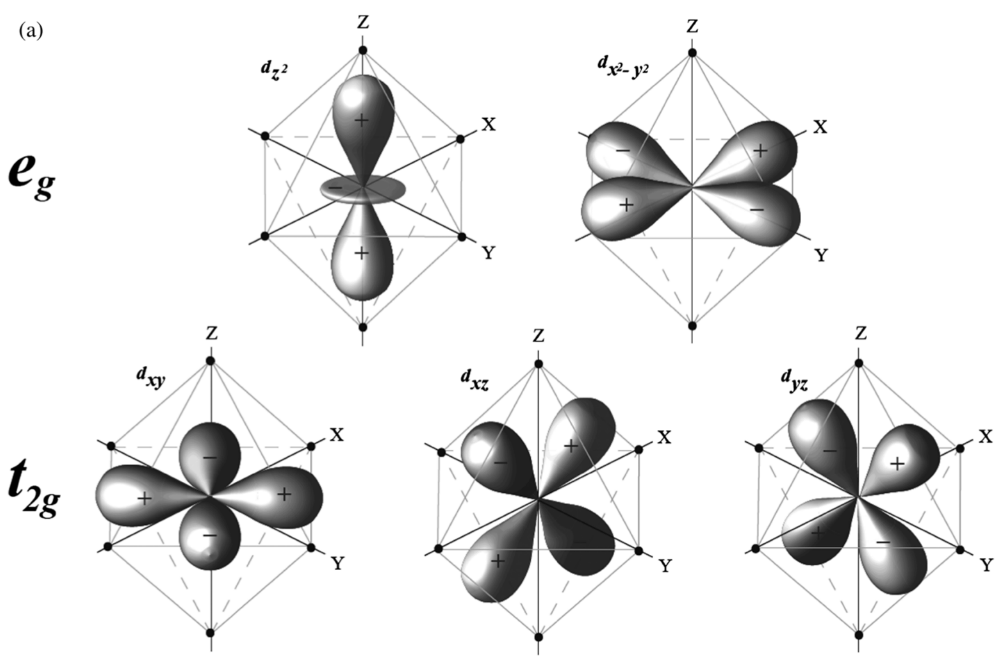

DFT+U: describe coulomb interactions among Fe 3*d* electron

Phonon Density of State of ^{57}Fe in $FeCO_3$

NRIXS results

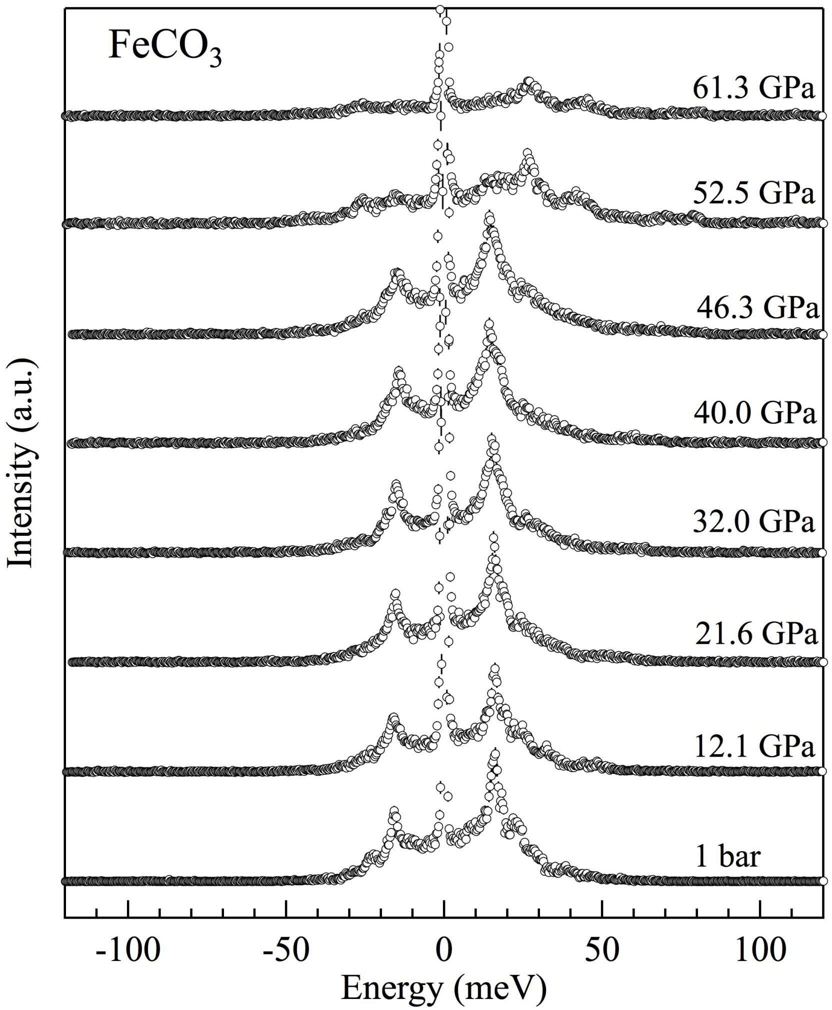

Experimental and theoretical results of PDoS of Fe are consistent

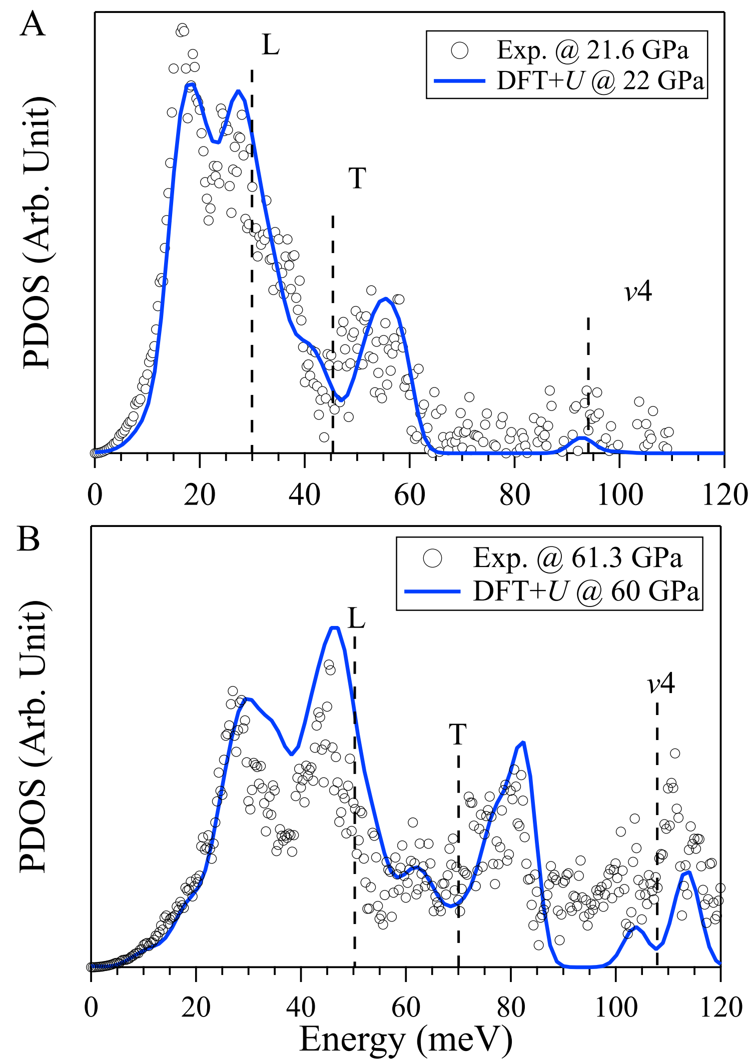

$(Mg_{0.75}Fe^{2+}_{0.25})SiO_3$ Bridgmanite

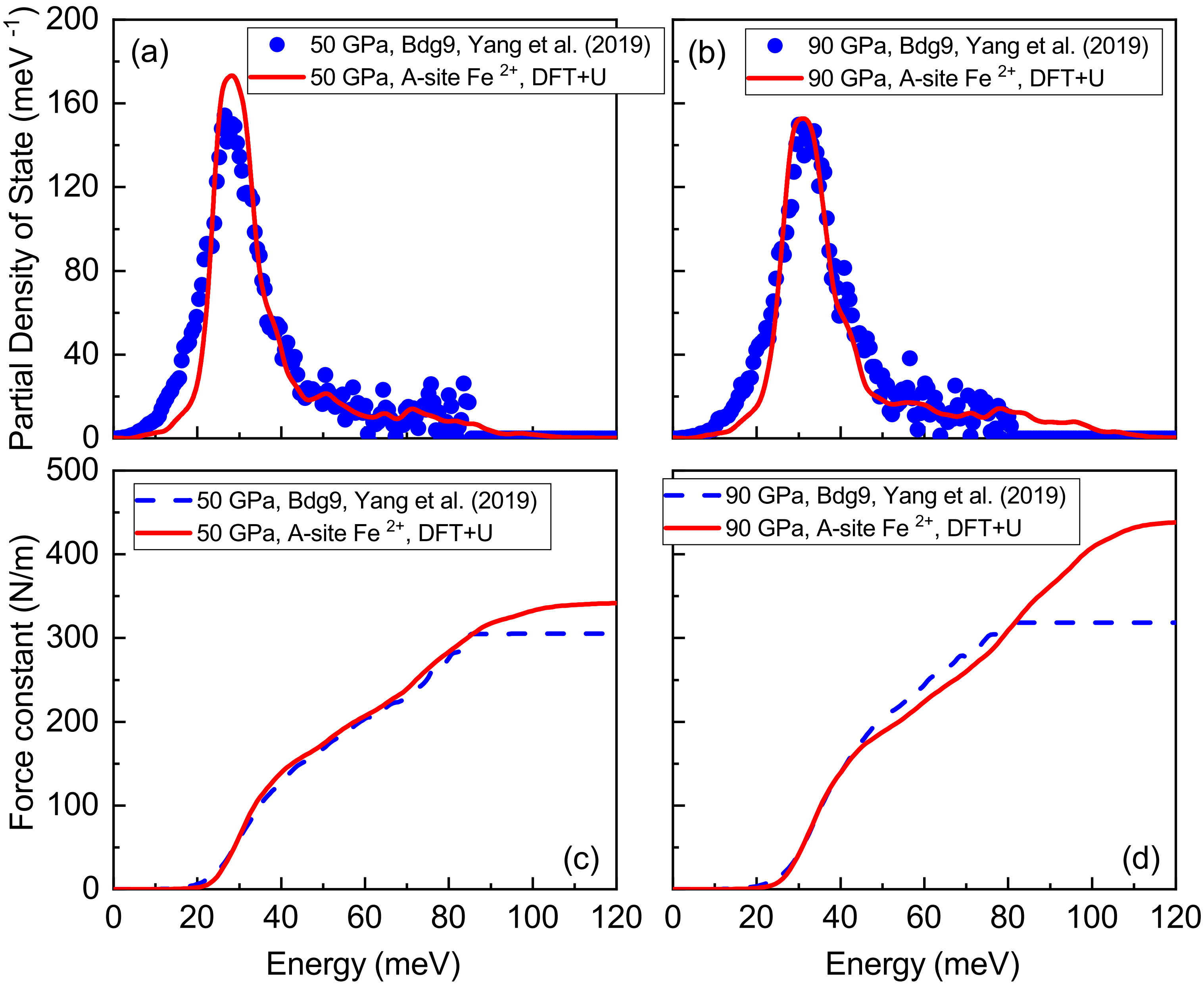

$(Mg_{0.75}Fe^{3+}{}_{0.25})(Si_{0.75}Al_{0.25})O_3$ Bridgmanite

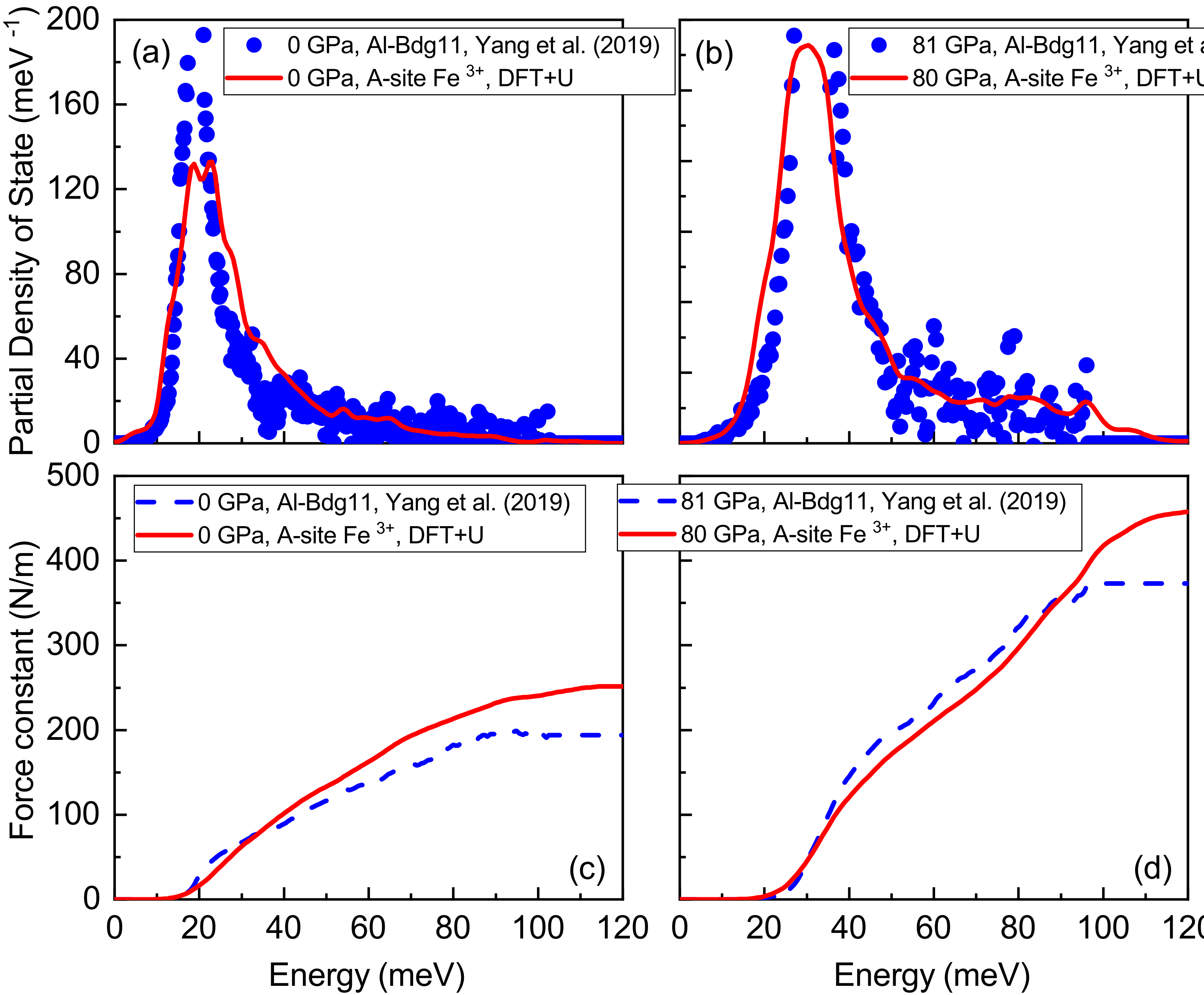

$(Mg_{0.5}Fe^{3+}{}_{0.5})(Si_{0.5}Fe^{3+}{}_{0.5})O_3$ Bridgmanite

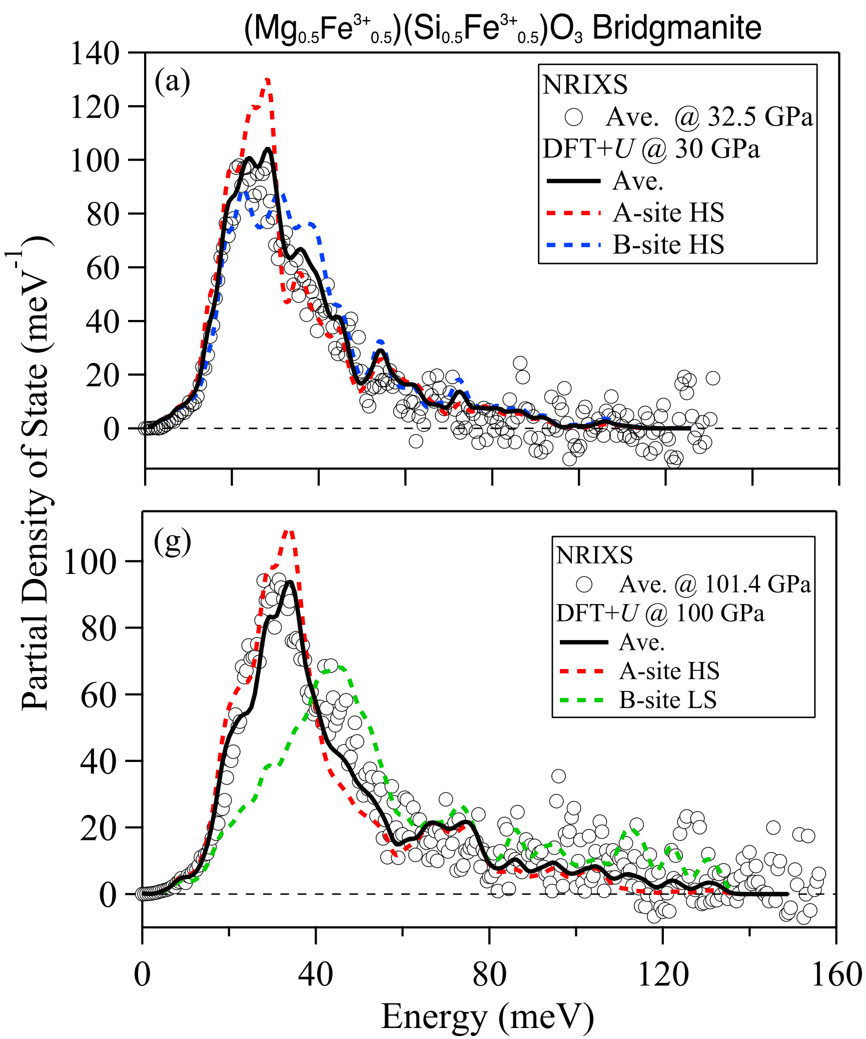

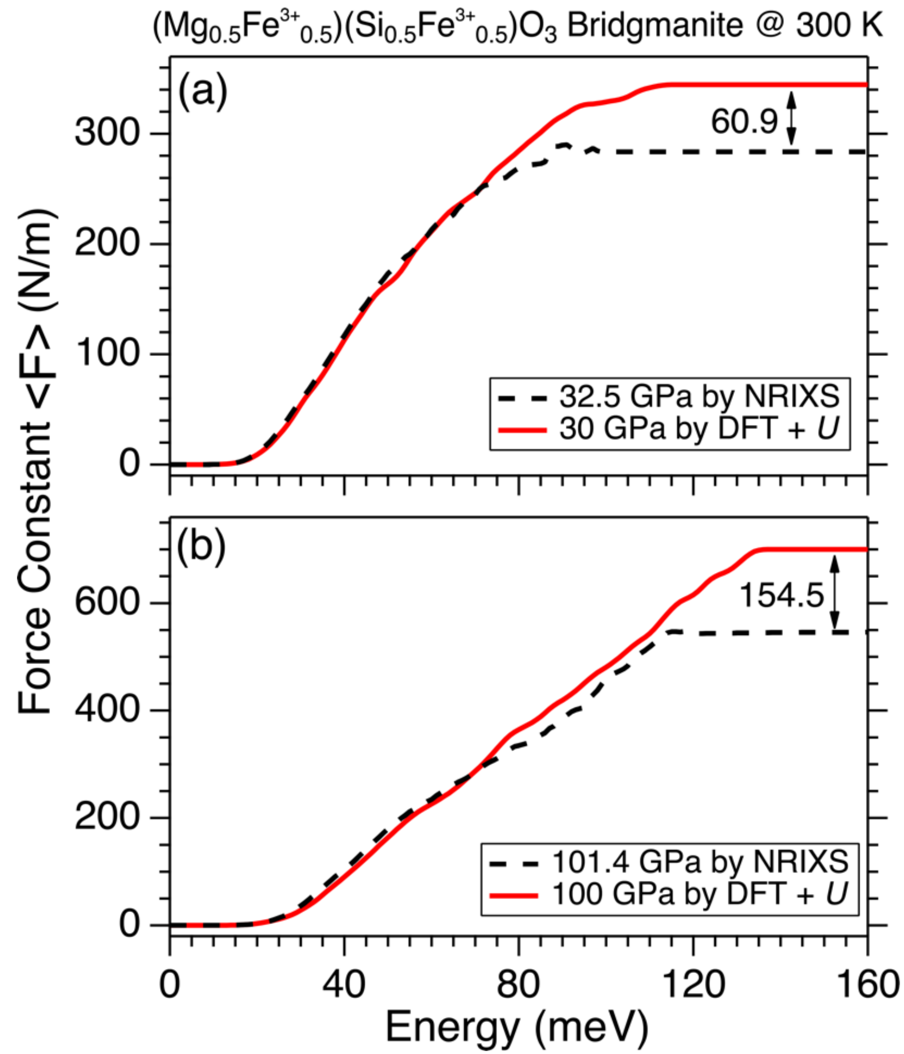

lnbeta of Fe in bridgmanite

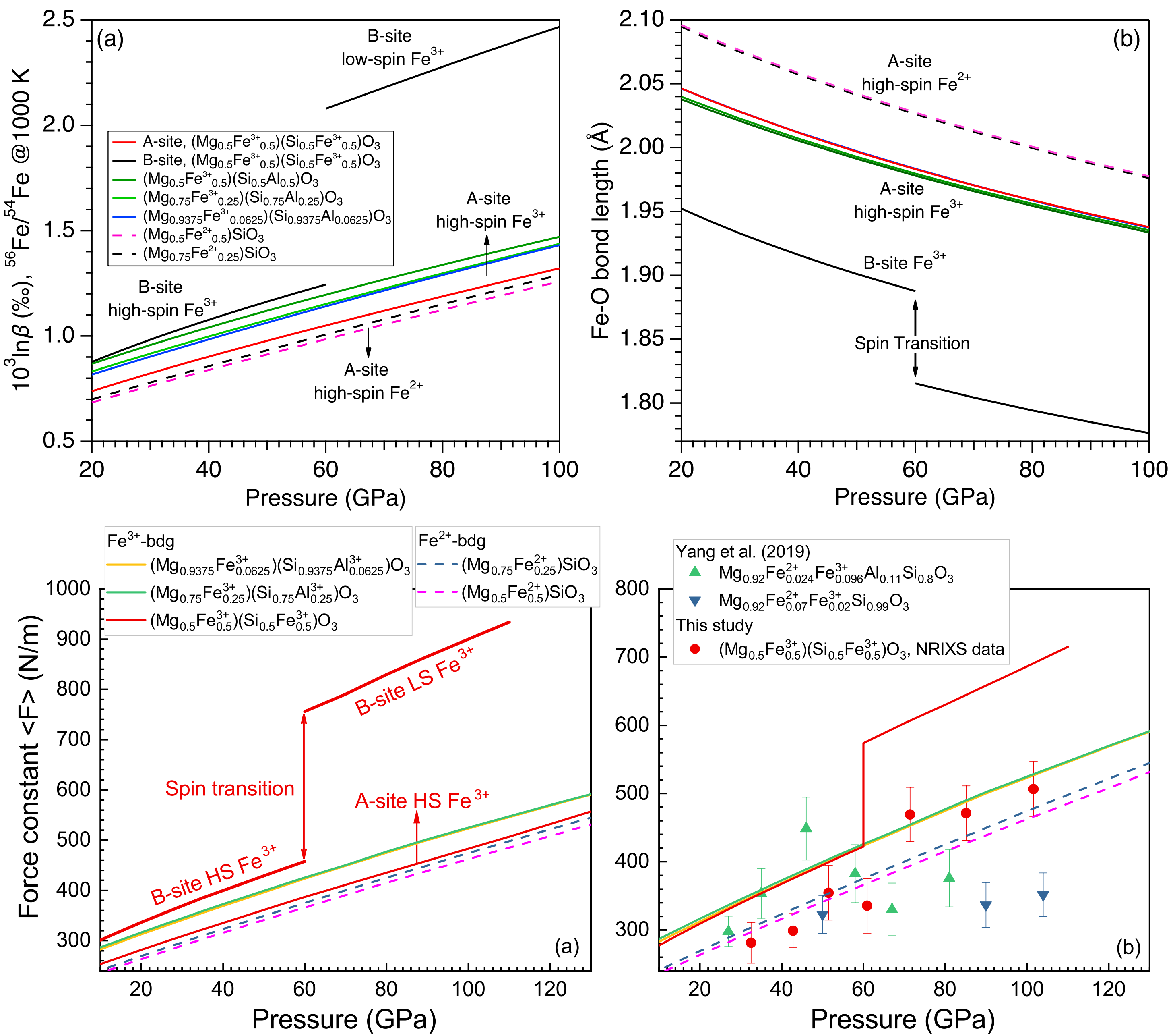

Magma ocean crystallization

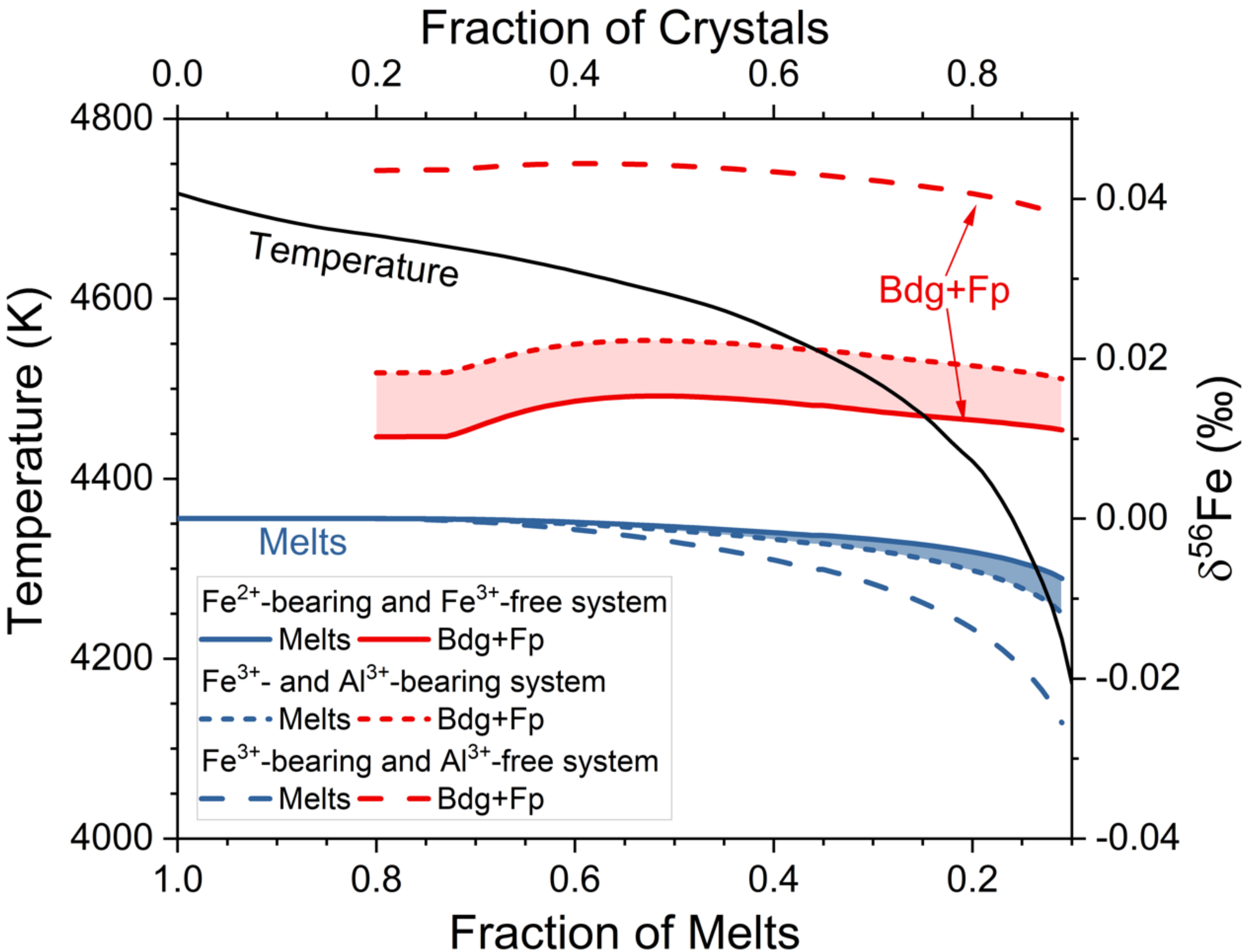

Fe isotope fractionation in the deep mantle

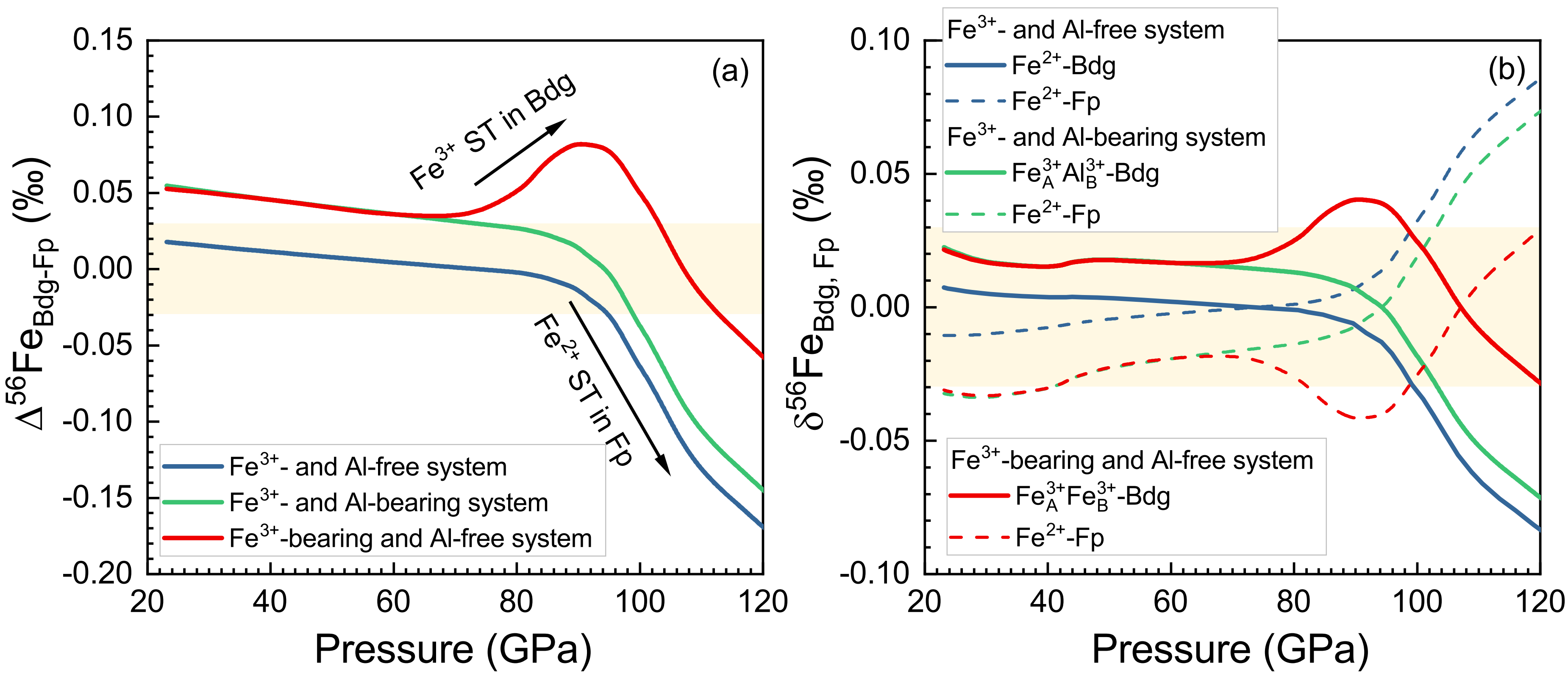

Fe isotope fractionation in the deep mantle

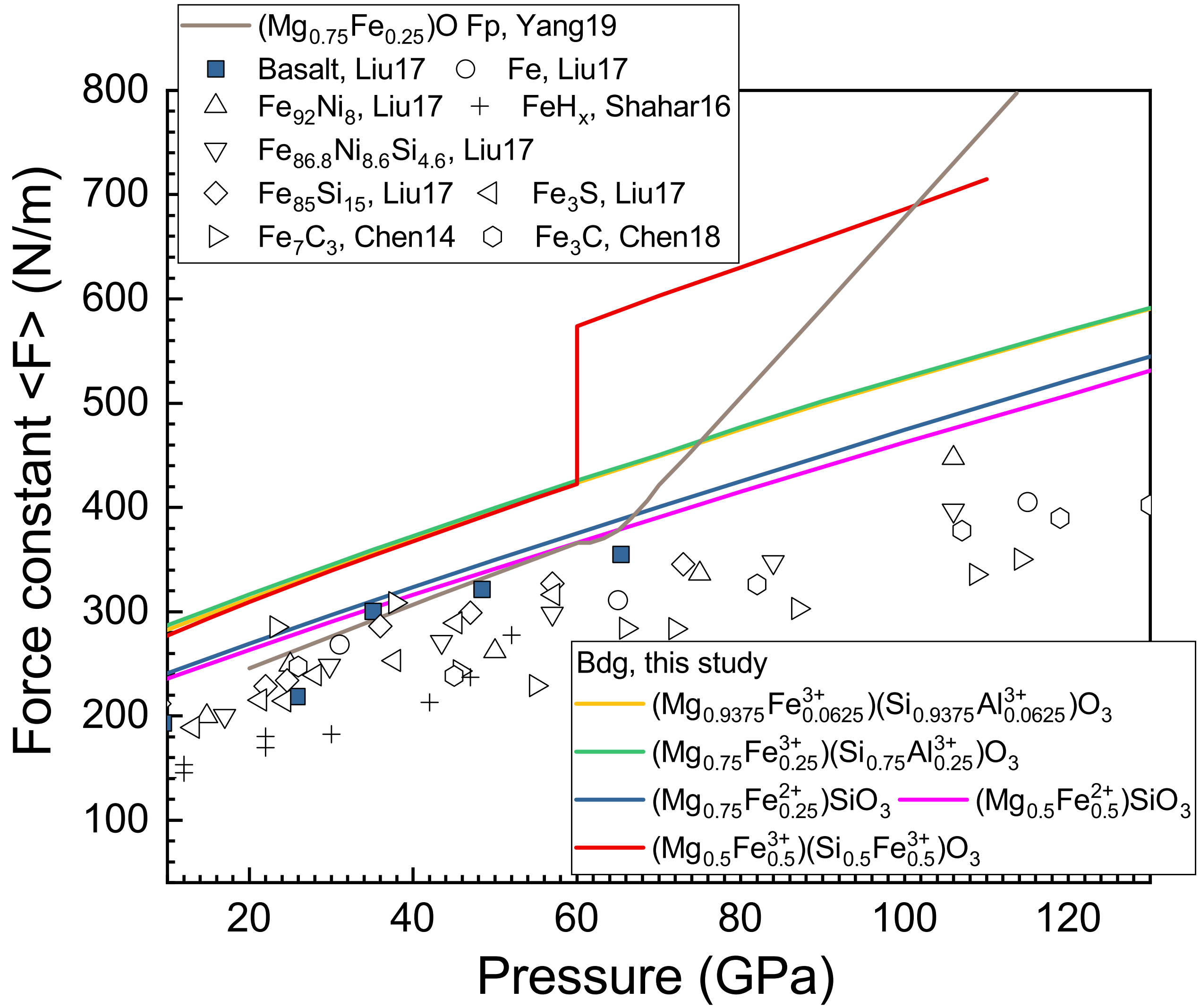

Part 3. EIFFs for aqueous solutions

Mg, Ba, Zn, Li, B, …

$$AX + X^* \rightleftharpoons AX^* + X$$

K=[AX*][X]/[AX][X*]=exp(-ΔG*/RT)

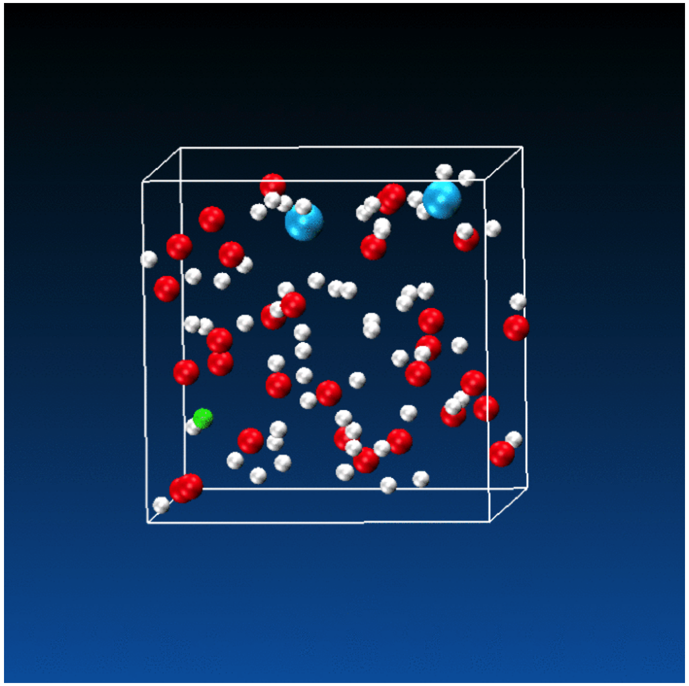

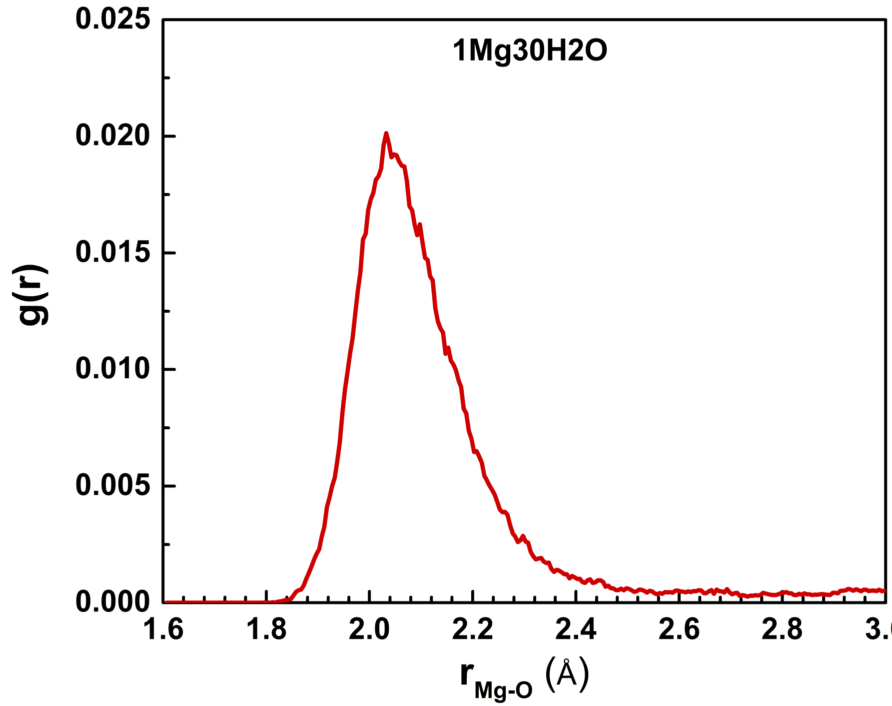

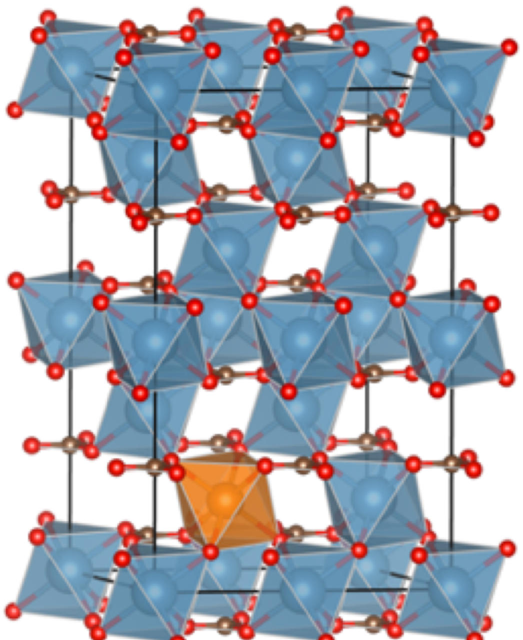

2.1425
2.1659
2.1482
2.1425
2.1659
2.1482

Statistical thermodynamics

Mechanical Properties of Individual Molecules → (average over molecules) 2 → (average over time) 3 → (statistical thermodynamics) 4 → Thermodynamic Properties

position, velocity energy, ...

temperature, pressure internal energy, enthalpy,...

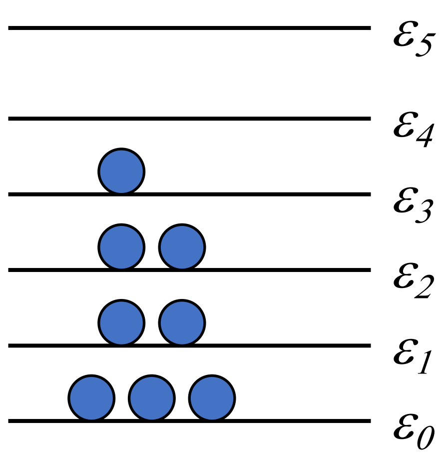

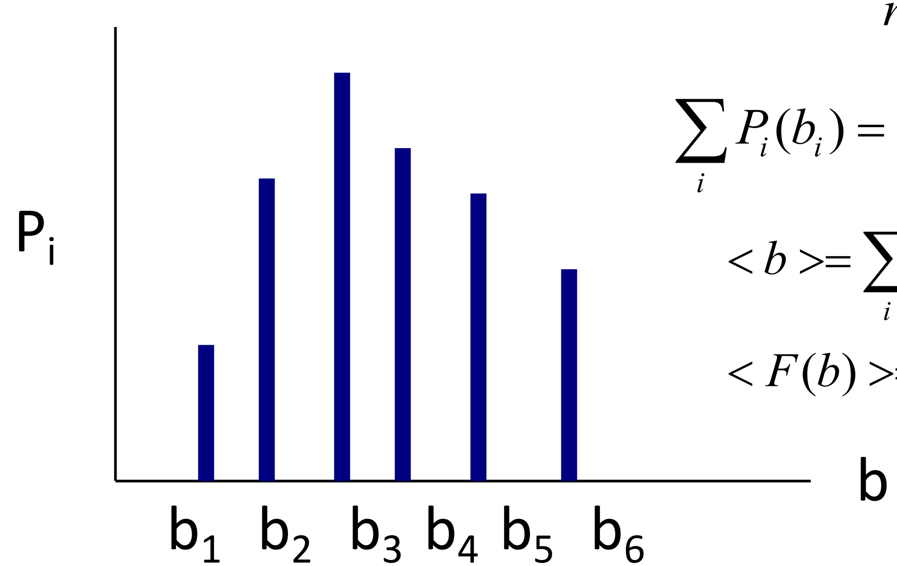

$$P_i(b_i) = \frac{n_i(b_i)}{n} = \frac{n_i(b_i)}{\sum_i n_i(b_i)}$$

$$\sum_i P_i(b_i) = 1$$

$$< b >= \sum_i b_i P_i$$

$$< F(b) >= \sum_i F(b_i) P_i$$

Thermodynamic integration

$$\ln(\beta(a,Y)) = -\frac{F^* - F}{k_B T} + \left(\frac{F^* - F}{k_B T}\right)_{classic}$$

Free energy of an isotopic species depends on its kinetic energy and mass:

$$\frac{\partial F}{\partial m} = -\frac{\langle K \rangle}{m}$$

The ideal limit the kinetic energy of an atom

$$\langle K \rangle = \frac{3k_B T}{2}$$

$$\ln(\beta(a,Y)) = \frac{1}{k_B T}\int_m^{m^*} dm' \frac{\langle K_a(m') \rangle}{m'} - \frac{3}{2}\ln\left[\frac{m^*}{m}\right]$$

First-principles molecular dynamics simulations (FPMD)

First-principles calculations

1. No empirical parameters
2. High precision
3. PT are parameters
4. Solve quantum equations

Kohn-Sham equation

$$\left(-\frac{\hbar^2}{2m}\nabla^2+\int\frac{n(r)dr'}{|r-r'|}+V_{ext}(r)+V_{xc}(r)\right)\psi_i(r)=\varepsilon_i\psi_i(r)$$

Molecular dynamics

$$\vec{r}(t)=\vec{r}_0+(\vec{v}_0t+\tfrac{1}{2}\vec{a}t^2)$$

$$\vec{a}=\vec{F}/m \qquad \vec{F}=-dU/d\vec{r}$$

$$K=\sum_i^N\tfrac{1}{2}m_iv_i^{\,2}=\tfrac{3}{2}Nk_BT$$

Energy & Force

Solution structures

Quantum mechanics + Statistical mechanics

Path Integral Molecular Dynamics

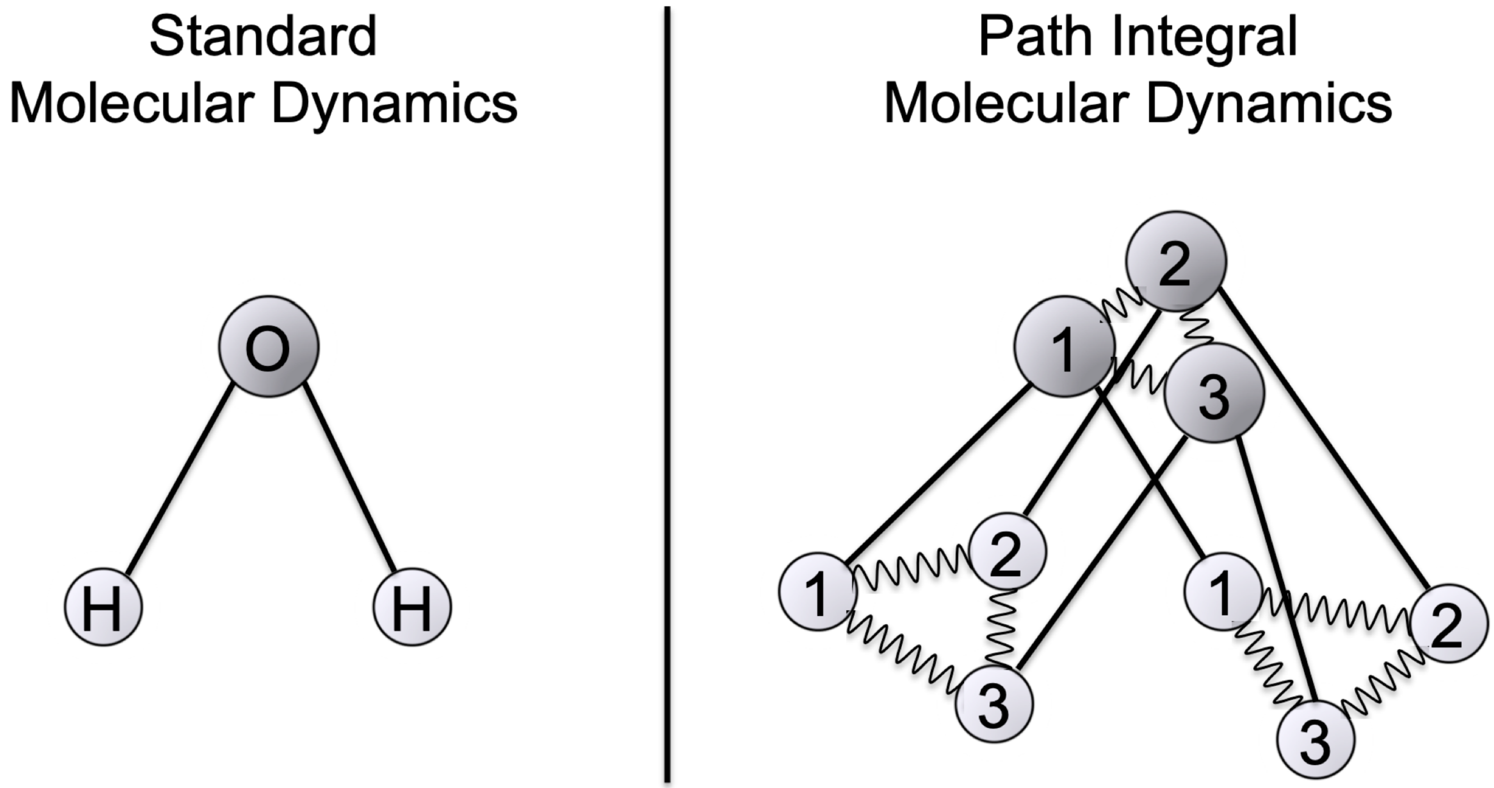

The drawback of PIMD methods is the computational cost that is almost prohibitive for treating at the ab initio level most of the systems relevant in geosciences

Equilibrium fractionation of H and O isotopes

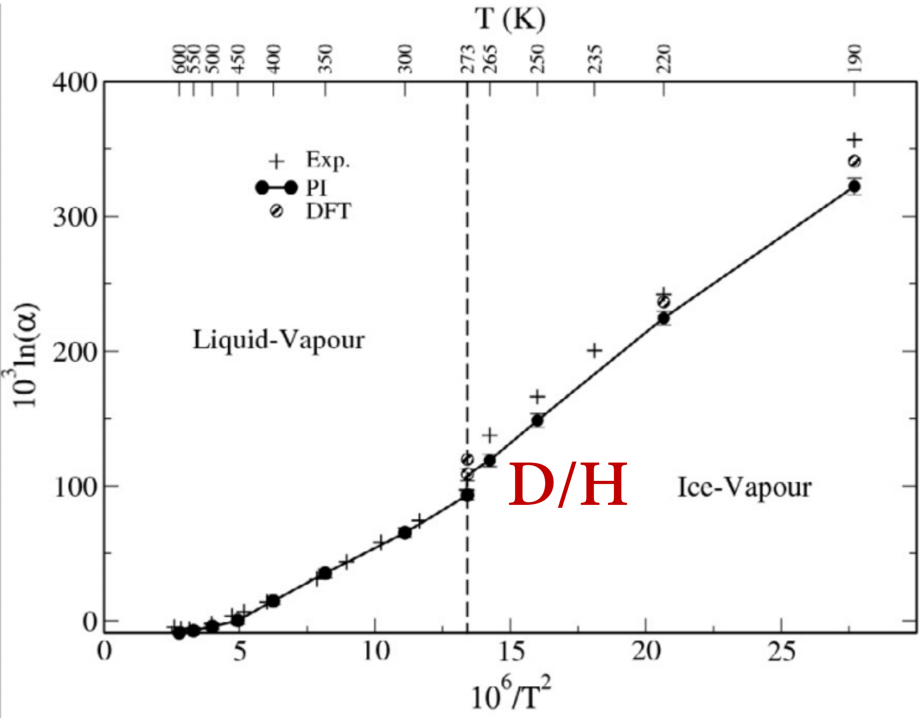

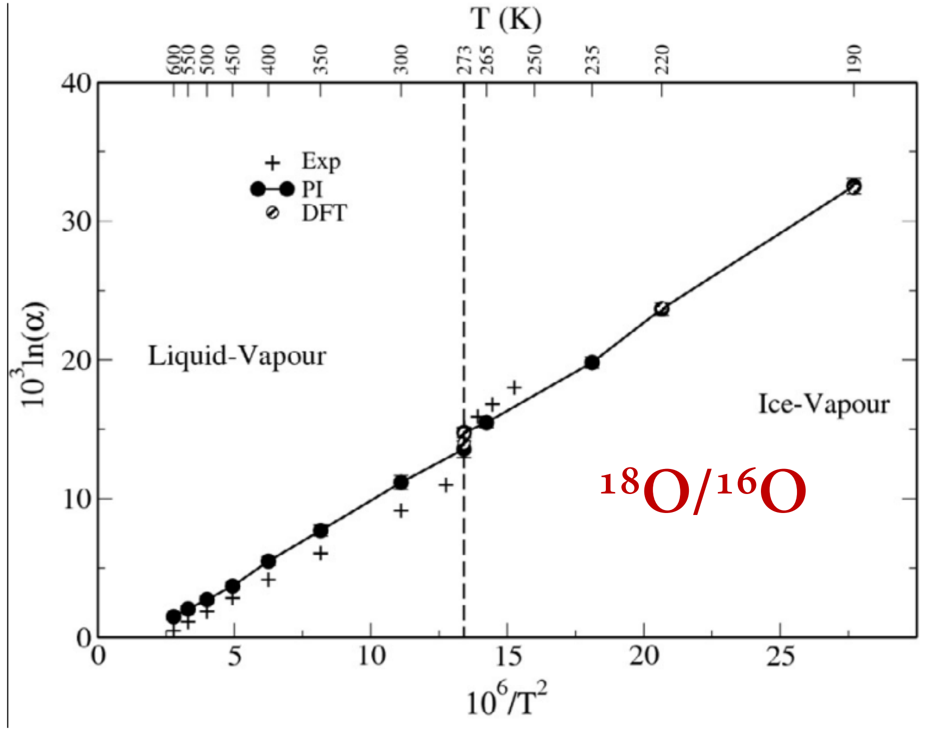

Pinilla et al. (2014)

Compromise strategy

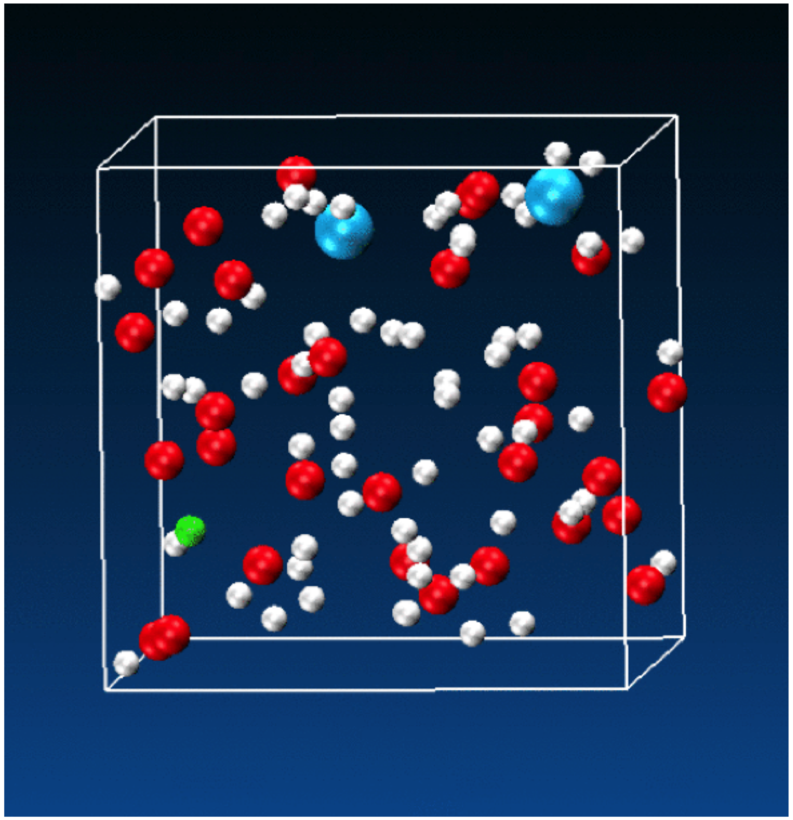

Capturing the structure of aqueous solution

Applications of Mg isotopes

- **Continental weathering** (Pogge von Strandmann et al., 2008; Teng et al., 2010; Pokrovsky et al., 2011; Huang et al., 2012; Wimpenny et al., 2014; Kasemann et al., 2014);
- **Paleo-environmental reconstruction** (Anbar and Rouxel, 2007; Higgins and Schrag, 2015; Husson et al., 2015);
- **Deep carbon recycling** (Yang et al., 2012; Huang et al., 2015; Liu et al., 2015; Li et al., 2016);
- **Mg global cycle** (Tipper et al., 2006; Higgins and Schrag, 2010; Beinlich et al., 2014; Fantle and Higgins, 2014);
- ……

Theoretical calculations

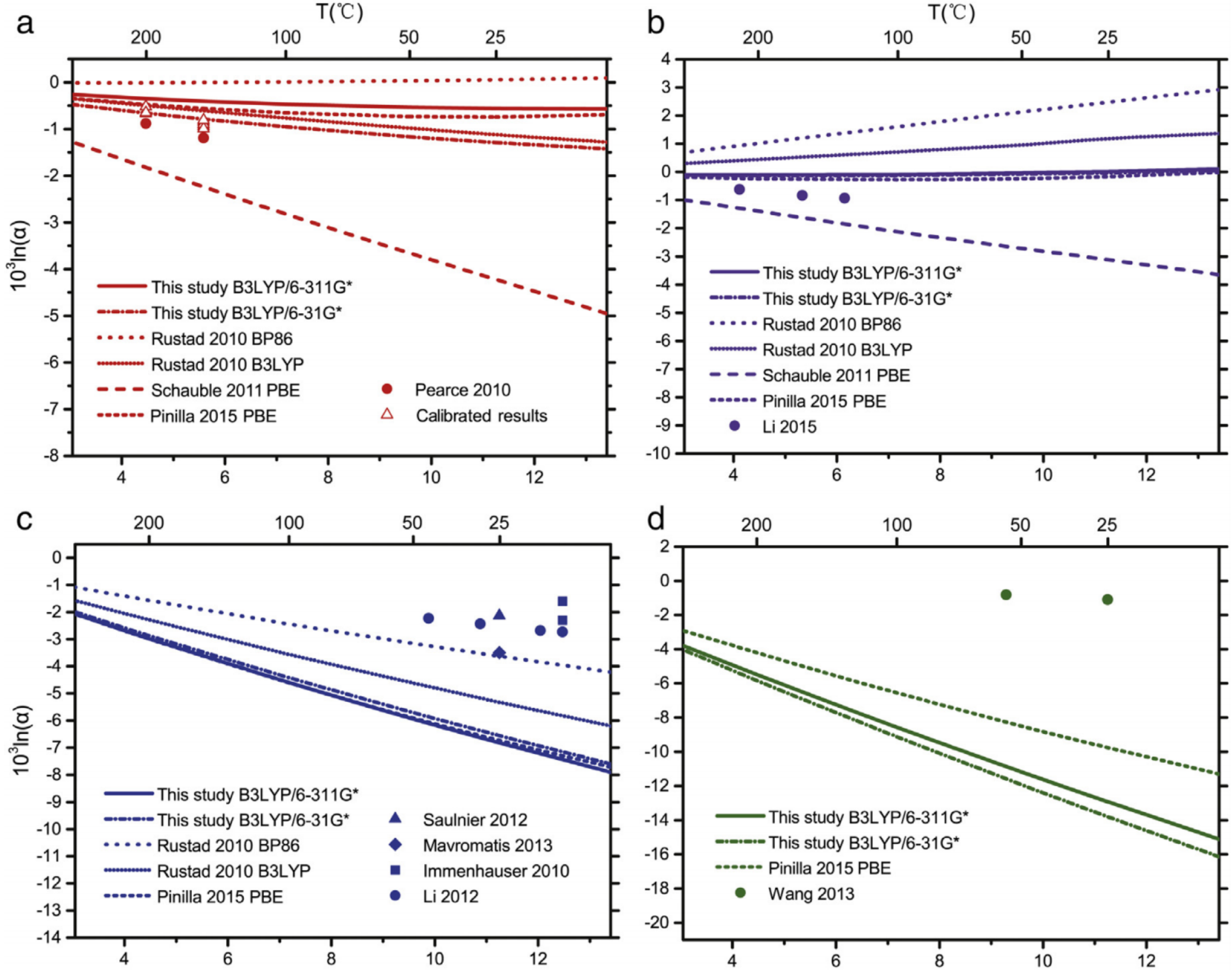

Big differences

Rustad et al., 2010; Schauble, 2011; Pinilla et al., 2015; Gao et al., 2018

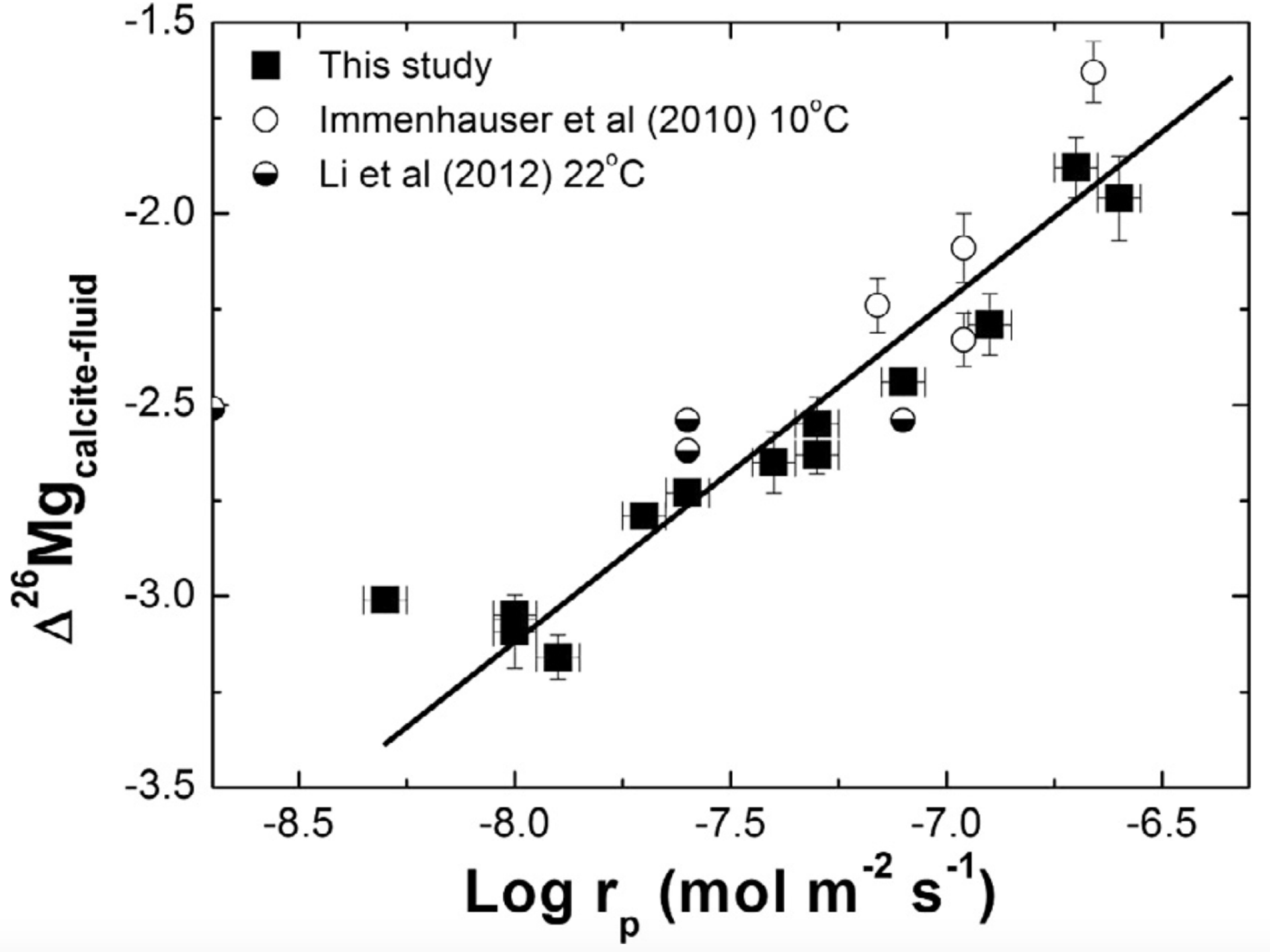

Mavromatis et al. (2013)

Radial distribution functions for Mg-O pairs

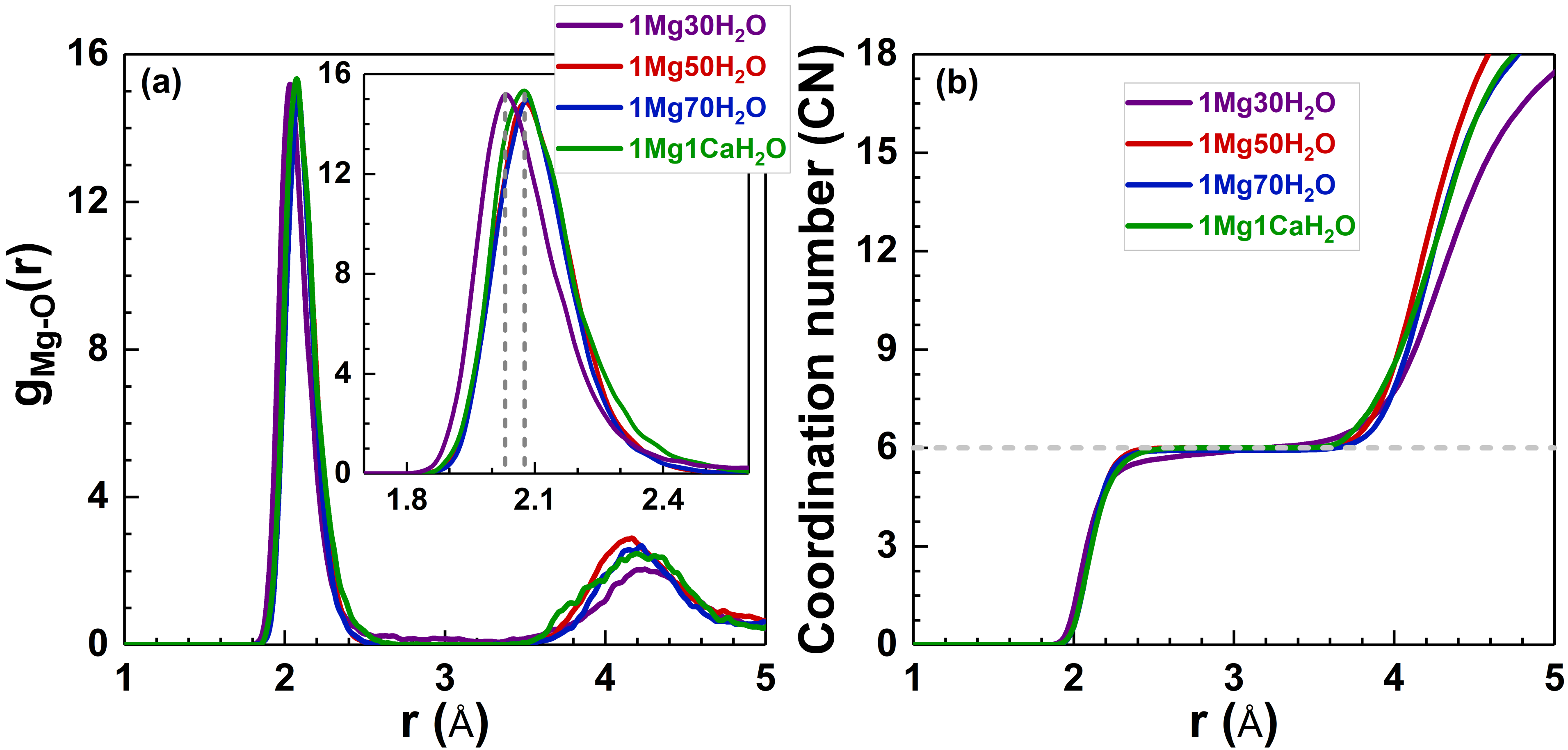

10^3lnbeta of aqueous Mg^{2+}

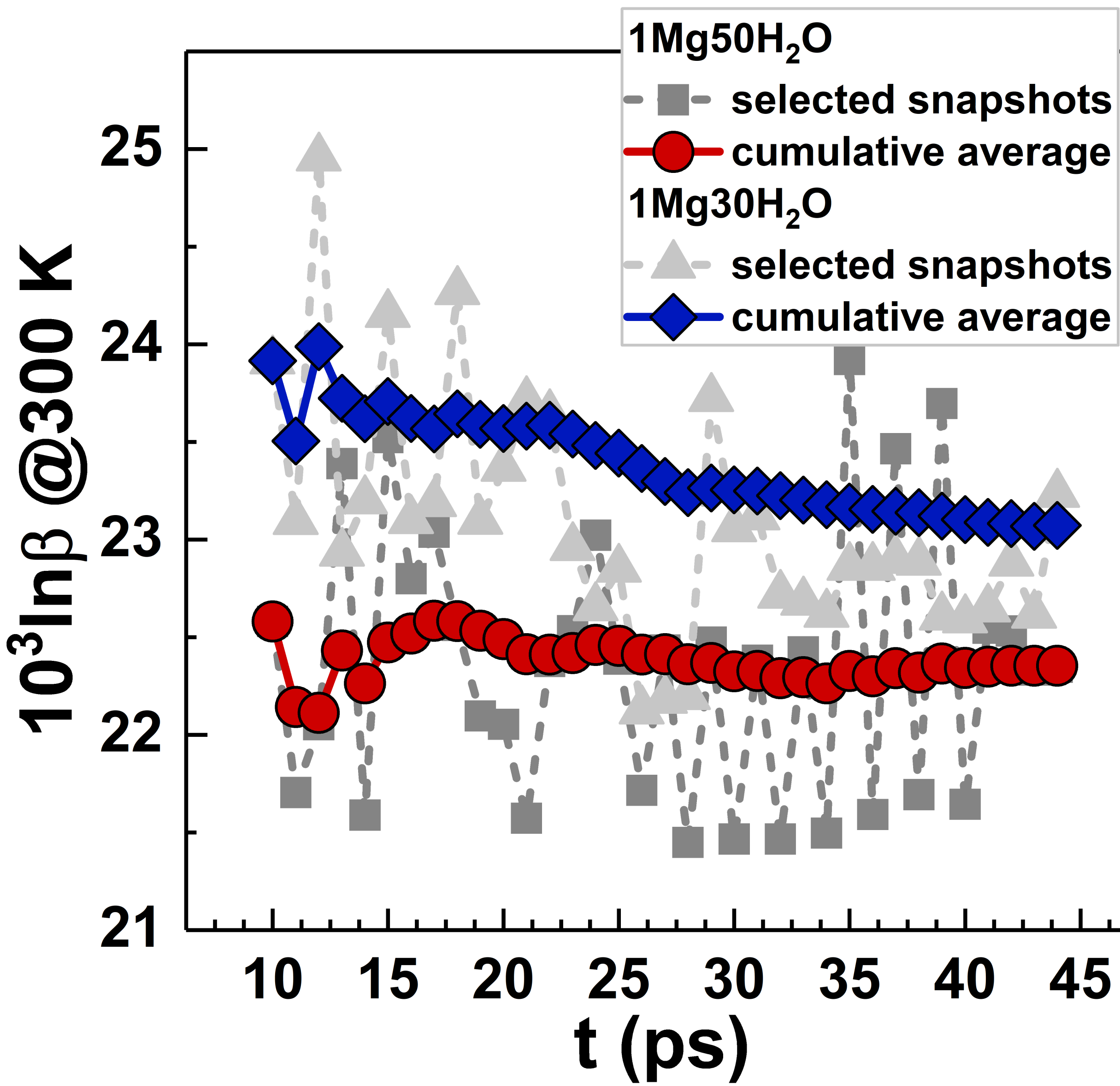

10^3lnbeta & 10^3lnalpha

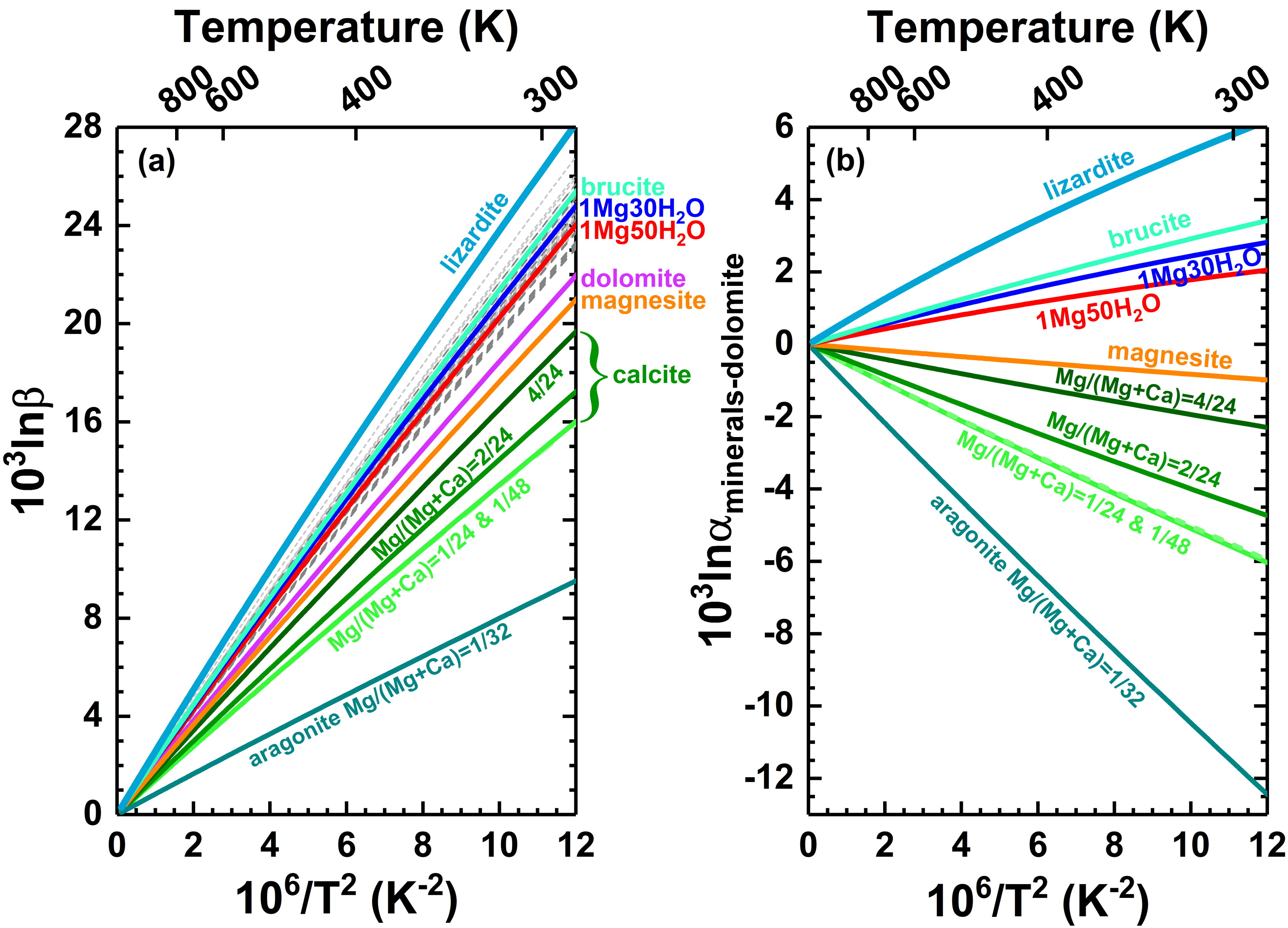

Dolomite-aqueous Mg^{2+}

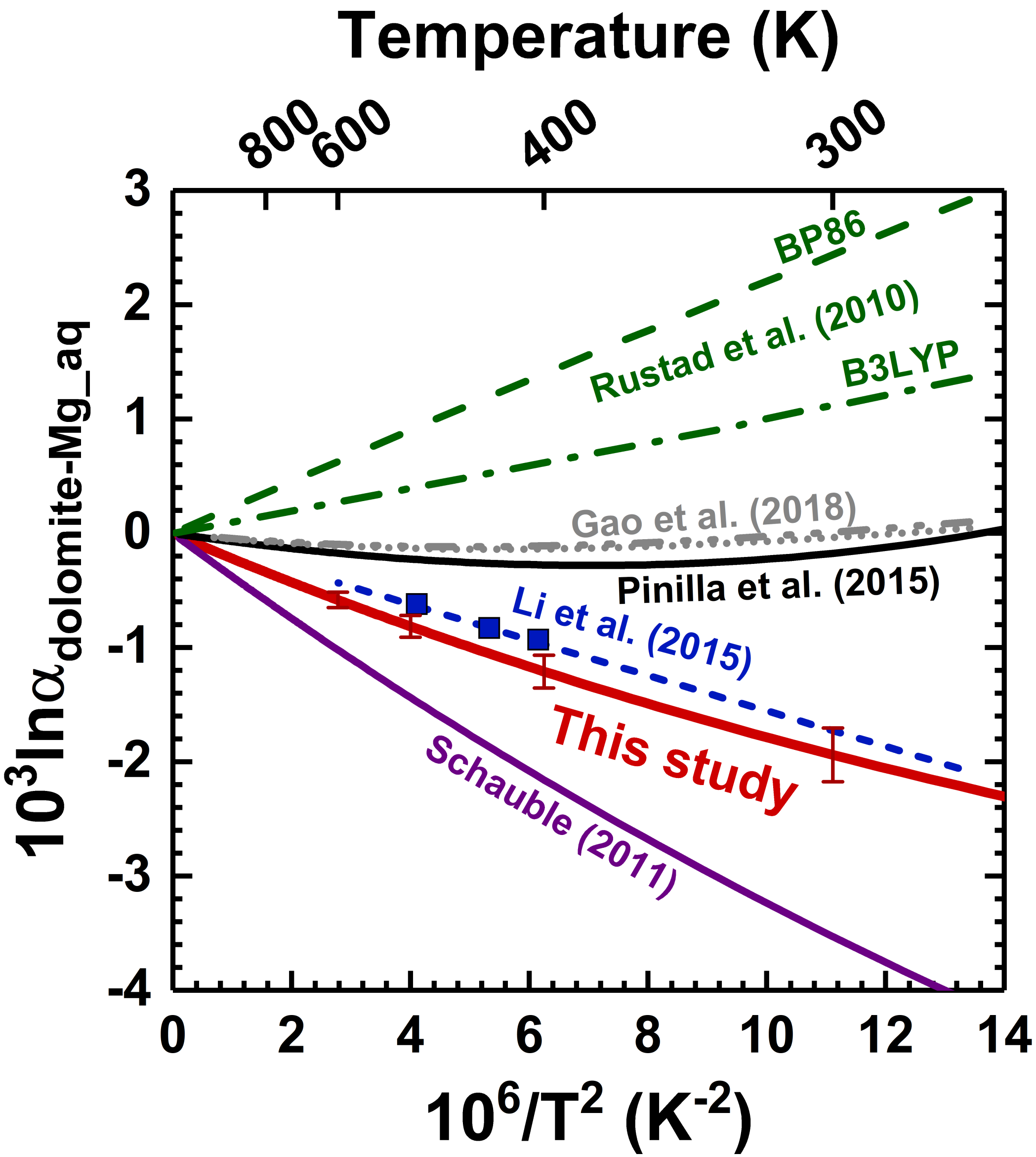

Magnesite-aqueous Mg^{2+}

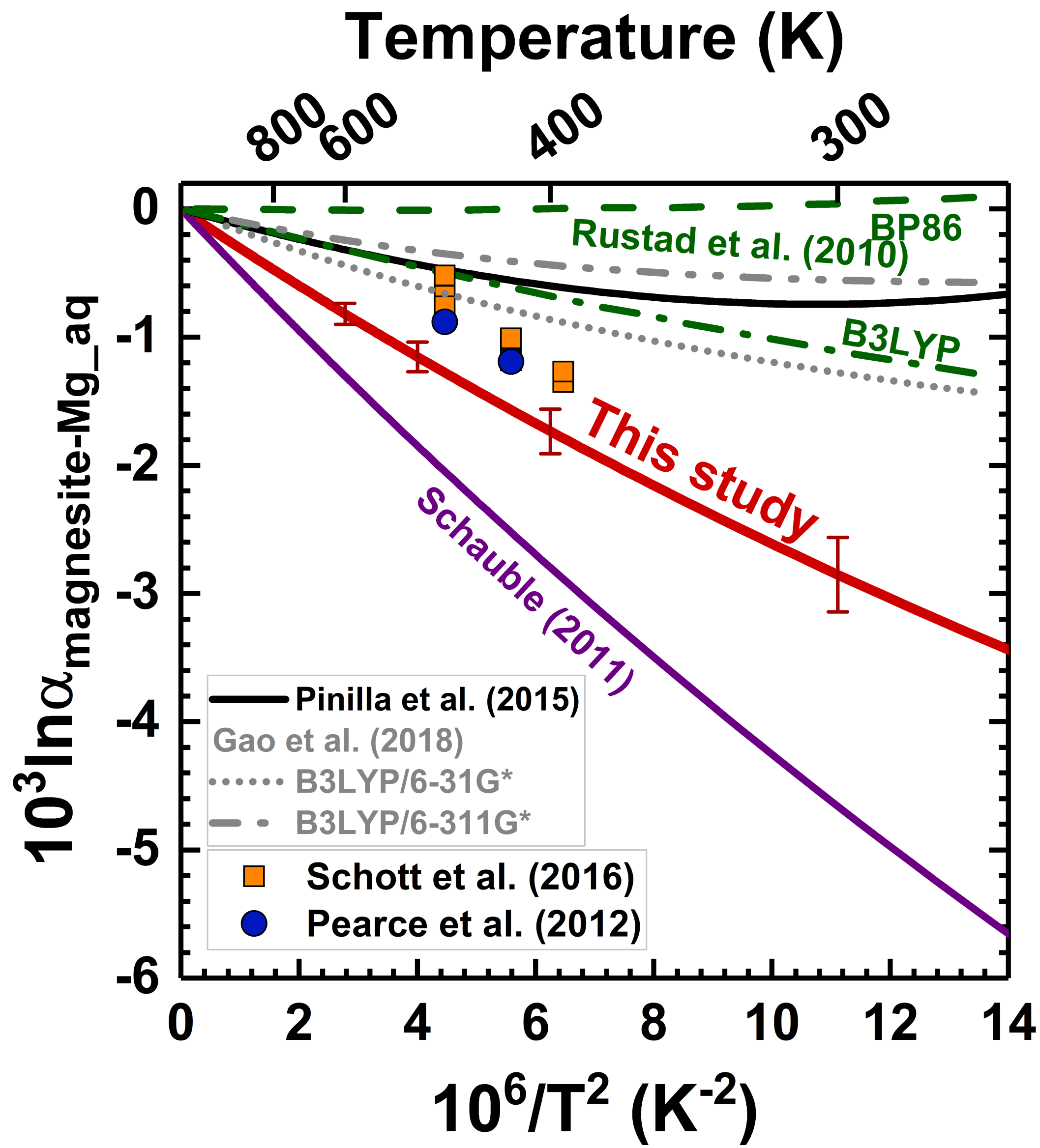

Calcite-aqueous Mg^{2+}

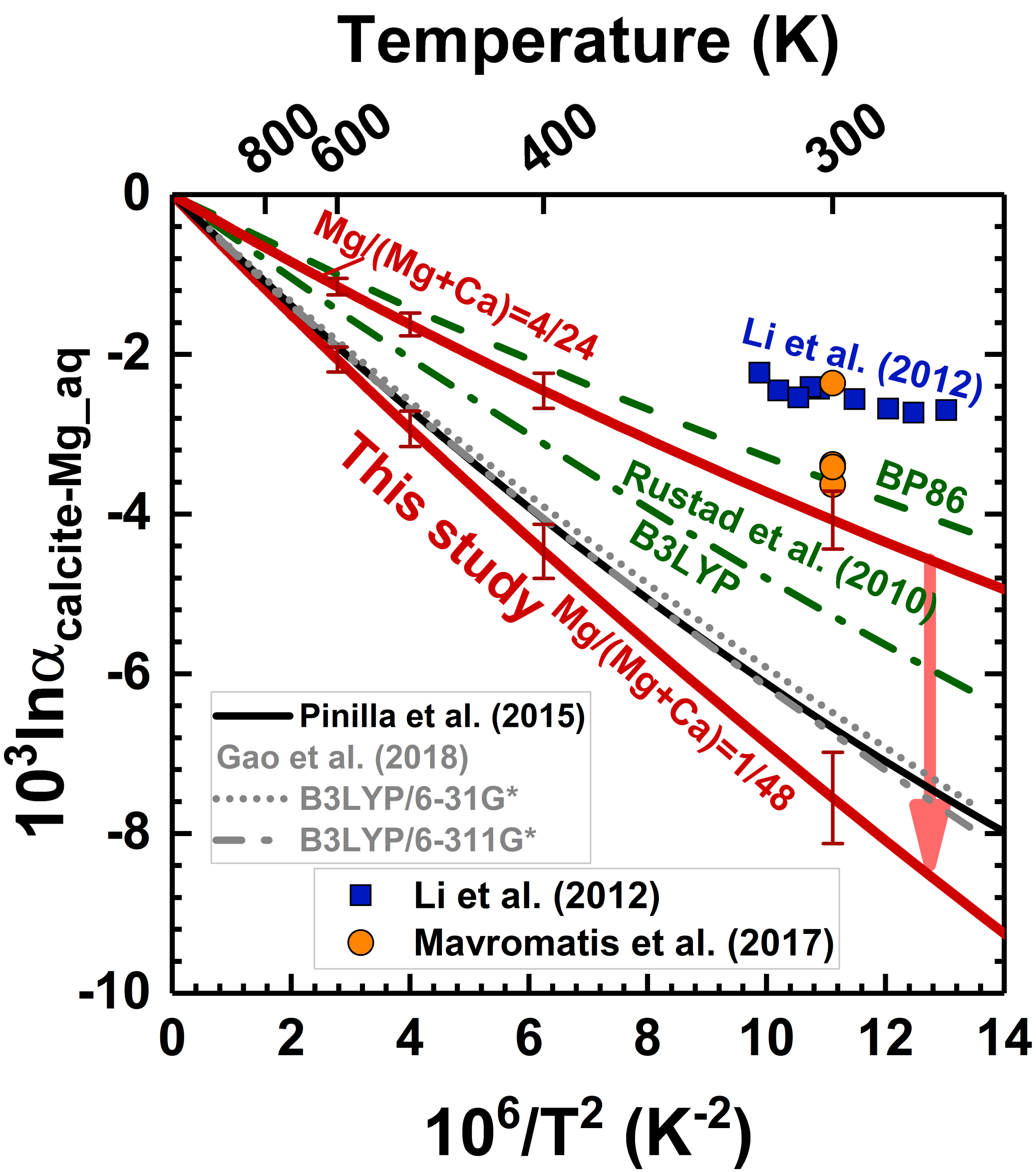

Aragonite-aqueous Mg^{2+}

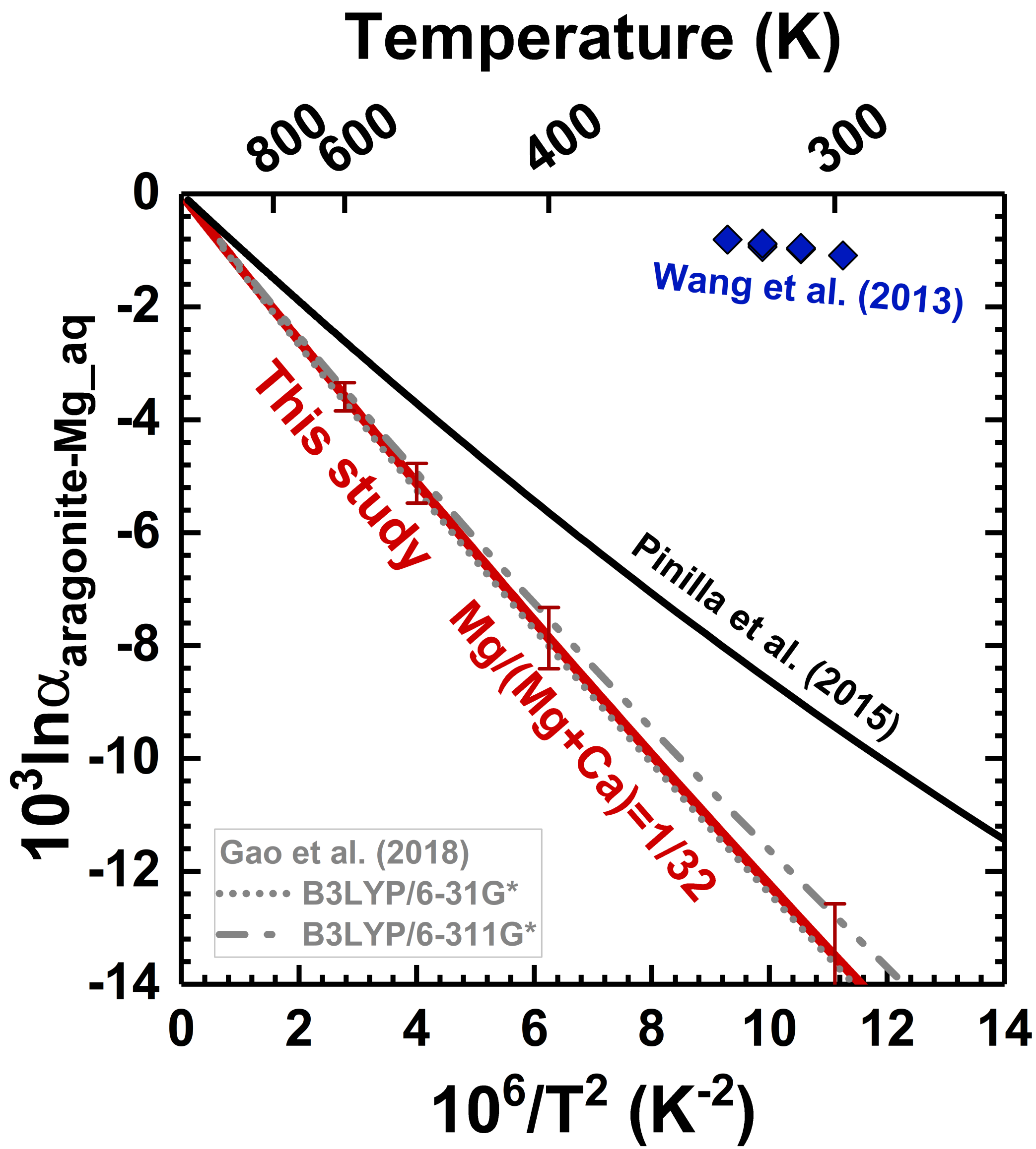

Brucite & Lizardite-aqueous Mg^{2+}

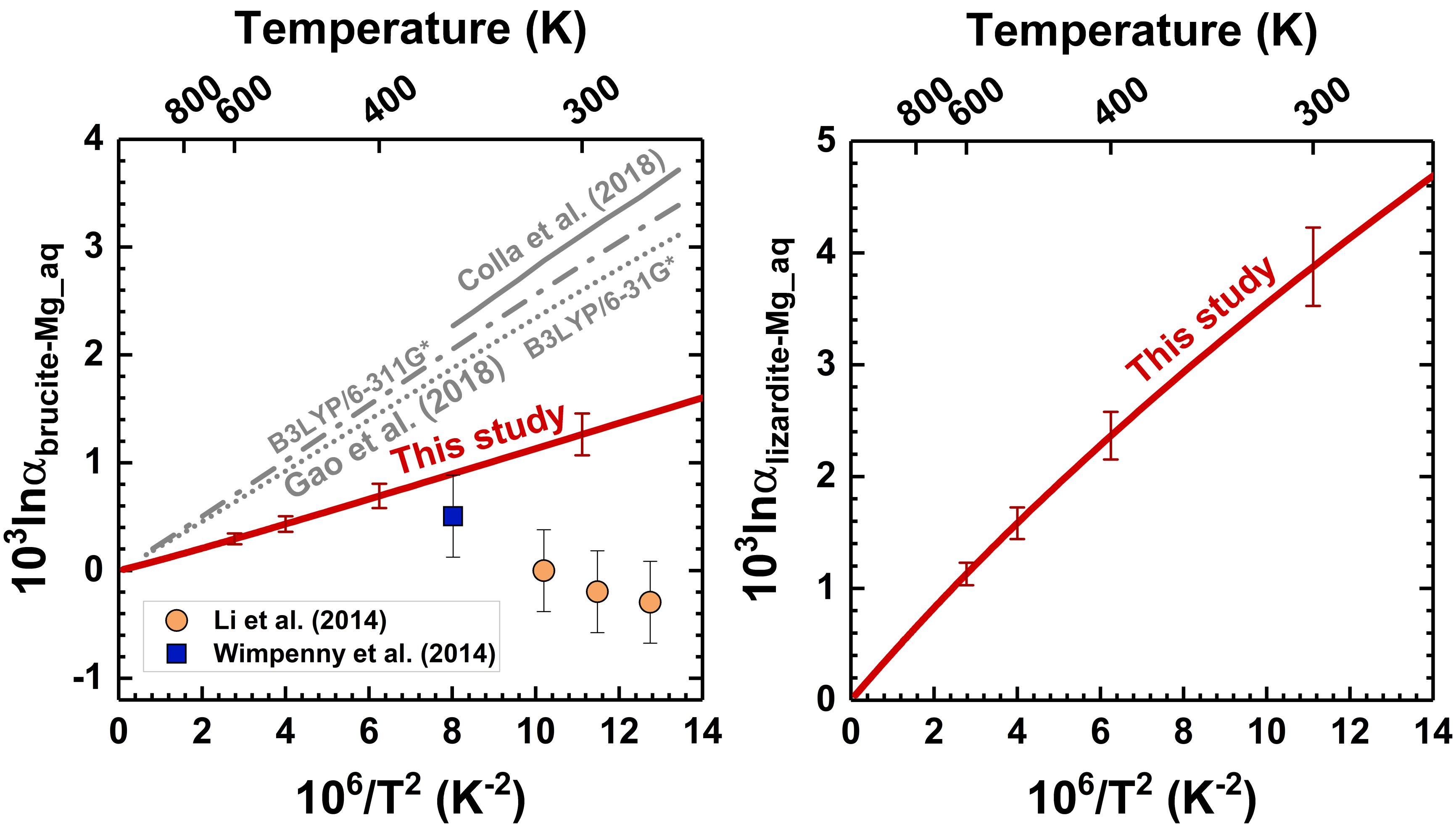

56 137.33
Ba
Barium
[Xe]$6s^2$ +2

Alkaline		Radius	253 pm
State @273 K	Solid	Modulus	9.6 GPa
Date of discovery	1808	Density	3510 kg/m^3
Melting point	1000 K	Conductivity	18 W/mK
Boiling point	2143 K	Heat capacity	205 J/kgK
Electronegativity	0.89	Abundance	$1x10^{-6}$ %
Ionization energy	502.9 kJ/mol	Electron affinity	13.95 kJ/mol

- Alkaline earth metal, found in Barite and Witherite
- Highly incompatible elements, **Crust/Mantle ~ 95**
- Element Linked to **Fluid Activity**
- Element related to **biological processes in the ocean**
- Seven stable isotopes: 130, 132, 134, 135, 136, 137, and 138

- A useful tracer of Fluid Mobility
- Tracing the recycling of subducting materials
- Ba cycling in the ocean
- Reconstruction of past productivity?

Ba cycling in the ocean

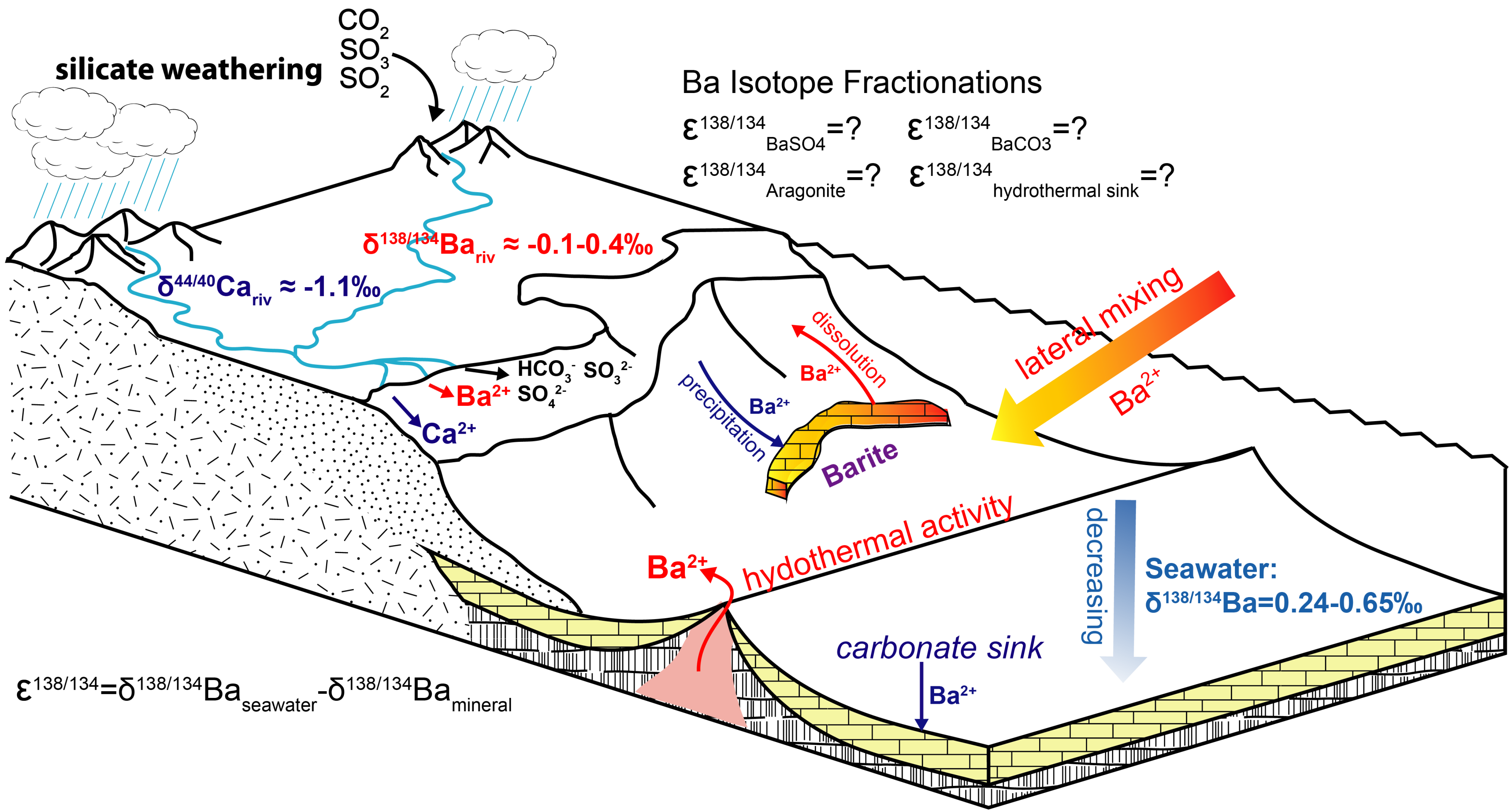

Ba isotope fractionations between solids and solutions

Process	$^{137/134}\varepsilon^{a}$ (‰)	$^{138/134}\varepsilon$ (‰)	*T*-range (°C)	Reference	Comment
Formation $BaSO_4$	−0.19	−0.25	21	This study	Precipitation experiment, with methanol
Formation $BaSO_4$	−0.21 to −0.26	−0.28 to −0.35	4–60	This study	Transformation experiment of precusors
Formation $BaSO_4$	−0.23 to −0.26	−0.31 to −0.35	21–60	[4]	Precipitation experiment
Formation $BaSO_4$	−0.14 to −0.34	−0.19 to −0.45	Ambient	[10,12]	Water column, Atlantic
Formation $BaSO_4$	−0.3	−0.4	Ambient	[11]	Water column, Lake Superior
Dissolution $BaSO_4$	0	0	95	[4]	Dissolution in concentrated Na_2CO_3 solution
Formation $BaMn(CO_3)_2$	−0.11	−0.15	21	[5]	Transformation experiment of precusors
Formation $BaCO_3$	−0.26	−0.35	21	This study	Precipitation experiment, slow, with methanol
Formation $BaCO_3$	−0.11 to −0.17	−0.15 to −0.23	4–80	This study	Transformation experiment
Formation $BaCO_3$	−0.06 to −0.14	−0.08 to −0.19	21–60	[4]	Precipitation experiment, fast
Formation $BaCO_3$	−0.26 to −0.32	−0.35 to −0.43	21–60	[4]	Precipitation experiment, slow
Formation $BaCO_3$	−0.07	−0.09	25	[14]	Precipitation experiment, fast
Ba incorporation $CaCO_3$	−0.01 to −0.26	−0.01 to −0.35	25	[6]	Aquarium experiment, corals
Ba incorporation $CaCO_3$	−0.16	−0.21	Ambient	[15]	Natural cold water corals
Dissolution $BaCO_3$	0	0	25	[14]	Experiment
Diffusion of $Ba^{2+}_{(aq)}$	−0.23	−0.31	10–25	[7]	Experiment, silica gel
Adsorption $Ba^{2+}_{(aq)}$	0.15	0.20	25?	[7]	Experiment, silica gel
Adsorption $Ba^{2+}_{(aq)}$	0	0	Ambient	[9]	Soil, field
Desolvation $Ba^{2+}_{(aq)}$	−1.1	−1.46	5–50	[13]	Modelling

Böttcher et al. (2018)

Ba isotope fractionations between solids and solutions

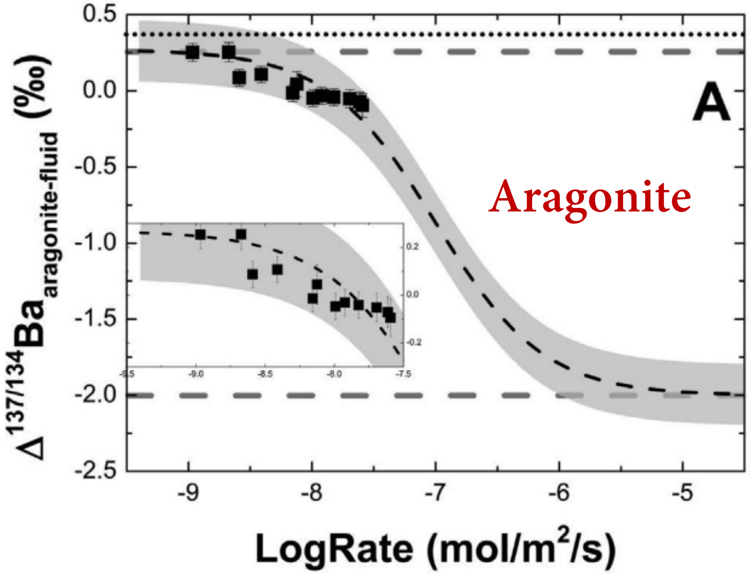

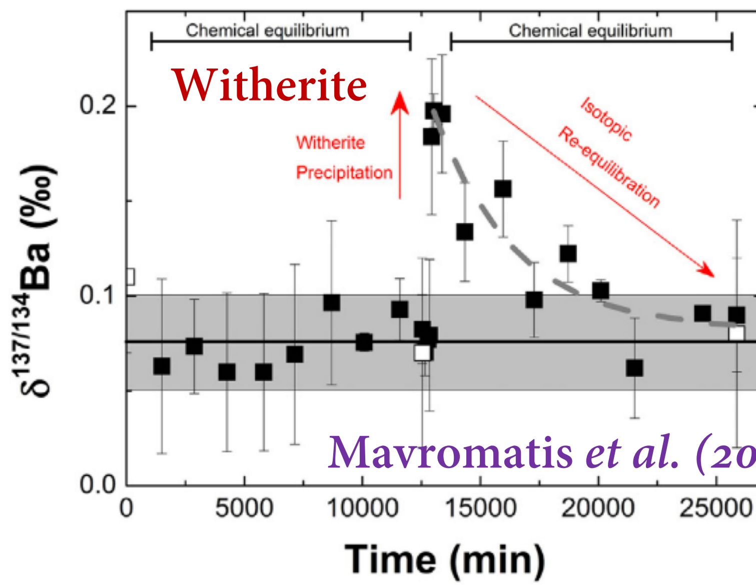

Mavromatis *et al.* (2016)

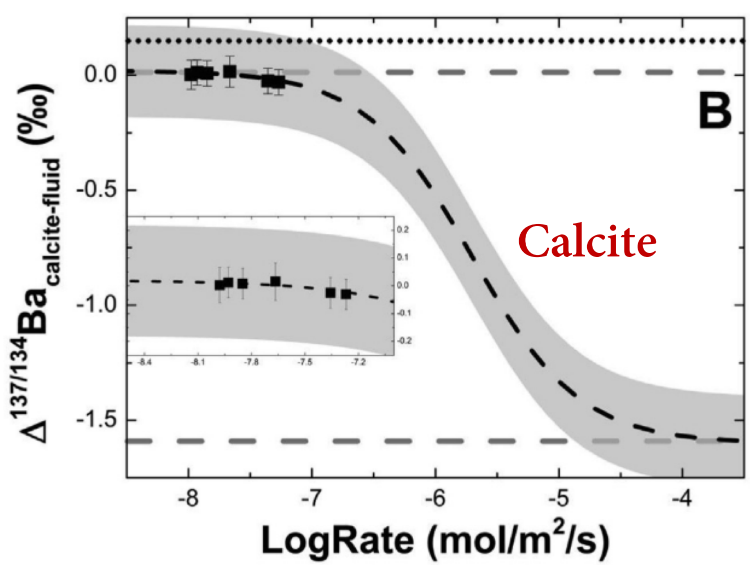

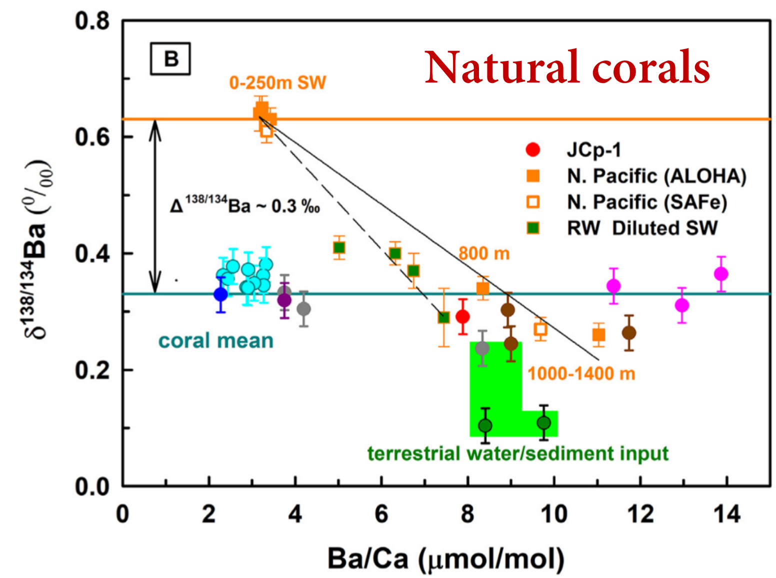

Mavromatis *et al.* (2020)

Liu et al. (2019)

Urey equation

$$\beta = \prod_{i=1}^{N_{dof}} \frac{u_i^*}{u_i} \exp\left[\frac{(u_i - u_i^*)}{2}\right] \frac{1 - \exp(-u_i)}{1 - \exp(-u_i^*)}$$

$$\beta = 1 + \sum_{i=1}^{N_{dof}} \left(\frac{1}{2} - \frac{1}{u_i} + \frac{1}{\exp(u_i) - 1}\right) \Delta u_i$$

$$G(u) = \frac{1}{2} - \frac{1}{u} + \frac{1}{\exp(u_i) - 1}$$

$$= \frac{u}{12} - \frac{u^3}{720} + \frac{u^5}{30240} - \frac{u^7}{1209600} + \ldots.$$

$$\beta = \beta_{exact} = 1 + \sum_{i=1}^{N_{dof}} \left(\frac{u_i}{12} - \frac{u_i^3}{720} + \ldots\right) \Delta u_i$$

$$u = h\nu_i / k_B T$$

$$\beta = 1 + \sum_{i}^{N_{dof}} \frac{u_i}{12} \Delta u_i$$

$$= 1 + \sum_{i=1}^{N_{dof}} \frac{\Delta u_i^2}{24} = 1 + \sum_{i=1}^{N_{dof}} \frac{u_i^2 - u_i^{*2}}{24}$$

$$\beta \simeq 1 + \sum_{i=1}^{N_{dof}} \frac{u_i^2 - u_i^{*2}}{24} = 1 + \frac{\Delta m}{mm^*} \frac{\hbar^2}{24 k_B^2 T^2} \sum_{i=1}^{3} A_i$$

Average Force Constant

"High-temperature" Approximation
ν [cm⁻¹] < 1.39 T [K]

Bigeleisen and Mayer (1947)

10^3lnbeta of aqueous Mg^{2+}: Force vs. Frequencies

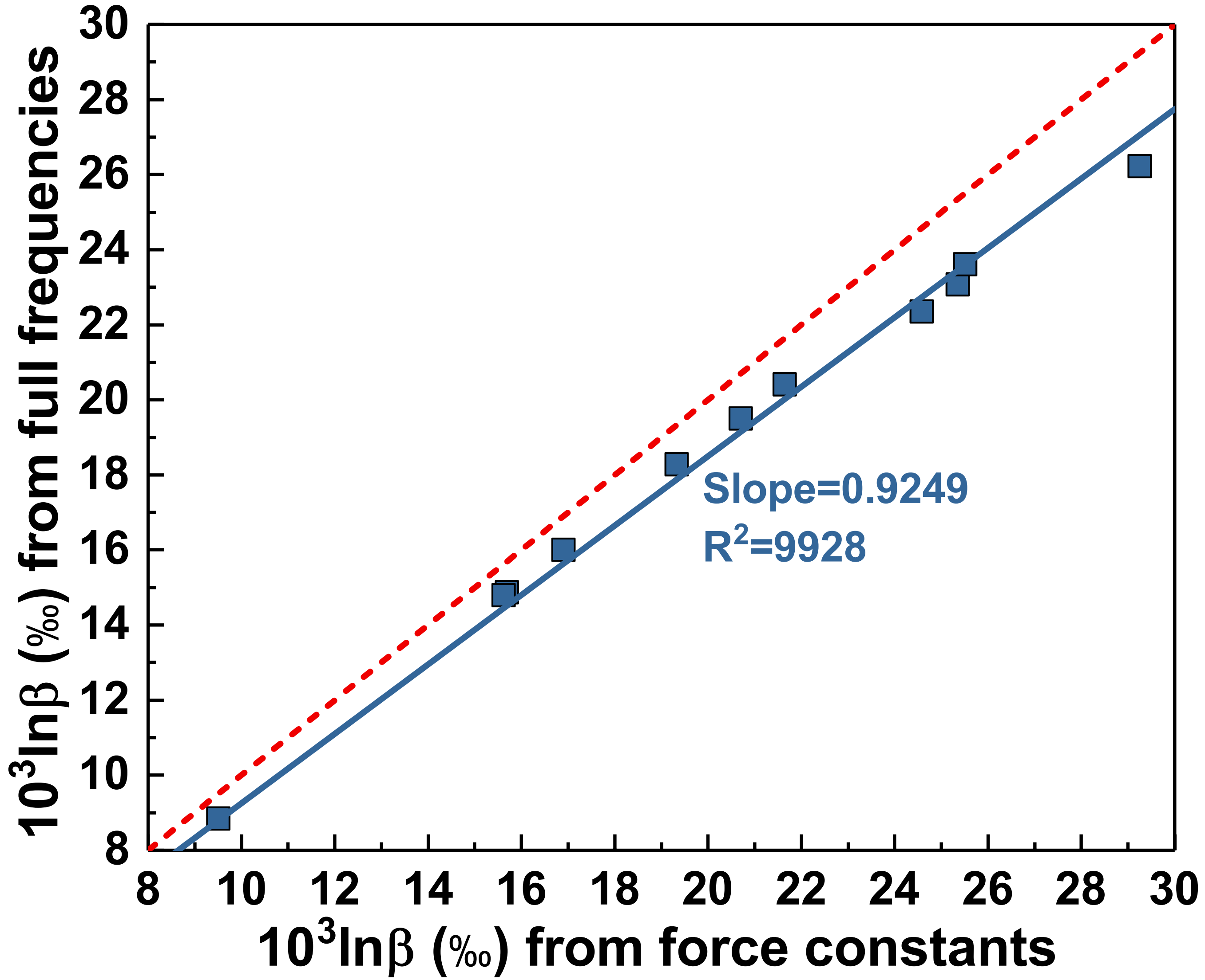

***Ionic** Radii (in Picometers) of the Most Common Oxidation States of the s-, p-, and d-Block Elements*

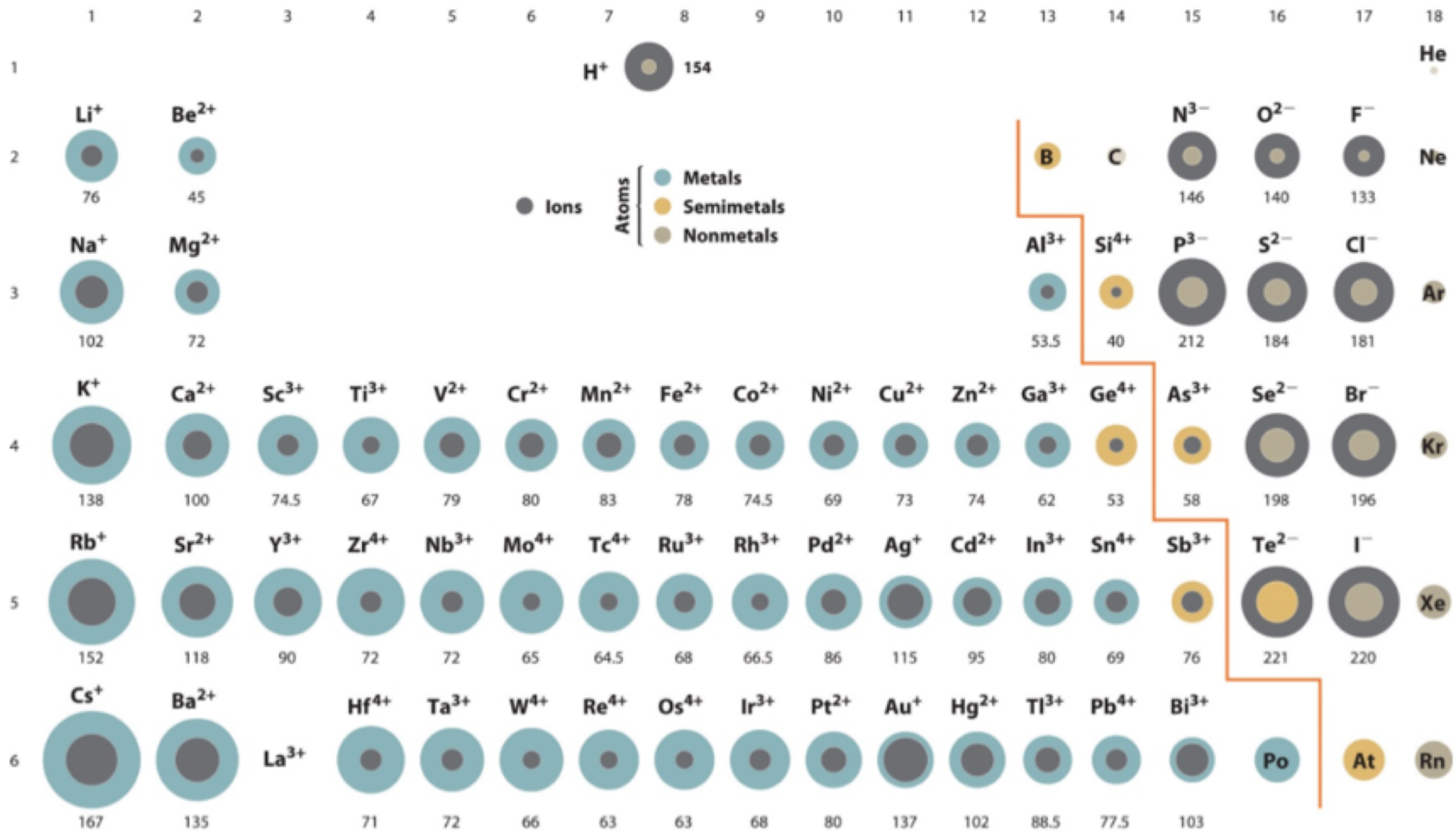

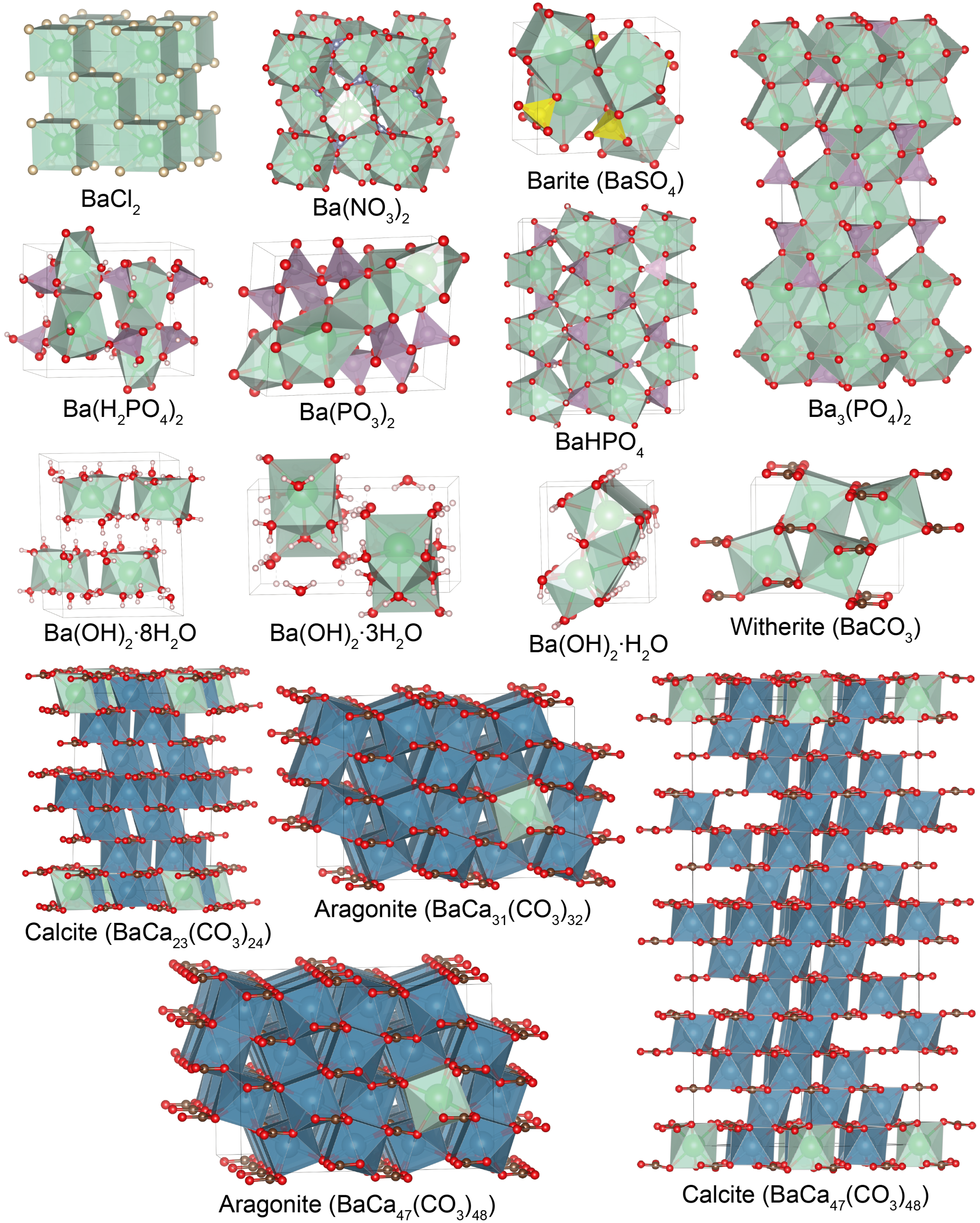
BaCl$_2$
Ba(NO$_3$)$_2$
Barite (BaSO$_4$)
Ba$_3$(PO$_4$)$_2$
Ba(H$_2$PO$_4$)$_2$
Ba(PO$_3$)$_2$
BaHPO$_4$
Ba(OH)$_2$·8H$_2$O
Ba(OH)$_2$·3H$_2$O
Ba(OH)$_2$·H$_2$O
Witherite (BaCO$_3$)
Calcite (BaCa$_{23}$(CO$_3$)$_{24}$)
Aragonite (BaCa$_{31}$(CO$_3$)$_{32}$)
Aragonite (BaCa$_{47}$(CO$_3$)$_{48}$)
Calcite (BaCa$_{47}$(CO$_3$)$_{48}$)

10³lnbeta and 10³lnalpha

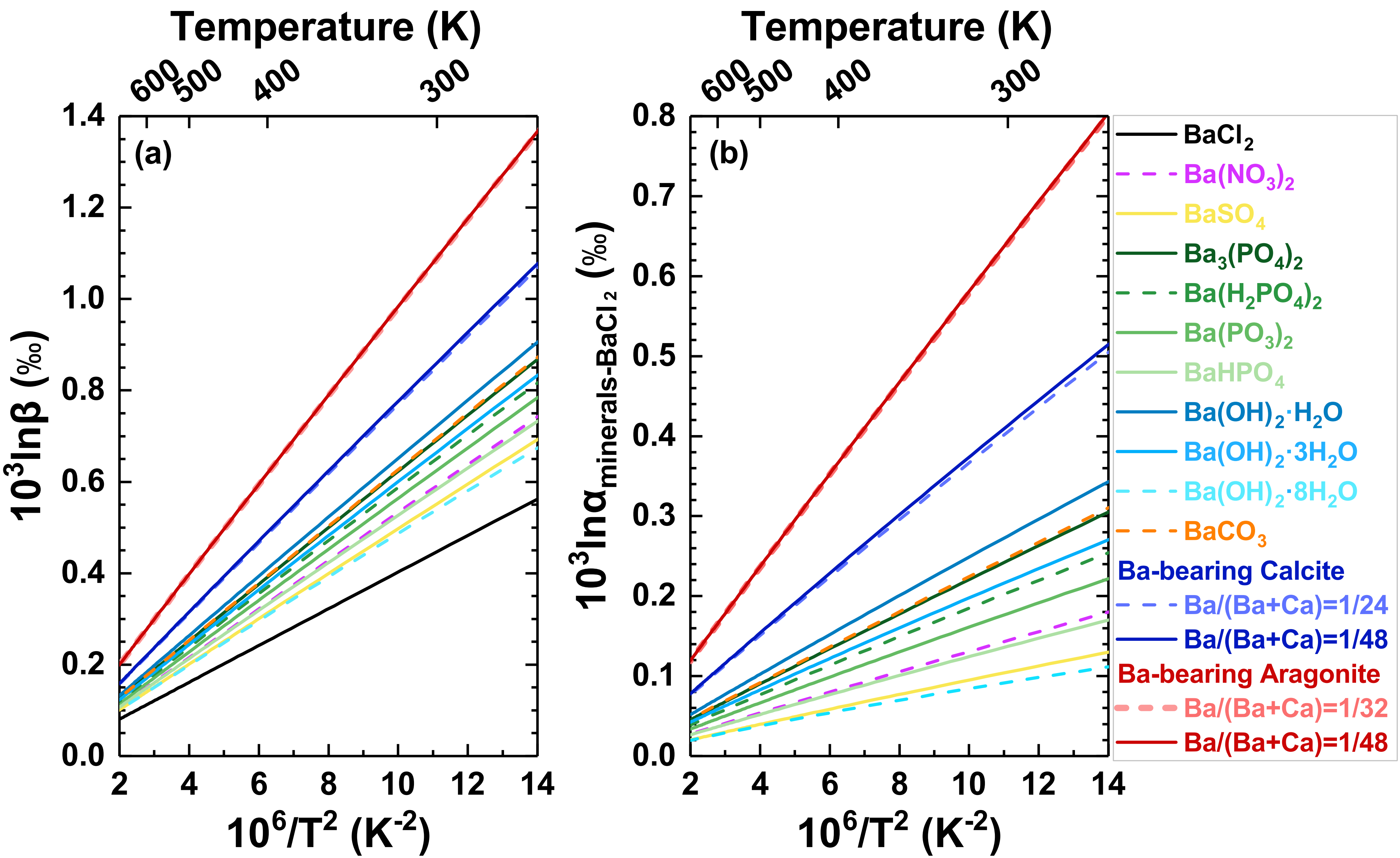

Controlling factors

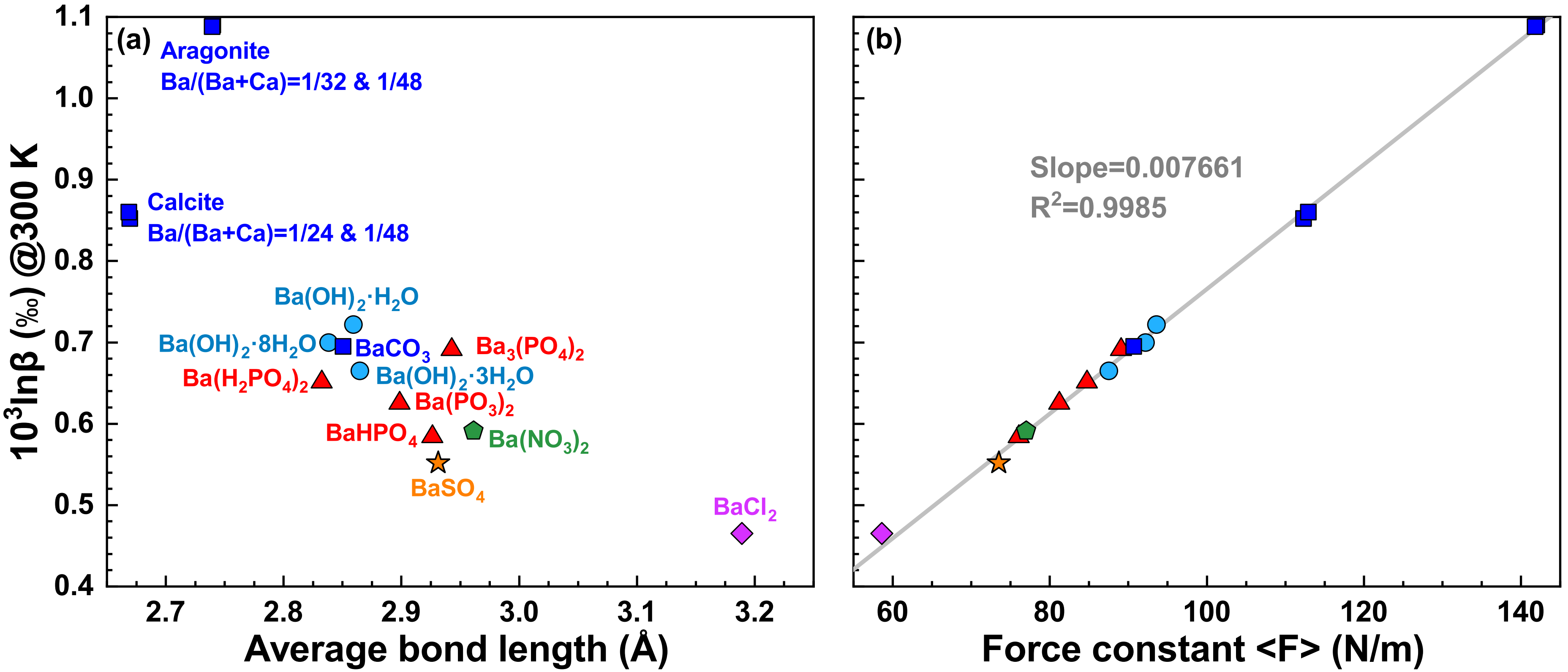

HT Approximation is valid for Ba isotopes?

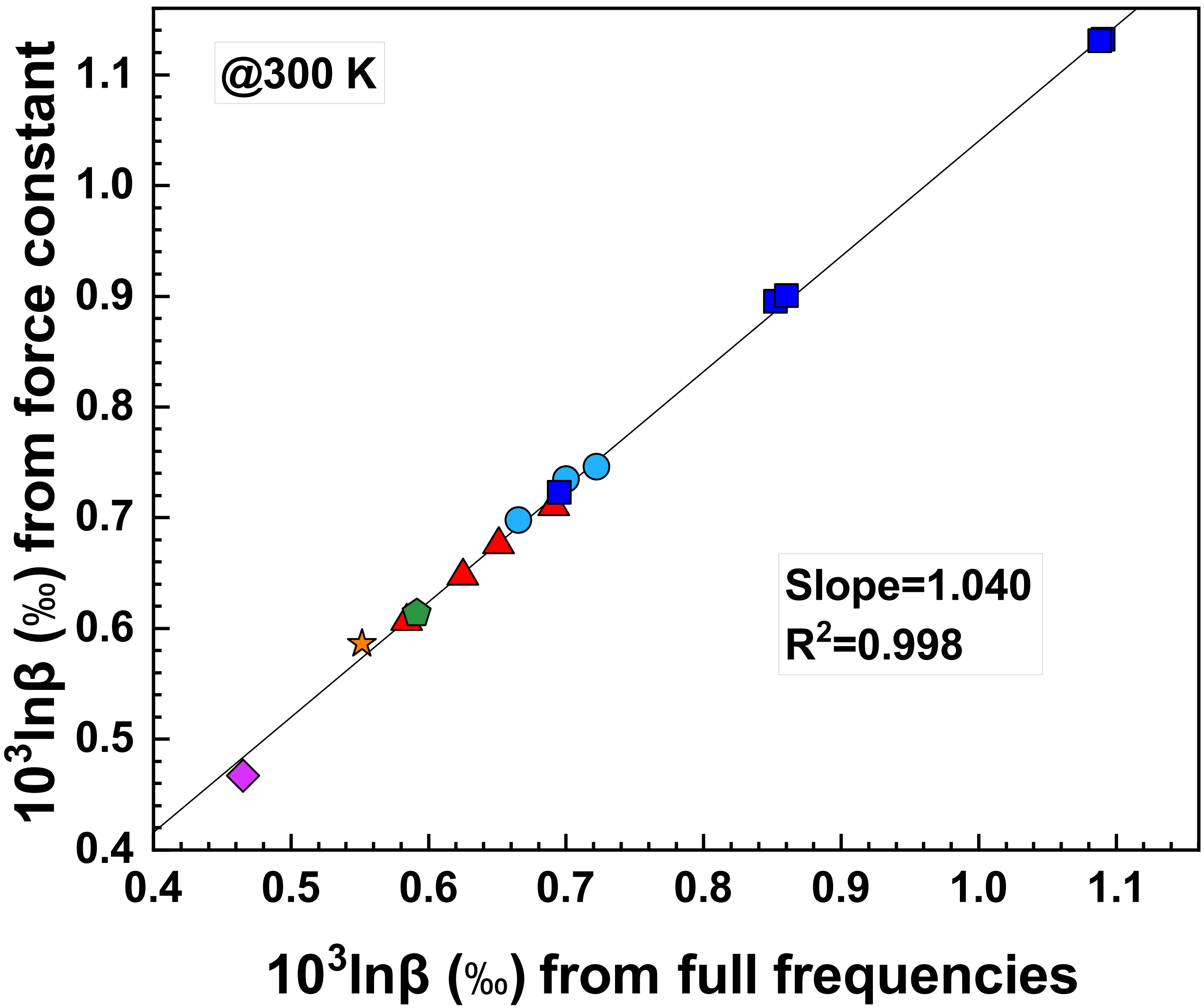

Aqueous Ba^{2+}: Structure & Force constant

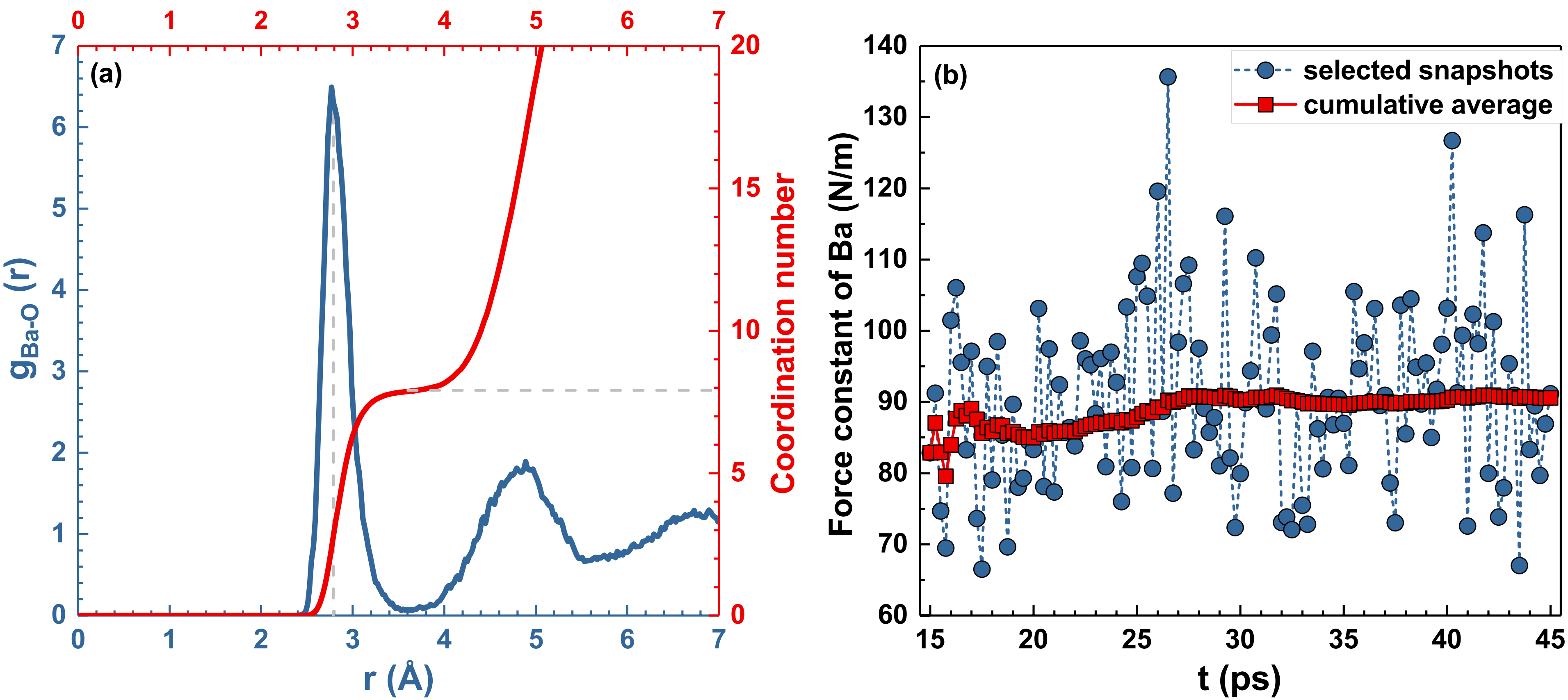

10^3lnalpha: mineral-aqueous Ba^{2+}

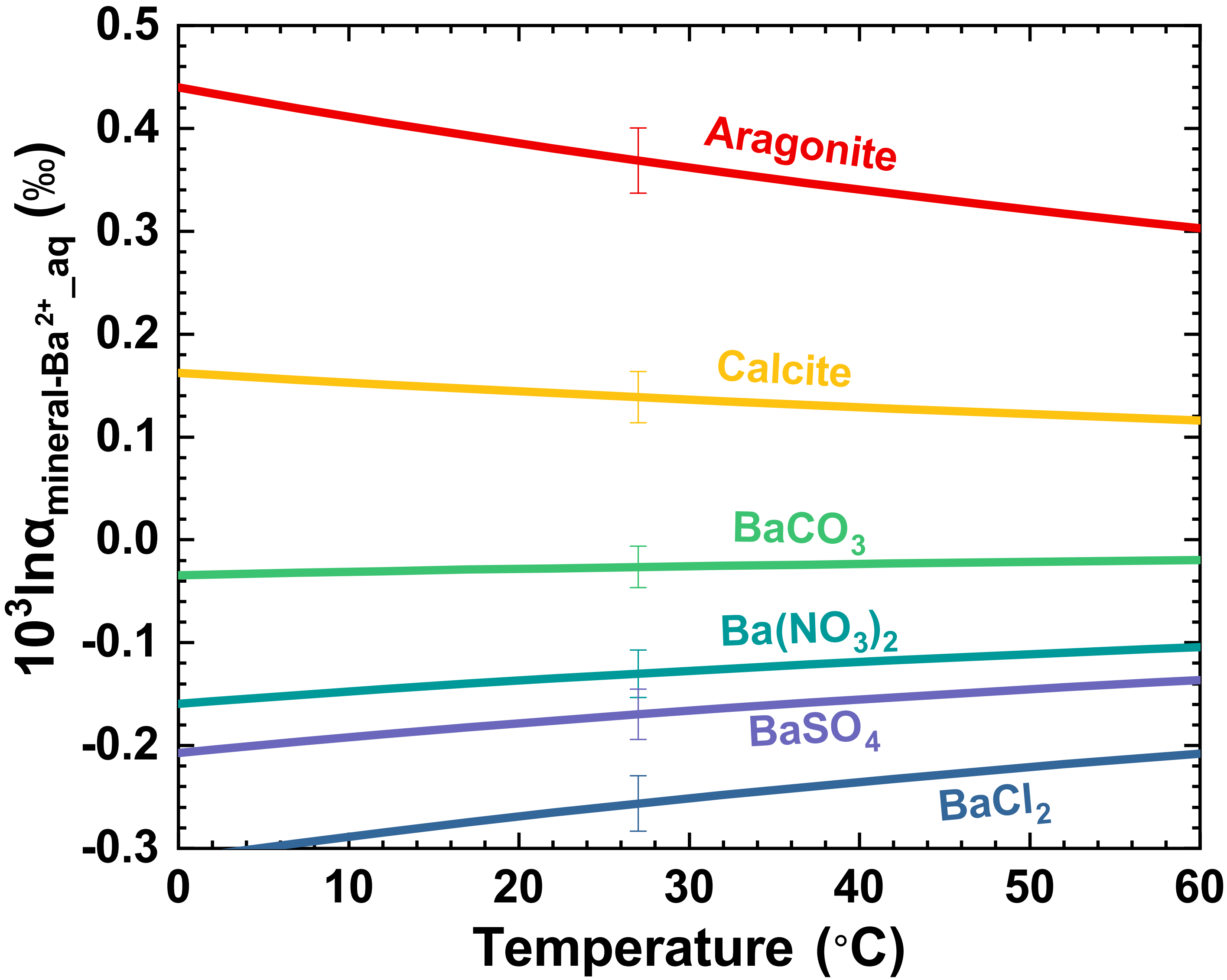

Summary

FPMD + Urey equation

4. Future prospects

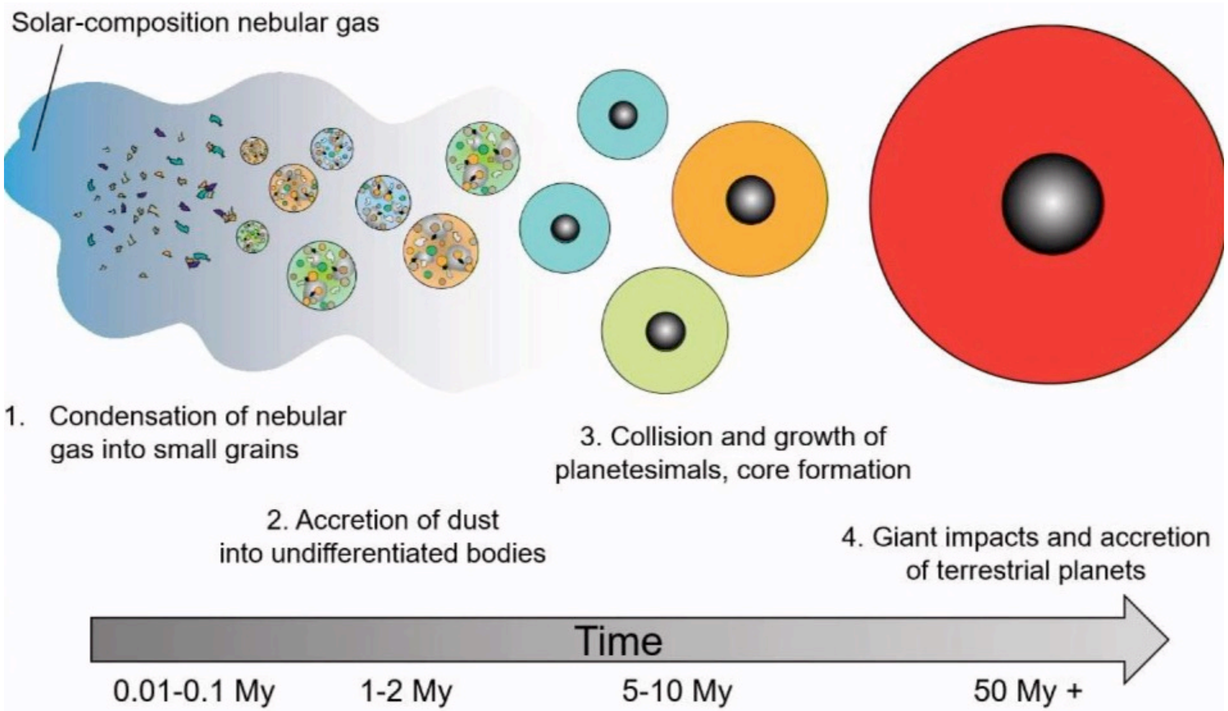

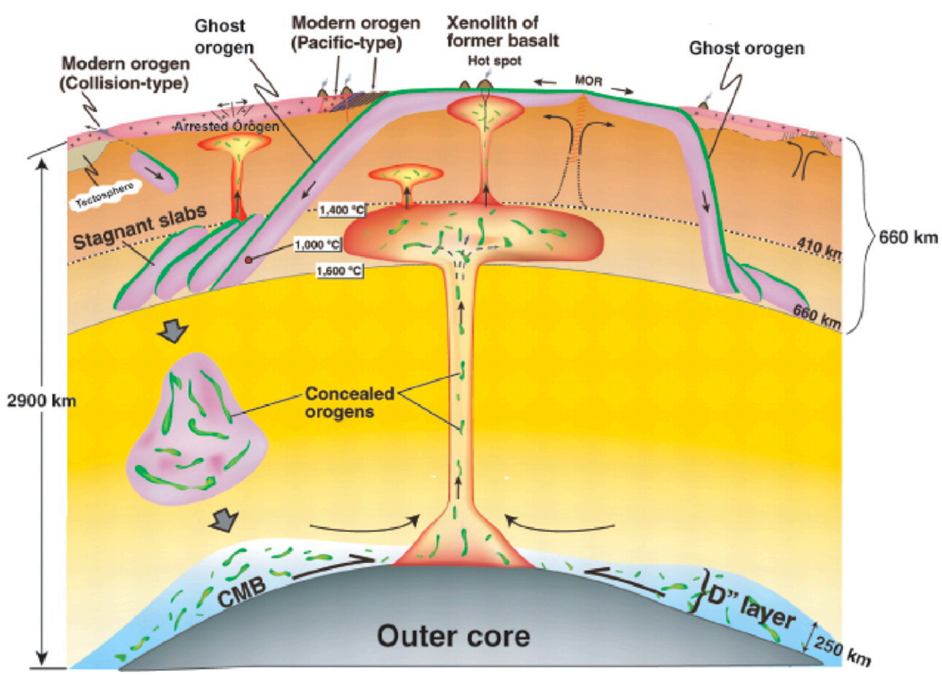

Santosh et al. (2015)

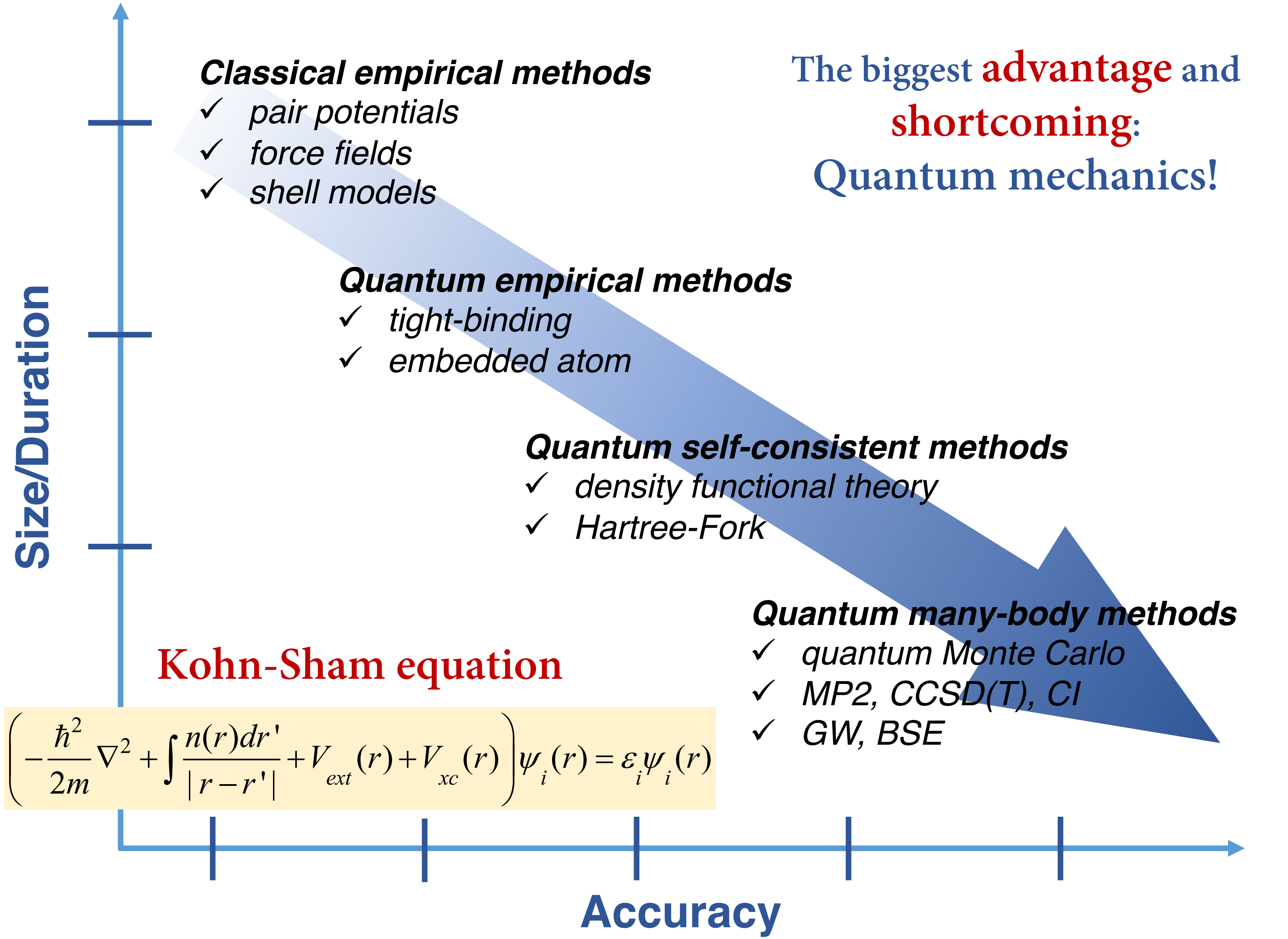
Classical empirical methods
✓ pair potentials
✓ force fields
✓ shell models
Quantum empirical methods
✓ tight-binding
✓ embedded atom
Quantum self-consistent methods
✓ density functional theory
✓ Hartree-Fork
Quantum many-body methods
✓ quantum Monte Carlo
✓ MP2, CCSD(T), CI
✓ GW, BSE
The biggest advantage and shortcoming: Quantum mechanics!
Kohn-Sham equation
$\left(-\frac{\hbar^2}{2m}\nabla^2+\int\frac{n(r)dr'}{|r-r'|}+V_{ext}(r)+V_{xc}(r)\right)\psi_i(r)=\varepsilon_i\psi_i(r)$
Size/Duration
Accuracy

Machine learning models density functionals

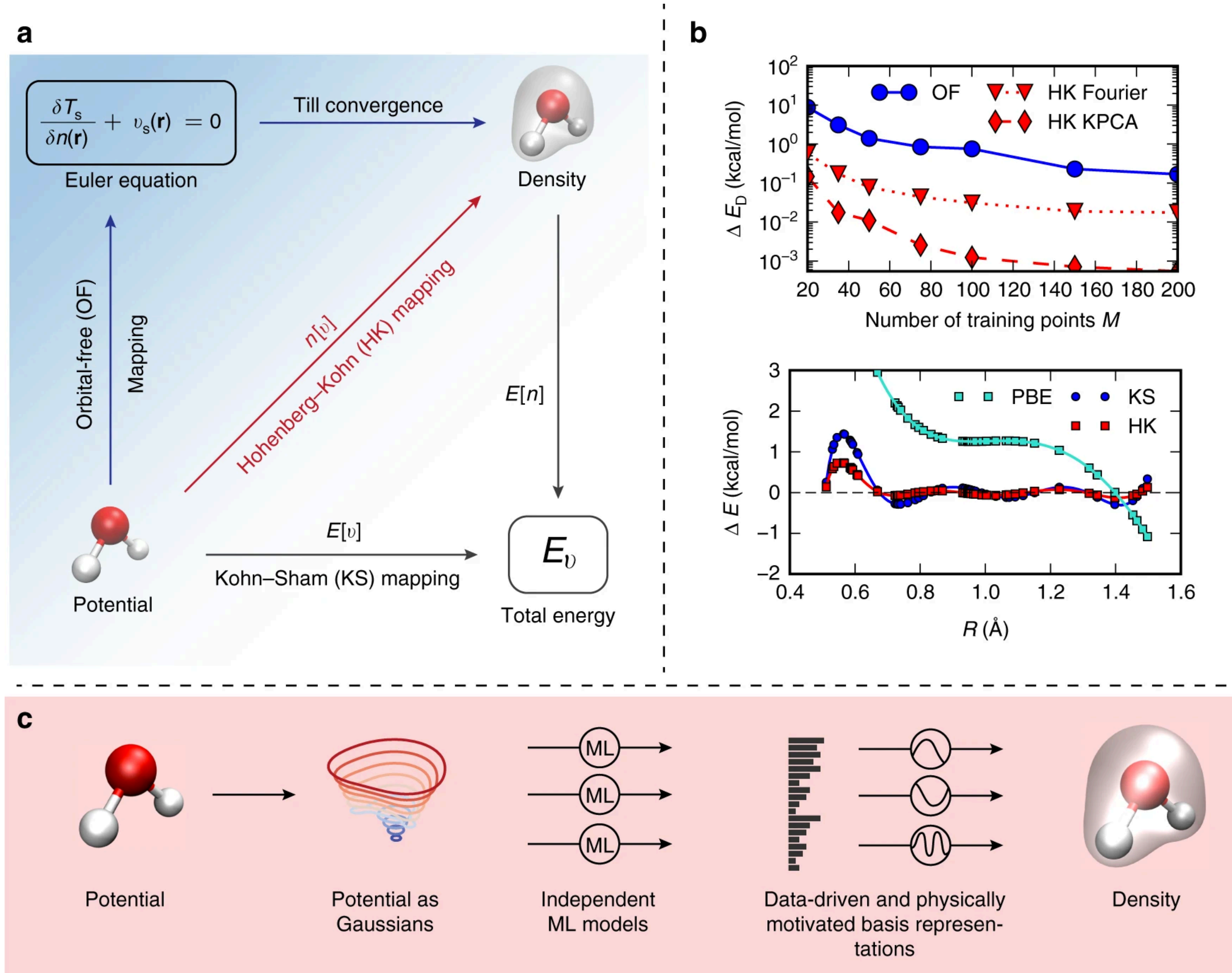

Brockherde et al. (2017)

Machine learning creates density functionals

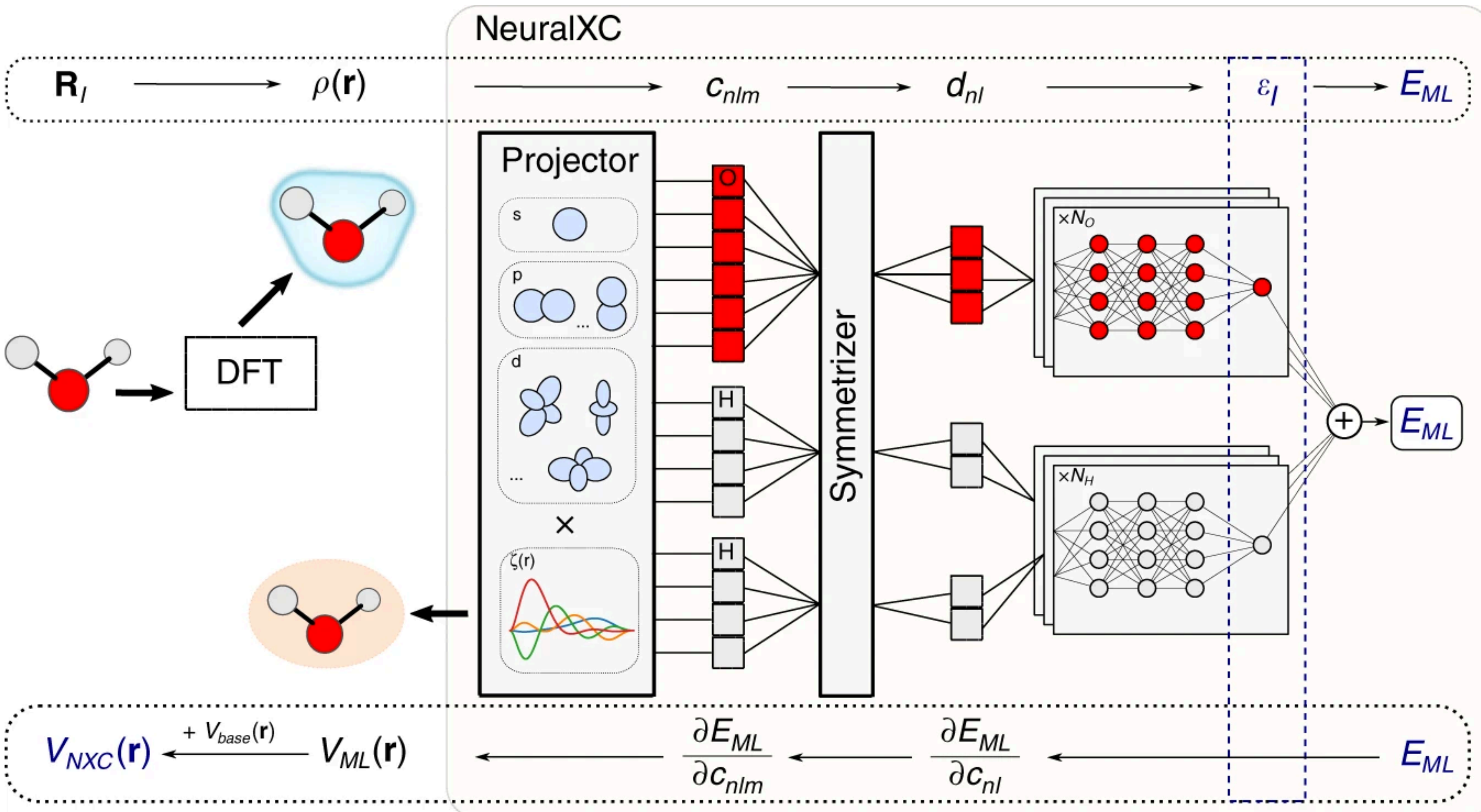

Dick & Fernandez-Serra (2020)